NOVEL IMPACTS OF HOST-ENVIRONMENT INTERACTIONS IN ENTERIC GLIA THROUGH SEQUENCING AND *IN-SITU* EXPRESSION

By

Christine Dharshika Ponnampalam

A DISSERTATION

Submitted to
Michigan State University
in partial fulfillment of the requirements
for the degree of

Genetics – Environmental Toxicology – Doctor of Philosophy

2021

ABSTRACT

NOVEL IMPACTS OF HOST-ENVIRONMENT INTERACTIONS IN ENTERIC GLIA THROUGH SEQUENCING AND *IN-SITU* EXPRESSION

By

Christine Dharshika Ponnampalam

The enteric nervous system (ENS) is comprised of enteric neurons and glia that facilitate essential gastrointestinal (GI) function including motility, visceral sensation, absorption, and gut permeability. Enteric neurons and glia are responsive to environmental cues and stressors ranging from the local gut microenvironment to the host's psychosocial state and understanding how the ENS integrates these cues to modulate local and systemic function is critical. Novel roles for enteric neurons in host-environmental interactions have been discovered using specialized sequencing technologies but these tools have not yet readily investigated enteric glia. The goal of this dissertation was to develop and utilize genetic technologies to characterize enteric glial responses to environmental mediators.

First we adapted existing genetic tools to study molecular changes in the ENS and specifically enteric glia. We developed effective means of characterizing enteric glial expression within complex *in vivo* models using the RiboTag model with RNA-sequencing and subsequently visualized changes in gene expression within enteric ganglia *in situ*. We then utilized these techniques to investigate sex-specific responses to early life stress in enteric glia. Enteric glia from male and female mice have contrasting expression profiles including differences in GPCR signaling that could contribute to sex-specific ENS signaling mechanisms and ultimately GI disease outcomes. This supports recent findings of sexual dimorphism in glial functional connectivity and may highlight a critical difference in the way enteric glia communicate with other cell types between males and females. Additionally enteric glia from male mice 'feminize' following early life stress through altered expression of GI and neurological disease genes including mechanisms of glial-immune communication like type I interferon signaling. Together these data

highlight striking differences in the physiologic molecular patterns and nature of stress response in enteric glia between males and females that likely contribute to sexually dimorphic GI disease patterns and symptom presentation.

Next we investigated ENS type I interferon responses through the stimulator of interferon genes (STING) pathway. STING responds to both microbial and host mediators to contribute to GI inflammation. However the role of STING signaling in the gut is complex and can either exacerbate or ameliorate inflammation likely dependent on complex microenvironmental factors. We provide the first known investigation of STING expression and signaling within the ENS. STING is expressed in both enteric neurons and glia but IFNB is only expressed in enteric neurons. ENS STING is activated by its canonical ligands to produce type I interferons. However this is likely primarily mediated through canonical activation of enteric neuronal STING and the contribution of enteric glial STING to type I IFN response is minor. Additionally enteric glial STING does not alter gastrointestinal outcomes during acute colitis within the DSS colitis model. Taken together these findings suggest enteric glia do not utilize STING for canonical type I IFN signaling or contribute to disease pathology in acute DSS colitis. Enteric glial STING may instead utilize primordial and specialized signaling pathways that more selectively alter local function.

Together our data provide novel genetic tools and data to further uncover molecular functions in enteric glia and their role in GI and systemic health. Using these we discovered entirely novel molecular interaction effects between sex and early life stress that shift the framework of these risk factors in GI disease. Furthermore we highlight a novel potential mediator of ENS-microbe communication with STING. Our findings further characterize the molecular patterns used by glia in response to complex environmental factors and highlight unique heterogeneity in glial intercellular communication.

TABLE OF CONTENTS

LIST OF TABLES

LIST OF FIGURES

KEY TO ABBREVIATIONS

2,3-cGAMP	2,3- cyclic guanosine monophosphate—adenosine monophosphate
3,3-cGAMP	3,3-cyclic guanosine monophosphate—adenosine monophosphate
AAALAC	Association for Assessment and Accreditation of Laboratory Animal Care
c-di-GMP	Cyclic diguanylate
CDNs	Cyclic dinucleotides
CMMP	Circular muscle—myenteric plexus
CNS	Central nervous system
DMEM/F-12	Dulbecco's modified eagle medium
DMXAA	5,6-dimethylxanthenone-4-acetic acid
DSS	Dextran sodium sulfate
ELISA	Enzyme-linked immunosorbent assay
ELS	Early life stress
ENS	Enteric nervous system
EW	Early weaning
FDR	False discovery rate
GI	Gastrointestinal
GPCR	G protein-coupled receptor
GSEA	Gene set enrichment analysis
H&E	Hematoxylin & eosin
HA	Hemagglutinin
IACUC	Institutional Animal Care & Use Committee
IBD	Inflammatory bowel disease
IBS	Irritable bowel syndrome
Ifit1	Interferon induced protein with tetratricopeptide repeats 1

IFN	Interferon
Ifnar	Interferon alpha/beta receptor
IFNB	Interferon beta
IHC	Immunohistochemistry
IPA	Ingenuity pathway analysis
KO	Knockout
LMMP	Longitudinal muscle—myenteric plexus
NH	Normal handled
NMS	Neonatal maternal separation
NMS + EW	Neonatal maternal separation + early weaning
Oasl2	2’,5’-oligoadenylate synthase-like protein 2
PASH	Periodic acid-Schiff with hematoxylin
PB	Phosphate buffer
PBS	Phosphate buffered saline
PCA	Principal component analysis
Rgs5	Regulator of G protein signaling 5
RIN	RNA integrity number
RNA-seq	RNA-sequencing
STING	Stimulator of interferon genes
Xist	X inactive specific transcript

CHAPTER ONE: ENTERIC NEUROMICS: HOW HIGH THROUGHPUT 'OMICS' DEEPENS OUR UNDERSTANDING OF ENTERIC NERVOUS SYSTEM GENETIC ARCHITECTURE

ABSTRACT

Recent accessibility to specialized high-throughput ‘omics’ technologies allows researchers to capture cell type- and subtype-specific biomolecular signatures. Omics methods are utilized in the enteric nervous system to further investigate enteric neuronal and glial subtypes. These results validate but also add complexity to our current understanding of ENS cellular makeup. Furthermore, these data provide the basis to begin linking both knowledge of ENS function and intestinal disease with ENS cellular type and subtype. In this review we discuss how high-throughput ‘omics’ data adds to our understanding of the cellular makeup of the ENS and how this may be perturbed in disease. These data identify several putative ENS cell subtypes that are likely altered in certain pathologies but the functional nature of these subtypes is still unclear. As the ENS omics field continues to grow we will answer these questions but undoubtedly uncover even more heterogeneity within the enteric nervous system.

INTRODUCTION

High-throughput “omics” research investigates molecular information on a large, comprehensive scale. The flexibility and resolution of omics technologies continues to increase while cost decreases[1]; making omics methods increasingly accessible and attractive to basic and clinical research. This is particularly true for work focused on understanding the enteric nervous system (ENS). The ENS is embedded in the gut wall and controls motility, fluid transport, and secretion in addition to integrating signals from other organs, the brain, and multiple cell types in the gastrointestinal tract.[2] The ENS is comprised of neurons and glia with generally well-known electrophysiological properties, anatomical features, and certain protein markers.[2–5] However, much of the complexity of the ENS remains to be understood and would benefit from developing a deeper understanding of cellular heterogeneity, functional attributes of cells and cellular networks, and genes that could contribute to disease.

Omics technologies are beginning to improve our ability to understand complexity within the ENS on a scale that was previously inaccessible. The advent of single cell sequencing technologies such as single cell RNA-sequencing (scRNA-seq) now allows investigators to delve even deeper and characterize heterogeneity between individual cells.[1] Cellular genomic libraries are now available to explore the cellular makeup of the ENS in fine resolution, which is useful to both build on prior knowledge and to generate new hypotheses. In this review we will begin by summarizing the ‘pre-omics’ understanding of the cellular makeup of the ENS and describe omics strategies that have been employed in ENS studies. Then we will focus on how omics data expand our knowledge of ENS cell diversity and how this changes in gastrointestinal disease. We conclude by discussing our thoughts on the strengths and weaknesses of current ENS omics data and suggest future directions for the field.

‘Pre-omics’ Understanding of ENS Cellular Makeup

Classification of Enteric Neurons

Enteric neurons are traditionally classified by their morphology, electrophysiological properties, and neurotransmitter expression.[2–4] Enteric neuron morphology was initially described by A.S. Dogiel[6] and has been characterized by imaging techniques that include intracellular dye filling, silver staining, retrograde tracing, immunohistochemistry, and electron microscopy. At least seven unique neuronal cell body types have been described by these assays. These are typified by the shape and number of axons and dendrites and by where their processes project. Dogiel type I and II are the predominant morphologies. Type I neurons have flat, long cell bodies with a single axon and short dendrites while type II neurons have round or ovoid cell bodies with multiple axons and longer dendrites. Type I neurons project through other ganglia and into musculature while type II neurons project within and to nearby ganglia.[4] Neurons are also classified by electrophysiological properties, which were characterized in early studies by Nishi and North[7] and later expanded upon by Hirst et al.[8] Two main types of enteric neurons were identified in these studies and categorized as having either S (synaptic) or AH (after hyperpolarization)-type electrophysiological properties. These differed based on action potential speed and magnitude, the length of after-hyperpolarizing potentials, and tetrodotoxin sensitivity. S-type neurons typically display a Dogiel type I morphology and include interneurons and motor neurons while AH-type neurons typically display a Dogiel type II morphology and are considered sensory neurons.[4]

Defining the neurochemical coding of enteric neuron subtypes was a significant advancement that allowed understanding how enteric neurons communicate amongst themselves and with target tissues. Enteric neurochemical coding has been defined by multiple approaches that include immunohistochemistry in combination with retrograde tracing, electrophysiology, and pharmacology. Understanding what neurochemicals enteric neurons express is important for developing models to understand cellular signaling and for identifying

unique cellular markers. Integration of this biomolecular data with morphological and electrophysiological properties was the basis for the current definitions of enteric neuron subtypes, which include motor neurons, interneurons, and sensory neurons. Motor neurons reside in the myenteric plexus and innervate the circular and longitudinal muscle of the intestine. These cells display a Dogiel type I morphology and include both excitatory and inhibitory subsets. Excitatory motor neurons are considered cholinergic based on acetylcholine (ACh) synthesis and release, but also release additional excitatory transmitters such as tachykinins. Inhibitory motor neurons are primarily considered nitrergic based on their use of nitric oxide (NO) as a transmitter.[2–4] Inhibitory neuromuscular transmission also involves purines and vasoactive intestinal peptide (VIP), but whether the same inhibitory neurons release both NO and purines or whether these are released by different subsets is not clear.[3,4] Excitatory motor neurons express choline acetyltransferase (ChAT) while inhibitory neurons express nitric oxide synthase (NOS), pituitary adenylyl cyclase activating peptide (PACAP), and neuropeptide Y (NPY). Secretomotor/vasodilator neurons have three known subtypes categorized as non-cholinergic VIP^+ neurons, $ChAT^+$/calretnin (*Calb2*)$^+$ neurons, and $ChAT^+/NPY^+$ neurons.[2–4]

At least four types of interneurons are present in the small intestine of the guinea pig and likely other species. Ascending interneurons are cholinergic and also utilize tachykinins and ATP as transmitters.[2–4] These neurons are involved in local motility reflexes.[3,4] Descending interneurons are also involved in local motility reflexes and include subtypes that are $ACh^+/NOS^+/VIP^+$ and others that are ACh^+/serotonin $(5\text{-HT})^+$. The latter is involved in secretomotor reflexes as well.[2,4] A third type of descending interneuron type is ACh^+/somatostatin $(SOM)^+$ and is involved in small intestinal migrating myoelectric complexes. This subtype is also characterized by distinct filamentous dendrites.[3,4]

Intrinsic primary afferent neurons (IPANs) regulate intrinsic reflex pathways of the intestine and are involved in chemo- and mechanosensation. IPANs have Dogiel type II morphology, AH-type electrophysiology[3,4], express ChAT, calcitonin gene related peptide (CGRP), tachykinins,

and calbindin, and also bind isolectin B4.[2,4] Intestinofugal/viscerofugal afferent neurons (IFANs) primarily reside in the myenteric plexus and project to prevertebral ganglia where they synapse with post-ganglionic sympathetic neurons. These cells contribute to intestinal reflexes that involve integration with other gastrointestinal organs. IFANs typically are Dogiel type I but occasionally type II.[4] IFANs utilize ACh and VIP signaling but also express cholecystokinin (CCK), gastrin releasing peptide (GRP), and opioid-related peptides.[2]

Classification of Enteric Glia

Enteric glial heterogeneity and functions were covered extensively in a recent review[9] and will not be reiterated here. Current glial subtypes are defined based on morphology and anatomical location in the gut wall and may include differences in marker expression and responses to various transmitters.[5,10] Canonical markers used to identify enteric glia include glial fibrillary acidic protein (GFAP), S100B, Sox10 [5,10,11] and *Plp1* [11]; however, expression of glial markers within a single cell varies over time and is reflective of their current state.[10,11] Therefore, whether expression patterns are indicative of different glial subtypes or ongoing cellular dynamics is unclear.

Omics in the Enteric Nervous System

The technical details of current omics techniques and strengths and challenges of applying these techniques to biomedical research are discussed in detail elsewhere.[1,12,13] Here we will briefly introduce those that have been employed to study the ENS. *Genomics* identifies variation in DNA sequence, primarily utilizing genome-wide association studies (GWAS). GWAS investigates diseased humans to identify genetic mutations (specifically single nucleotide polymorphisms, SNPs) that may confer disease risk. Sequencing the entire genome or coding 'exome' can also identify mutations. *Transcriptomics* identifies and quantifies RNA expression.

Transcriptomics initially used microarray platforms but now primarily consists of sequencing (RNA-seq). Typically RNA-seq focuses on which genes are expressed and how their expression level changes. However, this method can also identify noncoding RNAs such as microRNAs or long noncoding RNAs (lncRNAs) that influence transcription of coding genes. *Proteomics* quantifies protein abundance, modification, and interaction. Proteomics captures a related but separate understanding of gene expression than transcriptomics.[12]

Additional specializations of these primary 'omics' modalities also study the ENS. Sequencing the bacterial 16s rRNA gene studies the gut microbiome. Proteomics technology identifies host and microbial metabolites like amino acids, fatty acids, or carbohydrates.[12] RNA-seq combined with cell-specific isolation strategies investigates cell-specific expression. The most recent of these is single cell RNA-seq (scRNA-seq) which measures expression within individual cells.[1] ScRNA-seq is the primary technique used in the ENS to further resolve cellular subtypes of enteric neurons and glia. These data provide novel putative markers of cell type and subtype. Other omics technologies primarily investigate how the ENS is altered in physiology and disease. The details of omics methods used in the ENS and investigated in this review are summarized in **Table 1.1**.

Table 1.1 Omics dataset metadata and review criteria.

Number of Methods Utilized and Species/GI Regions Examined in ENS Omics Datasets						
Section	**Omics Method**		**Species**		**Region**	
Cell Subtype Markers	scRNA-seq	5	Mouse	5	Colon	3
	RNA-seq	1	Human	3	Ileum	1
					small intestine	4
Region-dependent	scRNA-seq	3	Mouse	5	Colon	5
	RNA-seq	1	Human	3	Ileum	1
	Cell-specific RNA-seq	2			Small intestine	4
Species-dependent	scRNA-seq	4	Mouse	5	Colon	3
	RNA-seq	1	Human	5	Ileum	1
	Cell-specific RNA-seq	1			Small intestine	3
					Cell culture	1
Sex-dependent	scRNA-seq	4	Mouse	4	Colon	3
	RNA-seq	1	human	1	Ileum	1
					Small intestine	3
Dysmotility	scRNA-seq	1	Mouse	2	Colon	4
	RNA-seq	3	Human	4	Small intestine	2
	WES	1	Rat	1		
	MALDI-TOF MS	1				
Development	scRNA-seq	2	Mouse	4	Colon	3
	RNA-seq	1	Human	3	Ileum	1
	Cell-specific RNA-seq	2	Zebrafish	1	Small intestine	4
	WES	1			Cell culture	1
	Microarray	1				
Neuroimmune Communication	scRNA-seq	1	Mouse	4	Colon	3
	Cell-specific RNA-seq	4	Human	2	Ileum	1
	Microarray	1	Rat	1	Small intestine	3
					Cell culture	1

Table 1.1 (cont'd)

Dysbiosis	**scRNA-seq**	**1**	**Mouse**	**11**	**Colon**	**11**
	RNA-seq	1	Human	1	Small intestine	4
	Cell-specific RNA-seq	2	Rat	3		
	GWAS	1				
	LCMS	1				
	16S sequencing	8				
GI Disease Markers	scRNA-seq	2	Mouse	5	Colon	7
	RNA-seq	1	Human	8	Ileum	1
	Cell-specific RNA-seq	2			Small intestine	3
	GWAS	2				
	Microarray	1				
	LCMS	1				
	16S sequencing	1				

scRNA-seq, single-cell RNA-sequencing; RNA-seq, RNA-sequencing; WES, whole exome sequencing; MALDI-TOF MS, matrix-assisted laser desorption/ionization time-of-flight mass spectrometry; GWAS, genome-wide association study; LCMS, liquid chromatography-mass spectrometry

Review Search Criteria

Full-text primary research articles were selected from the PubMed database using the following search term:

("neurons"[MeSH Terms] OR "neuroglia"[MeSH Terms] OR "Ganglia, Spinal"[MeSH Terms] OR "Enteric Nervous System"[MeSH Terms] OR "Colon/innervation"[MAJR] OR "dorsal root ganglia"[All Fields] OR "neuron"[Title/Abstract] OR "enteric glia"[All Fields] OR "glia"[Title/Abstract]) AND ("computational biology"[MeSH Terms] OR "sequence analysis"[MeSH Terms] OR "high throughput"[Title/Abstract] OR "sequencing"[All Fields] OR "next generation"[All Fields]) AND ("gastrointestinal diseases"[MeSH Terms] OR "gastrointestinal tract"[MeSH Terms] OR "Gastrointestinal Microbiome"[MeSH Terms] OR "gastrointestinal"[Title/Abstract] OR "bowel"[Title/Abstract] OR "gut"[Title/Abstract]) NOT Review[Publication Type]

From these results articles were screened for using high-throughput 'omics' methods in the enteric nervous system or referencing enteric nervous cells. A few newer articles were selected outside this due to backlog in MeSH classification.

OMICS CONTRIBUTION TO UNDERSTANDING ENTERIC NERVOUS SYSTEM CELL SUBTYPING

Genetic Markers of ENS Cell Subtypes

Several prominent scRNA-seq studies on the ENS vastly expand the data available to investigate the nature of ENS heterogeneity.[14–18] Here we highlight collective findings across these data and potential cellular subtypes and markers. While further examination is required to truly establish ENS cellular subtypes, these data suggest several subtypes of cells within the ENS that add additional complexity to the current neurochemical coding of enteric neurons and glia. Our interpretation of synthesized findings and potential ENS cell subtypes are summarized in **Figure 1.1 and Table 1.2**.

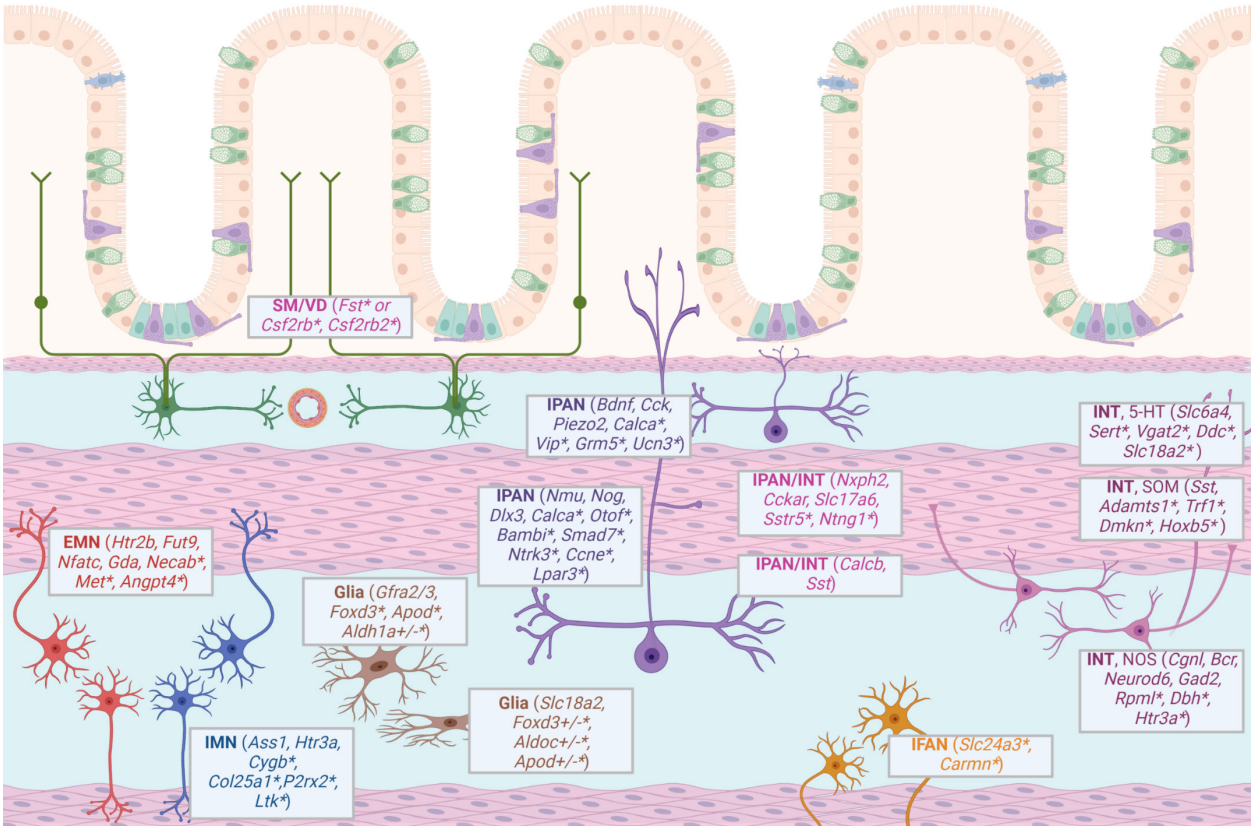

Figure 1.1 Putative markers of ENS cell subtypes.

Genetic markers of enteric neuron and glia subtypes from scRNA-seq research (created with Biorender.com). Future genetic and functional research could validate these molecules as important functional or developmental requirements for ENS cell subtypes. Genes mentioned in a single study from each cluster are denoted with an asterisk*. EMN, excitatory motor neuron; IMN, inhibitory motor neuron; INT, interneuron; IPAN, intrinsic primary afferent neurons; SM/VD, secretomotor/vasodilator neuron; IFAN, intestinofugal afferent neuron.

Table 1.2 Putative Number Enteric Neuron and Glia Subtypes and Co-Expression Markers.

Number of ENS cell subtypes proposed by scRNA-seq						
	Drokhlyansky et al.[14]	**May-Zhang et al.[15]**	**Morarach et al.[16]**	**Wright et al.[17]**	**Zeisel et al.[18]**	*functional classification of clusters not specified in research and estimated by expression of established markers
Species	mouse | human	mouse	mouse	mouse	mouse	
Age	adult	adult	PN21	E17.5 | adult	PN21	
Region	ileum, colon | colon	duodenum + ileum + colon	small intestine	intestine | colon	small intestine	
No. EMN	3, 3-5 | 4	2	3	1 | 1-2	2*	
No. IMN	2, 4-7 | 5	2	2	0-2 | 0-2	3*	
No. INT	2, 2-3 | 2	4	2-5	2-3 | 4-6	3*	
No. IPAN	3, 3-4 | 1	2	3	1 | 1-2	1*	
No. Glia	3 | 3-6	--	--	-- | 4	7	
Shared neurochemical markers of putative ENS cell subtypes						
Putative Cell Subtype	**Drokhlyansky et al.[14] (defining markers)**	**May-Zhang et al.[15] (defining markers)**	**Morarach et al.[16] (defining markers)**	**Wright et al.[17] (defining markers)**	**Zeisel et al.[18] (defining markers)**	**Shared Markers**
EMN, circular muscle	PEMN2	Cluster 3 (*Necab*)	ENC4	Chat3 (*Met*)	ENT6 (*Angpt4*)	*Htr2b, Fut9, Nfatc1, Gda, Penk*$^{-}$
IMN, longitudinal muscle		Cluster 1 (*Cygb, Col25a1*)		Nos1 (*P2rx2*)/Nos2	ENT2 (*Ltk*)	*Ass1, Htr3a*
INT, NOS^{+} descending	PIN1	Cluster 10	ENC6 (*Rpml*)	Nos cluster 2 (*Dbh, Htr3a*)	ENT7	*Nos1, Cgnl, Bcr, Neurod6, Gad2*
INT, SST^{+} descending		Cluster 9 (*Adamts1, Trf1, Gm30382*)		Chat 1 (*Dmkn, Hoxb5*)	ENT5	*Sst*
INT, 5-HT^{+} desending		Cluster 6s (*Sert,Vgat2*)	ENC12 (*Ddc, Slc18a2*)			*Slc6a4*

Table 1.2 (cont'd)

IN/IPAN	PSN4 (*Calca*$^{-}$)		ENC5			*Calcb, Sst*
IN/IPAN	PIN1	Cluster 6/ Cluster 7	ENC12 (*Sstr, Ntng1*)	Chat 4	ENT7/ENT8	*Nxph2, Cckar, Slc17a6*
IPAN	PSN1 (*Calca*)	Cluster 5 (*Otof*)	ENC6	Calcb(*Bambi, Smad7, Ntrk3*)	ENT9 (*Ccne, Lpar3*)	*Nmu, Nog, Dlx3*
IPAN	PSN2 (*Calca, Vip*)		ENC7 (*Grm5, Ucn3*)/ENC12			*Bdnf, Cck, Piezo2*
Dopaminergic Neurons	PEMN1/PSN4	Cluster 9	ENC11 (*Npy, Calb2*)	Nos cluster 2		*Th, Dbh*
Glia	Glia1 (*Gfra2*)				ENTG3-4 (*Gfra3, Foxd3, Apod, Aldh1a3*$^{+/-}$)	
Glia	Glia2 (*Lsamp, Ank2*)				ENTG5-7 (*Foxd3*$^{+/-}$, *Aldoc*$^{+/-}$, *Apod*$^{+/-}$)	*Slc18a2*

EMN, excitatory motor neuron; IMN, inhibitory motor neuron; INT, interneuron; IPAN, intrinsic primary afferent neurons

Motor Neurons

At least 2-5 subtypes of excitatory motor neurons are identified based on their gene expression profiles in single cell transcriptional studies.[14–18] Novel markers for excitatory motors neurons were identifies in these data and include *Gfra2,* the receptor for neurturin (NRTN),[17] and *Piezo1*. Since *Piezo1* encodes a mechanosensitive ion channel, these neuronal subtypes may sense colonic distension as well.[14] However, *Piezo1*$^{+}$ neurons could be intrinsic sensory neurons or mechanosensitive interneurons[17] and further functional studies are needed.

Most excitatory motor subtypes are difficult to align across multiple studies and could suggest complex expression patterns or technical differences. However, a neuronal subtype that excites circular muscle was identified across several studies including May-Zhang et al.[15] and Morarach et al.[16] where these cells are defined as Cluster 3 and ENC4, respectively. Cells within these clusters expressed high levels of the 5-HT2B receptor gene *Htr2b* in addition to genes encoding a calcium binding protein (*Necab2*), an enzyme that catalyzes the last step in the biosynthesis of Lewis X antigen (*Fut9*), and a transcription factor involved in inducible gene transcription during immune responses (*Nfatc1*). *Fut9* and *Nfatc1* were also expressed by the Chat 3 neuron cluster defined by Wright et al.[17] and by the ENT6 neuron cluster in Zeisel et al.,[18] which additionally co-expressed the guanine deaminase gene (*Gda*) and the gene encoding angiopoietin-4 (*Angpt4*). This cluster could correspond to PEMN2 in Drokhlyanksy et al.[14] due to higher enkephalin (*Penk*) expression compared to other putative excitatory motor neurons, as also seen in other datasets.[15,16,18] Other markers identified in clusters corresponding to excitatory motor neurons include *Brinp2*, *Fbxw15*, and *Specc1* in cells proposed to innervate longitudinal muscle (cluster 0 in May-Zhang et al.[15]) and the D2 dopamine receptor *Drd2* (PEMN3 in Drokhylansky[14]).

At least 2-4 inhibitory motor neuron subtypes have also been identified based on gene expression profiles in single cell transcriptional studies[14–18]. Potential new markers for inhibitory motor neurons include *Gfra1*, the receptor for glial cell line-derived neurotrophic factor (GDNF)[17]

and *Etv1*, a gene encoding the transcription factor Etv1.[17,18] A cluster proposed as inhibitory motor neurons projecting to longitudinal muscle also co-expressed genes encoding arginosuccinate synthase 1 (*Ass1*), cytoglobin (*Cygb*), and a brain-specific membrane associated collagen (*Col25a1*) (cluster 1 from May-Zhang et al.[15]). This overlaps with two *Nos1*$^{+}$*Ass1*$^{+}$ inhibitory subtypes defined by Wright et al.[17] as Nos1 and Nos2. The Nos1 cluster also expressed genes encoding 5-HT3A (*Htr3a*) and P2X2 (*P2rx2*) receptors. This cluster may correspond to ENT2 or ENT3 from Zeisel et al.[18] as these cells are *Nos1*$^{+}$*Htr3a*.[18] There is less consistency in the genetic profiles of other clusters identified as inhibitory motor neurons between datasets. Certain clusters express *Vip* while others do not. These subtypes could be further resolved by investigating their specific markers, including adrenomedullin (*Adm*), the GPCR *Lgr5*, or desmocollin 2 (*Dsc2*).[14,15]

Drokhlyansky et al.[14] identified 2-3 clusters that potentially correspond to secretomotor/vasodilator neurons. These clusters were characterized as secretomotor/vasodilator neurons based on expression of the glucagon like peptide 2 receptor (*Glp2r*). One subtype (PSVN1) co-expressed follistatin (*Fst*) while another (PSVN2) co-expressed Csf2 receptor genes *Csf2rb* and *Csf2rb2*. While these may indicate specialized growth function and immune communication respectively further investigation is required.

Dopaminergic Neurons

Dopaminergic enteric neurons are rare neurons that develop relatively late (after E18)and express tyrosine hydroxylase (*Th*), dopamine active transporter (*Dat*), and the dopamine metabolite DOPAC.[19,20] These neurons are important regulators of gastrointestinal motility[21] and therefore involved in motor circuitry, but what specific types of neurons express dopamine is unclear. ScRNA-seq studies suggest subtypes of motor neurons, interneurons, and sensory neurons are dopaminergic.[14,15] However, these data suggest some co-expression markers which future studies could use to further characterize dopaminergic neurons. These neurons may express dopamine beta-hydroxylase (*Dbh*), *Npy,* and *Calb2*[16] and/or the combination of *Ebf1, Meis2, Etv1, Satb1, Klf7,* and *Sox6.*[20].

Interneurons

Interneurons are more difficult to define by gene signatures in scRNA-seq studies due to the overlap of their established markers with other neuron types. Despite this, between 2-5 subtypes of putative interneurons have been proposed [14–18]. May-Zhang et al.[15] identified four interneuron subtypes (three descending and one ascending) that may align with current functional classifications. One subtype (cluster 10) corresponds to *Nos1*$^{+}$ descending interneurons. These align with *Nos1*$^{+}$ interneuron clusters from other datasets and suggest co-expression of several markers including neuronal differentiation 6 gene (*Neurod6*) and glutamate decarboxylase 2 (Gad2).[14–18] The second descending interneuron subtype identified by May-Zhang et al.[15] (cluster 9) are *Sst*$^{+}$ and co-expressed *Adamts1, Gm30382,* and *Trf1*. This aligns with *Sst*$^{+}$ clusters in other datasets and suggest co-expression of dermokine (*Dmkn*) and homeobox gene *Hoxb5*.[17,18] The third descending interneuron subtype is serotonergic and identified by expression of serotonin transporter *Sert*, dopa decarboxylase (*Ddc*), *Vgat2,* and *Slc6a4.*[15,16] The ascending interneuron subtype identified by May-Zhang et al.[15] (cluster 3s) was characterized by high *Chat* and *Tac1* and co-expression of *Kctd16* and *Unc5d.*

One cell type is conserved amongst datasets but classified as both a potential interneuron[14,17] or potential IPAN.[15,16] These cells co-expressed combinations of markers *Nxph2*, *Cckar*, *Slc17a6*, *Sstr5*, and *Ntng1*.[14–18] It is unclear if cells with this expression profile represent a single subtype, genes upregulated in multiple subtypes in response to a particular microenvironment, or both. *Nxph2* is part of the neurexophilin family and modulates synaptic plasticity and supports this expression profile as a transitional state for multiple neuronal subtypes. These cells required *Pbx3* expression at E18.5 for fate determination[16] and perhaps lineage tracing could resolve their identity in adulthood.

Intrinsic Primary Afferent Neurons (IPANs)

Between 1-4 cell clusters are proposed to correspond to IPANs based on transcriptional signatures[14–18] and differential expression of CGRP genes (paralogs *Calca* and *Calcb,* coding for

CGRPα and CGRPβ respectively) may help differentiate subtypes. *Calca* is only expressed in a subset of IPAN clusters[14] and immunolabeling confirms this in both juvenile (PN21) and adult mice.[16,22]

One *Calca*$^{+}$ subtype co-expressneuromedin U (*Nmu*), noggin (*Nog*), and homeobox *Dlx3*.[14–18] Developmental differences in gene expression in these cells are also characterized. At E17.5 this subtype also expressed *Bambi*, *Smad7*, *Ntrk3*, and *Adra2a*.[17] However, *Adra2a* is expressed across all IPANs in adulthood.[14] suggesting that this subtype-specific expression is limited to the developmental period. At PN21, these cells are the only neuron subtype that does not express Phox2a.[16] These expression patterns may help further identify this cell type. A second *Calca*$^{+}$ IPAN subtype expresses a combination of brain-derived neurotrophic factor (*Bdnf*), mechanosensitive ion channel *Piezo2,* and *Cck*. Drokhlyansky et al.[14] suggest this is a single subtype (PSN3) while Morarach et al.[16] identified a *Bdnf*$^{+}$*Piezo2*$^{+}$ subtype (ENC12) and a separated cluster (ENC7) as *Bdnf*$^{+}$*Cck*$^{+}$*.* ENC12 appeared morphologically as IPANs while ENC7 were characterized as atypical IPANs or perhaps even viscerofugal neurons, adding additional complexity to this expression pattern.

One *Calca*$^{-}$ subtype identified by Drokhlyansky et al.[14] (PSN4) is *Sst*$^{+}$ and may correspond to a *Calcb*$^{+}$*Sst*$^{+}$ cluster defined as interneurons (ENC5) by Morarach et al.[16]. These discrepancies could suggest developmental differences in IPAN clustering. May-Zhang et al.[15] identified *Klhl1* as a novel marker of *Nmu*$^{-}$ IPANs in mice. Whether this marker labels all *Nmu*$^{-}$ subtypes or one particular subtype remains to be investigated. This study also identified a single neuronal cluster as intestinofugal and these cells co-express *Slc24a3* and *Carmn* in mice and humans. *Carmn* is a long noncoding RNA critical for cardiac muscle development and pathological remodeling.[23] While this may have interesting implications for either the development or function of IFANs this remains to be seen.

Enteric Glia

While data on glial subtypes is limited 3-7 subtypes are classified based on expression patterns. The number of glial subtypes may differ throughout development or by gut region, as 7 subtypes were identified in PN21 mice ileum[18] while adult mice colon only have 3-4 subtypes.[14,17] One glial subtype in PN21 mice is classified as a progenitor cell due to topoisomerase *Top2a* expression.[18] This is not a defining marker identified in adult enteric glia and suggests this glial subtype plays a larger role in the juvenile development period than adulthood. Expression of the vesicular monoamine transporter *Slc18a2* and GDNFα receptors further supports developmental convergence of glial subtypes, as these mark 2-3 subtypes at PN21 and only one subtype each in adulthood.[14,18] Several other markers of enteric glial subtypes are identified only in a single study. These include differential expression of *Foxd3* and *Aldh1a3* in PN21 subtypes[18] and neurotensin receptor *Ntsr1* in adult subtypes.[14] In humans, one glial subtype expressed *P2Y12R, NRXN1,* and *XKR4*[14] which could also be potential markers. While differential expression of these markers could reflect developmental and species differences these may also require further investigation. Several studies created glial expression datasets[14,17,18] and with re- or meta-analysis of these data with a glial focus will likely help resolve these differences and identify additional subtype expression patterns.

Region-, Species- and Sex-Dependent Expression

Region-Dependent Expression

The number of neuronal subtypes is mostly conserved across gut regions[14,15]; however, the proportion of neuronal types and subtypes varies. The ileum contains more sensory neurons than the colon while the colon contains more secretomotor/vasodilator neurons. This difference likely reflects the colon's need to regulate fluid absorption and secretion.[14] Subtype-specific genes also vary between regions of the small and large intestine. *Chat*$^{+}$*/Nos*$^{+}$ descending interneurons,

Gad2^{+} interneurons[15–17] and/or *Gad2*$^{+}$ secretomotor/vasodilator neurons[14] are more prevalent in the small intestine. Genes including *Unc5d*, *Col25a1,*[24] *Htr2b,*[14,25] and *Htr3a*[14] are all highly enriched in the colon and are putative markers for subtypes of ascending interneurons, inhibitory motor neurons,[15] excitatory motor neurons,[15,16] and IPANs/inhibitory motor neurons,[17] respectively.

Regional expression patterns also reflect gut physiology. Genes involved in signaling with enteroendocrine cells such as *Cckar,*[15]*Tacr3, Npy,* and the glucagon receptor *Gcgr* are highest in duodenal neurons.[25] Meanwhile distal gut segments are enriched for the glutamate receptor[14], *Sst, Cartpt, Penk,* and *Grp*.[25] Glutamate is mostly absorbed in terminal ileum[14] while these other distally-enriched genes are important in colonic motility.[25] Transcription factor *Pou3f3* (*Brn1*) is also higher in the colon than small intestine.[15,17,24,25] This gene is important in CNS development,[17] so perhaps it plays a role in colonic ENS development as well. Finally, *Ahr* is highly expressed in colonic neurons[17] and neuronal *Ahr* integrates microbial cues with colonic motility.[24] For other genes with regional variation their expression may be functionally relevant but is currently unclear. Duodenal neurons enrich for growth factors such as *Fst1* and *Wif1* while distal neurons enrich for *Agrp,*[25] *Ano5, Pde1c, Panrt2*,[24] *Pantr1,* and *Zfhx3*.[17]

Neurotransmitter ligand/receptor expression differs across the colon as well and highlight colonic region-dependent signaling priorities. Somatostatin (*Sst*) signaling may be more prominent in proximal colon. Meanwhile several pathways are distally enriched, including serotonin (*Htr3a* and *Htr3b*), glutamate (*Gria3* and *Grid1*), acetylcholine (*Chrna7* and *Chrm1*), chromogranin B (*Chgb*), enkephalin (*Penk*), norepinephrine (NE), secretogranin II (*Scg2*), and *Vip*.[14] However, *Htr3a* and *Htr3b* are higher in the duodenum than ileum,[25] suggesting additional roles for these receptors proximally. Particular neuronal subtypes also demonstrate regional colonic distribution. *Calca*$^{+}$*/Nog*$^{+}$*/Nmu*$^{+}$ sensory neurons are more highly prevalent in the proximal colon while *Lgr5*$^{+}$ inhibitory motor neurons are more common distally.[14]

Differences between enteric glia in human colonic mucosa and *muscularis externa* have been characterized. Mucosal glia more highly expressed ferritin genes (*FTH1* and *FLT*), heat shock protein *CRYAB*, and galectin-1 (*LGALS1*) while myenteric glia expressed genes involved in cell adhesion like *NRXN1* and *CADM2*.[14] These are likely also reflective of known gut physiology. Ferritin helps regulate iron absorption in the mucosa[26] while CRYAB modulates mucosal inflammation and barrier integrity,[27] suggesting mucosal glia participate in these functions. Cellular adhesion is likely important for the structural integrity of myenteric ganglia. This is not a surprising role for enteric glia as it is important in other peripheral glia like Schwann cells as well.[28]

Species-dependent expression

Historically enteric neurons from smaller mammals are considered smaller, simpler, and easier to classify than those from larger species such as humans. Perhaps this is in part due varying abundances of neuronal cell types, as these types display varying cell body size and complexity.[4] ScRNA-seq research supports this phenomenon as the proportions of neuronal types differs between species. Both excitatory and inhibitory motor neurons are enriched in humans while all the other types (sensory neurons, interneurons, and secretomotor/vasodilator neurons) are less abundant. However single cell collection methods have variable efficacy in capturing rare cells or cells with differing morphologies,[29] so to what extent these findings are due to technical limitations is unknown. ScRNA-seq research highlights both conserved functions and complex molecular differences. For instance, development of the ENS is highly conserved. Parallel scRNA-seq of mouse and human neural crest cells identified similar progression of gene expression patterns between both species, suggesting conserved mechanisms of neural fate determination.[30] Specifically, ligand-receptor interactions important for neuronal development are highly conserved between mice and humans.[20] However, hedgehog signaling is subtly different

between species, promoting both neuronal and glial differentiation in mice but only neuronal differentiation in humans.[30]

The number of classified neuronal subtypes is also relatively conserved between species[14,16] and some co-markers are also shared. Excitatory motor neurons in mice and humans express *Galntl6, Tshz2, Alk, Bnc2*,[14] *Rbfox1, Pbx3,* and *Tbx2.*[17] Inhibitory motor neurons in both species express *Dgkb*[14] and *Tbx3.*[17] Interneurons express *Grm7* and sensory neurons express *Cbln2*.[14] Interestingly, secretomotor/vasodilator neurons from both species share markers with other neuron types and therefore may require co-expression patterns to identify. These neurons express *Vip, Kcnd2, Etv1,* and *Scgn*.[14]

However murine and human enteric neuronal expression patterns are more different than similar and may reflect divergent molecular signaling mechanisms. May-Zhang et al.[15] estimate that only 40% of neuron-specific genes are conserved between mice and humans, with variations in subtype- and location-dependent expression as well. This is interesting considering mouse and human gene expression are considered more similar than different within brain regions,[31] however these findings may also be influenced by technical differences. Nonetheless these suggest differential regulation of feeding and energy within the ENS through the melanocortin, leptin, and serotonin pathways. Human neurons highly expressed the melanocortin receptor *MC1R* while mouse neurons expressed its antagonist *Agrp*. Similarly, human neurons highly expressed leptin receptor *LEPR* and serotonin synthesis enzyme *TPH2* while mouse neurons did not.[14]

Differences in gene expression between mice and humans further complicates discovery of subtype markers as well. Drokhlyansky et al.[14] were unable to observe *CHAT* in human neurons and utilized expression of the choline transporter *SLC5A7* to mark these neurons instead. They hypothesize the lack of *CHAT* is due to their specific methods[14], which is likely the case since other studies do not report this same concern in scRNA-seq human data.[17] It is important to note that the strategy of using *Slc5a7* to mark cholinergic neurons would not likely be appropriate in mice since *Slc5a7* may also be expressed by nitrergic neurons.[18] For IPANs, specific subtype

markers are entirely different between mice and humans. While subtypes of murine IPANs express *Klhl1*, *KLHL1* labels an entirely different subset of neurons in humans, classified as *CALB1*$^{+}$*/NXPH2*$^{+}$ Dogiel type III neurons of the small intestine.[15]

Enteric glial subtypes may also be conserved between humans and mice, where three clusters were identified in each species by Drokhlyansky et al.[14] These clusters may correspond to one other but are not explicitly compared. However human glia demonstrate higher complexity as patient-specific subtypes also clustered, likely reflecting the impact of human genetic variability and disease status on gene expression.

Sex-dependent expression

Many of the established concepts regarding ENS neurochemical coding and physiology relied on data from studies that either did not consider sex as a variable or aimed to remove it as a variable. Current omics studies investigating sex differences also remain relatively limited. However, scRNA-seq studies that did assess sex differences did not observe overt sex-related differences in clustering of enteric neuron subtypes, regardless of age or species.[14,16,17] While ENS cell clustering is similar between sexes, there are still differentially expressed genes within all or specific clusters.[14,15] Most of these genes are X- and Y-chromosome related, however some are not. May-Zhang et al.[15] observed that *SLC6A14* and *MUC5B* are enriched in female human neurons, while *Cntnap5a* is higher in putative IPANs (cluster 5) and *Sst* is higher in excitatory motor neurons innervating longitudinal muscle (cluster 0) in female mice. Similarly glial cell subtypes do not appear to have robust sex differences. Perhaps these data are still underpowered to detect subtle sex differences and future research will uncover these. This is especially true for enteric glia given their relatively minor focus in current literature.

OMICS CONTRIBUTION TO UNDERSTANDING ENTERIC NERVOUS SYSTEM DYSFUNCTION AND DISEASE

High-throughput omics data highlights ENS expression patterns and how they are altered in different abnormal states. Here we discuss ENS gene expression in the context of dysmotility, development, communication with immune cells, and dysbiosis. Finally, we link known genetic disease markers with ENS expression. Highlights of these findings are summarized in **Figure 1.2**.

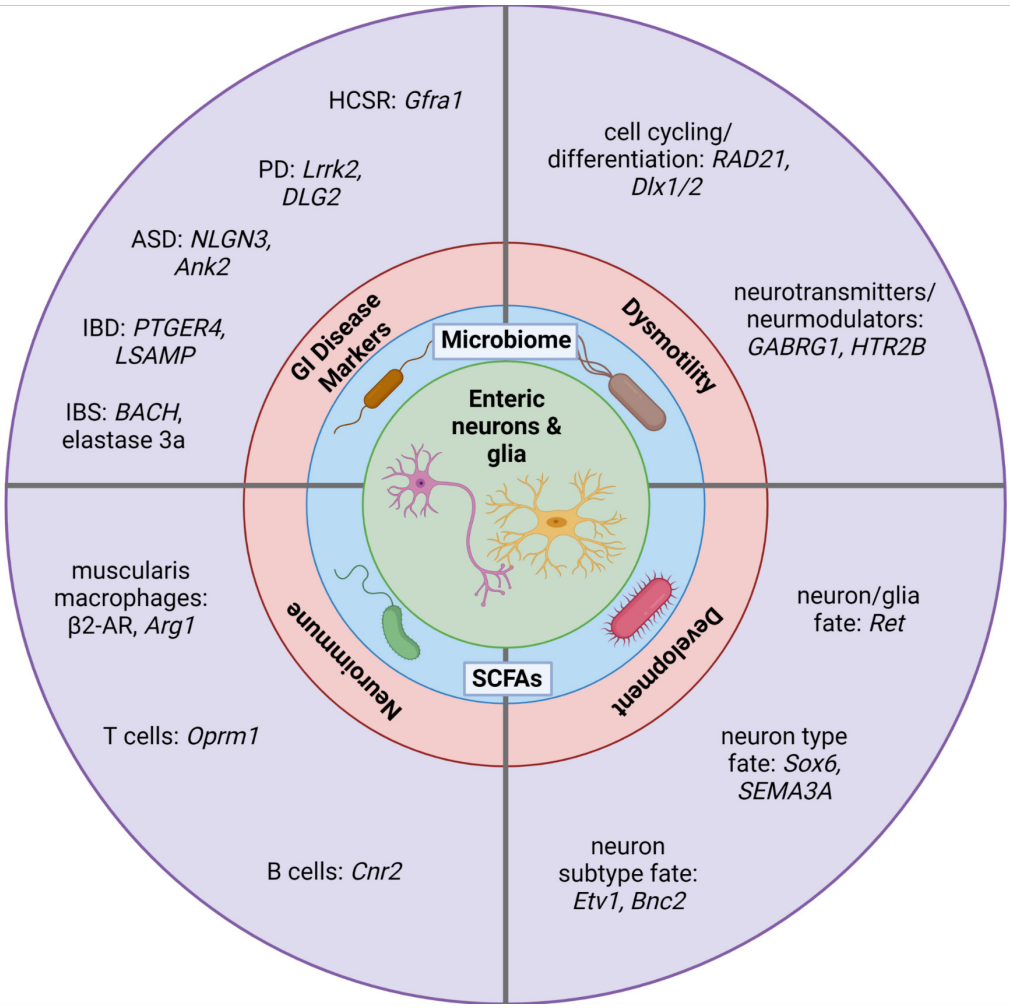

Figure 1.2 ENS-specific gene expression in development and disease.

Several genes expressed by enteric neurons and glia that play a role in gastrointestinal health and pathology are determined through omics research (created with Biorender.com). These data help elucidate the role of the ENS in known pathologies. HSCR, Hirschsprung disease; PD, Parkinson's disease; ASD, Autism spectrum disorder; IBD, inflammatory bowel disease; IBS, irritable bowel syndrome.

Dysmotility

GWAS and related genetic studies have identified mutations associated with dysmotility in humans. However how these mutations contribute to disease risk through gene expression is often unclear. Omics data suggest some of these mutations affect expression of genes involved in cell cycling and differentiation in the ENS. For instance, mutations in DNA repair gene *RAD21* are associated with chronic intestinal pseudo-obstruction. This mutation lowers expression of neuronal differentiation factor *Runx1* and subsequently reduces enteric neuron numbers and slows intestinal transit in zebrafish.[20,32] Transcription factors *Dlx1* and *Dlx2* are also important for bowel motility, where *Dlx1/2* mutants have decreased *Vip* and increased *Penk* and *Plp1* expression,[33] suggesting Dlx1/2 signaling modulates neuronal subtype populations and peripheral glia.

Not surprisingly omics data also support that altered neurotransmitter and neuromodulator signaling in the ENS contribute to dysmotility. A mutation in GABA-A subunit gene *GABRG1* is associated with irritable bowel syndrome (IBS) and decreased *GABRG1* expression in IBS patients.[34] Expression of serotonin receptor *HTR2B* decreases in obstructed defecation patients.[35] *Htr2b* is primarily expressed by excitatory motor neuron subtypes[15,16] and in the distal gut.[14,25] These data suggest decreased prevalence or activity of excitatory motor neurons contributes to dysmotility, while others suggest roles for inhibitory neurons. GDNF signaling is important for neuronal development[36,37] and loss of this signaling leads to intestinal obstruction in mice.[38] Initially GDNF signals through GDNF receptor alpha 1 (*Gfra1*) on nitrergic neurons and subsequently these neurons signal to non-nitrergic populations to enhance contractility.[17] For other neuropeptides involved in dysmotility the neuron populations affected are unclear. Secretoneurin is involved in gastrointestinal motility[39,40] and expressed by the majority of interganglionic enteric neurons.[41] Its precursor protein secretogranin II increases in these neurons in response to early life stress[39] and therefore may impact stress-dependent dysmotility.

Development

Genetic and omics studies investigating neuronal development are often in the context of Hirschsprung's disease. These studies could encompass their own review and here we focus instead on increased resolution of the enteric neuronal development timeline and where differential expression of developmental genes may disrupt this.

Enteric neuronal expression of canonical developmental markers like *Phox2b* and *Elavl4* are validated in omics studies.[40,42] Interestingly, while *Dlx2* is also important in neuronal development[33] and decreased in aganglionic mouse bowel[42] its expression is enriched in non-neuronal cells.[40] This suggests *Dlx2* is primarily expressed in non-neuronal cells but dependent on communication with neurons. Since the deleterious effects of *Dlx2* are studied in whole-body knockouts,[33] this intercellular communication may help regulate neuronal development.

Important expression patterns for ENS cell development and differentiation are identified by omics. At E12.5 the ENS clusters into glial progenitors, neuronal progenitors, and mixed groups.[43] Determination of neuronal type occurs in the following days, signified by the expression of canonical neuronal type markers. Excitatory neurons emerge first followed by inhibitory neurons at E14. *TAC1*$^{+}$ and *VIP*$^{+}$ neurons continue to differentiate until E16. Electrical excitability also begins to form at this point with the expression of voltage-gated sodium channel *SCN3A*.[44] Dopaminergic neurons appear later at E18.[19,20] Specific transcription factors help regulate these fates, where *Sox6* helps drive dopaminergic differentiation[20] while *SEMA3A* may regulate *TAC1*$^{+}$/*VIP*$^{+}$ neuron development.[44] Co-expression of other genetic markers suggest neuronal subtype differentiation also occurs between E 15.5 and E18. This begins with an initial binary split where one group expresses *Etv1* and contains inhibitory motor neurons and select sensory neurons/interneurons while another group expresses *Bnc2* and contains excitatory motor neurons and additional sensory neurons/interneurons. The gene expression patterns of these initial two subtype clusters remain into adulthood as *Nos1*$^{+}$*Npy*$^{+}$ inhibitory motor neurons and *Ndufa4l2*$^{+}$

excitatory motor neurons, respectively. Meanwhile other neuronal types and subtypes downregulate these markers to diversify into the other characterized enteric neuronal subtypes.[16] Taken together these data suggest that enteric neuronal subtypes are already forming as neuronal types emerge.

Neuroimmune Communication

Neuroimmune communication within the gut was initially suggested by innervation surrounding Peyer's Patches and immune cells in the lamina propria and immunostaining for neurotransmitter receptors on these cells[3,4] Omics data supports molecular mechanisms of interaction between specific neuronal types or subtypes and immune cells.. For instance, secretomotor/vasodilator neurons communicate with monocytes via chemokine *CX3CL1* to *CX3CR1*.[14] Adrenergic neurons communicate with muscularis macrophages through β2 adrenergic receptors (β2-AR) during bacterial infection and increase expression of protective and wound-healing genes such as Fizz1 (*Retnla*) and *Il10* in these cells.[45] Muscularis macrophages in turn communicate with enteric neurons using arginase 1 (Arg1) to protect them from NLRP6-inflammasome activation and cell death.[46] Together these highlight protective signaling mechanisms in enteric neuroimmune communication.

Neurons may also communicate with immune cells through opioid and cannabinoid receptors, but it is unclear if these signals would ameliorate or exacerbate inflammation as the impact of opioid and cannabinoid signaling on gut inflammation is complex.[47–49] Neurons could use enkephalins to signal opioid receptor mu 1 (*Oprm1*) on T cells and Dagla to signal cannabinoid receptor 2 (*Cnr2*) on B cells. Inhibitory motor neurons also produce interleukins IL-12 and IL-18 that may interact with T cells.[14] However these are transcriptional data and require mechanistic studies to validate and determine the role of these specified communications.

Neuronal IL-18 regulates antimicrobial activity in goblet cells[50] and therefore may play a similar role in T cells.

Specific mechanisms of communication between enteric glia and immune cells were recently reported.[51,52] Omics literature supports glial-immune interactions but provide little insight into specific pathways. In dinitrobenzene sulfonic acid (DNBS) colitis enteric glia upregulate genes in immune-related pathways including cytokine activity and antigen processing and presentation.[53] Glia treated with LPS+IFNγ also upregulate several proinflammatory cytokines, chemokines, and interleukins in cell culture[54] and rat small intestine.[55] Interestingly, glial *S100b* decreased in both models. Typically S100b release increases iNOS expression and NO production[54,55] so perhaps this is a compensatory/protective mechanism.

Dysbiosis

Omics research primarily uses 16s rRNA sequencing to correlate altered microbiome diversity with gastrointestinal disease but here we will focus on host ENS changes. Not surprisingly the microbiome alters enteric neuronal gene expression in the ileum and colon but not proximal intestinal regions.[24,25] Many genes are regulated by colonic microbes and affect ENS function. For instance, the microbiome impacts colonic motility by upregulating *Ahr* expression on enteric neurons.[24] Commensal bacteria release extracellular vesicles containing heat shock system proteins like chaperonin 60 which increase both colonic motor complex amplitude and IPAN activity,[56] suggesting roles for this communication in both motor and afferent intrinsic pathways. Microbial dysbiosis also correlates with afferent signaling in visceral hypersensitivity. Specifically taxa that produce short-chain fatty acids (SCFAs) increase in multiple inflammatory disease models.[57–59] Intrinsic enteric neurons are not considered directly involved in pain transduction pathways[4] but communication between the ENS and extrinsic sensory neurons can modulate pain perception.[53] SCFAs increase expression of enteric glial GFAP and nerve growth

factor (NGF), where NGF contributes to visceral hypersensitivity.[60] Taken together these data suggest that microbial regulation of visceral pain may involve enteric glial NGF.

Microbial dysbiosis likely impacts motor neuron development. Mice that receive antibiotics at PN10 have increased colonic motility corresponding with increased cholinergic neurons and decreased nitrergic neurons while antibiotic-treated 6-week old or adult mice had the opposite results.[61–63] While these findings suggest age-dependent relationships between enteric neurons and microbiota, these groups also received different antibiotics and this may also explain these results. Commensal microbiota also regulate the survival of specific intestinofugal neurons (IFANs) by preventing inflammasome-dependent cell death.[25] These IFANs express the marker cocaine- and amphetamine-regulated transcript (*Cartpt*) and help regulate blood glucose levels through communication with the liver and pancreas. Conversely enteric neurons prevent infection by pathogenic bacteria. Neuronal IL-18 promotes goblet cell production of antimicrobial peptides and subsequently prevents invasion of the pathogenic species *Salmonella* typhimurium.[50] Together these data highlight signaling mechanisms between enteric neurons and gut bacteria that help regulate homeostasis and prevent infection.

Dysbiosis is also associated with disease pathogenesis and/or disease markers, particularly in IBS. While taxonomic changes of the microbiome in IBS are subtle these bacteria alter host serum metabolites,[64] likely reflecting altered bacterial metabolites as well. This metabolic disturbance contributes to enteric neuron dysfunction and dysmotility in IBS. For instance, mice that receive fecal transplants from IBS-D patients recapitulate decreased colonic transit times despite little change in microbial composition.[64] Additionally SCFAs can regulate colonic motility through the monocarboxylate transporter 2 (MCT2), where mutations in the gene for MCT2 ligand delphilin (*GRID2IP*) confer IBS disease risk.[65] This similarly suggests disturbances in microbial metabolites may be key in IBS dysmotility though functional studies are required to validate this connection.

ENS Expression of Gastrointestinal Disease Markers

Many previously identified disease markers and risk genes are enriched in enteric neurons compared to other colonic cell types. In Hirschsprung disease (HSCR) this includes *RET, PHOX2B, GFRA1,* and *ECE1*.[14] Since *Gfra1* is preferentially expressed in nNOS$^+$ inhibitory neurons[14,16,17] this may reflect specific pathology in these neuronal subtypes. Many canonical HSCR-related genes are also downregulated in patients with obstructed defecation (including *RET, PHOX2B,* and *GFRA1*).[35] Since these genes are important in enteric neuronal development[40,42,43] this indicates that for at least a subset of patients obstructive defecation is a developmental disorder. Meanwhile ENS expression of Parkinson's disease (PD) risk genes supports neurodegenerative processes that may preferentially affect certain neuronal subtypes. PD risk genes *DLG2, SNCA*, and *SCN3* are enriched across most neuron subtypes in humans but murine *Lrrk2* is more highly expressed in inhibitory motor neuron and secretomotor/vasodilator neuron subtypes. *Lrrk2* expression in enteric neurons also increases with age.[14] LRRK2 dysfunction in the brain contributes to neuroinflammation and subsequent neuronal death in late-onset PD.[66] Similar mechanisms may occur in the GI tract and preferentially target certain neuronal subtypes to produce symptoms. However, whether these are species differences or LRRK2 functions similarly in the ENS is unclear.

The effects of Autism spectrum disorder (ASD) risk genes in the ENS may also reflect CNS pathology. Enteric neurons enrich for genes expressed in the CNS like GABA receptor *GABRB3* and adhesion molecules *DSCAM* and neuroligin-3 (*NLGN3*).[14,67] The effects of this ASD *NLGN3* mutant in the brain recapitulate in the ENS, where enteric neurons have increased GABA-A sensitivity and subsequently shortened intestinal transit time.[67] ASD may also involve enteric glial pathology as glia enrich for risk genes *NRXN1* and *ANK2* compared to other intestinal cell types[14] but the effect of this on gastrointestinal dysfunction in ASD is unknown. *Ank2* is also enriched in a specific glial subtype in mice[14] and perhaps this glial subtype contributes to disease.

Glia are also implicated in inflammatory bowel disease (IBD). Mutations in the prostaglandin receptor EP4 (*PTGER4*) confer risk in IBD[68–70] and *Ptger4* is expressed in enteric glia.[53] Enteric glial *Ptger4* decreases with DNBS colitis but increases if the tachykinin receptor NK2R is blocked, indicating that communication between $NK2R^+$ enteric neurons and/or extrinsic afferents and enteric glia may play a role. A mutation in *LSAMP* is associated with IBD risk in African Americans.[69] *Lsamp* is also expressed in murine enteric glia and decreases in DNBS colitis.[14,53] Furthermore *Lsamp* is preferentially enriched in glial subtypes.[14] Taken together these data suggest certain enteric glial subtypes may play a role in ASD and IBD but follow-up investigation is required to validate this.

Novel disease biomarkers are also suggested by omics research and may serve to further classify and identify patients. A mutation in lncRNA NONHSAG044354 is associated with IBD risk and may regulate *BACH2* expression in the transverse colon.[71] *BACH2* is enriched in enteric neurons and most highly expressed in excitatory motor neuron subtypes.[14] Perhaps *BACH2* expression in these neurons is altered by lncRNAs in certain IBD patients and differential expression of either this lncRNA or BACH2 may confer disease risk. IBS patient may also be diagnosed by co-expression of biomarkers, where expression of elastase 3a, cathepsin L, and proteasome alpha subunit-4 effectively distinguishes IBS supernatants from healthy controls.[72] Furthermore, elastase 3a from IBS patients activates enteric neurons, suggesting this may not only be a potential biomarker of IBS but also involved in enteric neuronal dysfunction.

CONCLUSIONS

ScRNA-seq identifies several novel putative markers of ENS cell subtypes, many of which are congruent among multiple studies and suggest distinct neuronal and glial populations (**Figure 1.1** and **Table 1.2** and similarly assessed by Wright et al.[17]). These data expand our understanding of ENS cellular heterogeneity and highlight further complexity in enteric neuron and glial classification. Meanwhile, other omics methods supplement these findings by elucidating

ENS cell type- and subtype-specific roles in physiology and disease. Together these findings demonstrate the ability of omics data to identify novel molecules and pathways in the ENS.

Current omics methods can generate data in a relatively unbiased manner. Combining this potential for novelty with the ever-increasing power and sensitivity of omics technology make omics an ideal methodology for exploring complex and multi-modal questions. These characteristics also make omics data exponential hypothesis-generating tools that will promote scientific advancement for years beyond their creation. This is demonstrated by the sheer number of downloads, citations, and re-analyses of recent omics publications.[73]

However, some of these same characteristics also present current challenges in omics methods. Because of the sheer amount of data created in any given experiment it can be difficult to synergize and make overall sense of collective findings. This is especially the case when accessing data through publications as opposed to datasets. In most cases it may be better to access the data directly, but this can prove challenging without bioinformatics expertise. We hope that as omics data continues to grow, means of improving accessibility will improve in tandem. These include meta-analyses and standardized means of accessing, searching, and representing omics data. The latter includes websites like the Single Cell Portal by the Broad Institute for scRNA-seq data, among others.[74] We hope these sites continue to grow in popularity for both depositing and accessing data.

Another challenge in omics is that it easily generates comparative data but requires specific experimental design to provide causative data. This historically made understanding expressional changes in the ENS challenging as it meant correlating tissue-level differential expression with genes known to have ENS expression without actually knowing if this change occurred in ENS cells. Thankfully newer omics technologies allow ENS-specific sequencing, where techniques like scRNA-seq clearly demonstrate their ability to identify enteric neurons and glia out of many other cell types. As these modalities continue to grow future research may integrate single cell techniques for multiple biomolecules together to provide a better mechanistic

picture.[1] Future research may also resolve whether some ENS cell clusters are distinct cell populations or temporal expression patterns responding to the current microenvironment. Given the rate omics technology improves and ENS omics research is recently published, it is only a matter of time until our understanding of the ENS genetic architecture deepens once again.

SUMMARY AND AIMS OF DISSERTATION

High-throughput 'omics' technologies have greatly contributed our knowledge of complex enteric neuronal mechanisms and their perturbations in disease. However these techniques are underutilized to study enteric glia and represent an ideal method for characterizing complex molecular patterns within enteric glia and how these are altered in relevant multimodal disease pathways. The objective of this dissertation is to develop and utilize genetic technologies to characterize enteric glial responses to environmental mediators. Chapter two describes how we adapted high-throughput and *in situ* genetic technologies for use in the enteric nervous system and specifically for studying enteric glia. Chapter three utilizes these techniques to investigate sex-specific gene expression patterns and key responses to early life stress in enteric glia. Chapter four investigates mechanisms of enteric glial and gut microbe communication through stimulator of interferon genes (STING) signaling and type I interferon responses. Finally chapter five discusses the contribution of these findings to our understanding of complex glial-environmental interactions and future directions for understanding patterns of enteric glial and enteric neuronal communication to determine targeted key interactions determined by sex and early life stress. The work in this dissertation further characterizes the molecular patterns used by enteric glia in response to complex environmental factors and highlights unique heterogeneity in glial intercellular communication in addition to providing the scientific community with valuable resources for understanding genetic expression patterns within the ENS.

REFERENCES

REFERENCES

1. Shapiro E, Biezuner T, Linnarsson S. Single-cell sequencing-based technologies will revolutionize whole-organism science. *Nat Rev Genet*. 2013;14(9):618-630. doi:10.1038/nrg3542

2. Furness JB. The enteric nervous system and neurogastroenterology. *Nat Rev Gastroenterol Hepatol*. 2012;9(5):286-294. doi:10.1038/nrgastro.2012.32

3. Furness J. Types of neurons in the enteric nervous system. *J Auton Nerv Syst*. 2000;81(1-3):87-96. doi:10.1016/S0165-1838(00)00127-2

4. Furness JB. *The Enteric Nervous System*. (Furness JB, ed.). Malden, Massachusetts, USA: Blackwell Publishing; 2006. doi:10.1002/9780470988756

5. Gulbransen BD, Sharkey KA. Novel functional roles for enteric glia in the gastrointestinal tract. *Nat Rev Gastroenterol Hepatol*. 2012;9(11):625-632. doi:10.1038/nrgastro.2012.138

6. Dogiel AS. Zur Frage über den feineren Bau der Herzganglien des Menschen und der Säugethiere. *Arch für Mikroskopische Anat*. 1898;53(1):237-281. doi:10.1007/BF02976730

7. Nishi S, North RA. Intracellular recording from the myenteric plexus of the guinea-pig ileum. *J Physiol*. 1973;231(3):471-491. doi:10.1113/jphysiol.1973.sp010244

8. Hirst GDS, McKirdy HC. A nervous mechanism for descending inhibition in guinea-pig small intestine. *J Physiol*. 1974;238(1):129-143. doi:10.1113/jphysiol.1974.sp010514

9. Seguella L, Gulbransen BD. Enteric glial biology, intercellular signalling and roles in gastrointestinal disease. *Nat Rev Gastroenterol Hepatol*. March 2021. doi:10.1038/s41575-021-00423-7

10. Boesmans W, Lasrado R, Vanden Berghe P, Pachnis V. Heterogeneity and phenotypic plasticity of glial cells in the mammalian enteric nervous system. *Glia*. 2015;63(2):229-241. doi:10.1002/glia.22746

11. Rao M, Nelms BD, Dong L, et al. Enteric glia express proteolipid protein 1 and are a transcriptionally unique population of glia in the mammalian nervous system. *Glia*. 2015;63(11):2040-2057. doi:10.1002/glia.22876

12. Hasin Y, Seldin M, Lusis A. Multi-omics approaches to disease. *Genome Biol*. 2017;18(1):83. doi:10.1186/s13059-017-1215-1

13. Misra BB, Langefeld C, Olivier M, Cox LA. Integrated omics: tools, advances and future approaches. *J Mol Endocrinol*. 2019;62(1):R21-R45. doi:10.1530/JME-18-0055

14. Drokhlyansky E, Smillie CS, Van Wittenberghe N, et al. The Human and Mouse Enteric Nervous System at Single-Cell Resolution. *Cell*. September 2020:1-17. doi:10.1016/j.cell.2020.08.003

15. May-Zhang AA, Tycksen E, Southard-Smith AN, et al. Combinatorial transcriptional profiling of mouse and human enteric neurons identifies shared and disparate subtypes in situ. *Gastroenterology*. 2020;160(3):1-16. doi:10.1053/j.gastro.2020.09.032

16. Morarach K, Mikhailova A, Knoflach V, et al. Diversification of molecularly defined myenteric neuron classes revealed by single-cell RNA sequencing. *Nat Neurosci*. December 2020. doi:10.1038/s41593-020-00736-x

17. Wright CM, Schneider S, Smith-Edwards KM, et al. scRNA-sequencing reveals new enteric nervous system roles for GDNF, NRTN, and TBX3. *Cell Mol Gastroenterol Hepatol*. January 2021:140981. doi:10.1016/j.jcmgh.2020.12.014

18. Zeisel A, Hochgerner H, Lönnerberg P, et al. Molecular Architecture of the Mouse Nervous System. *Cell*. 2018;174(4):999-1014.e22. doi:10.1016/j.cell.2018.06.021

19. Li ZS, Pham TD, Tamir H, Chen JJ, Gershon MD. Enteric Dopaminergic Neurons: Definition, Developmental Lineage, and Effects of Extrinsic Denervation. *J Neurosci*. 2004;24(6):1330-1339. doi:10.1523/JNEUROSCI.3982-03.2004

20. Memic F, Knoflach V, Morarach K, et al. Transcription and Signaling Regulators in Developing Neuronal Subtypes of Mouse and Human Enteric Nervous System. *Gastroenterology*. 2018;154(3):624-636. doi:10.1053/j.gastro.2017.10.005

21. Rao M, Gershon MD. The bowel and beyond: the enteric nervous system in neurological disorders. *Nat Rev Gastroenterol Hepatol*. 2016;13(9):517-528. doi:10.1038/nrgastro.2016.107

22. Spencer NJ, Sorensen J, Travis L, Wiklendt L, Costa M, Hibberd T. Imaging activation of peptidergic spinal afferent varicosities within visceral organs using novel CGRPα-mCherry reporter mice. *Am J Physiol Liver Physiol*. 2016;311(5):G880-G894. doi:10.1152/ajpgi.00250.2016

23. Ounzain S, Micheletti R, Arnan C, et al. CARMEN, a human super enhancer-associated long noncoding RNA controlling cardiac specification, differentiation and homeostasis. *J Mol Cell Cardiol*. 2015;89:98-112. doi:10.1016/j.yjmcc.2015.09.016

24. Obata Y, Castaño Á, Boeing S, et al. Neuronal programming by microbiota regulates intestinal physiology. *Nature*. 2020;578(7794):284-289. doi:10.1038/s41586-020-1975-8

25. Muller PA, Matheis F, Schneeberger M, Kerner Z, Jové V, Mucida D. Microbiota-modulated CART + enteric neurons autonomously regulate blood glucose. *Science (80-)*. 2020;6176(August):eabd6176. doi:10.1126/science.abd6176

26. Charlton RW, Jacobs P, Torrance JD, Bothwell TH. The Role of the Intestinal Mucosa in Iron Absorption. *J Clin Invest*. 1965;44(4):543-554. doi:10.1172/JCI105167

27. Xu W, Guo Y, Huang Z, et al. Small heat shock protein CRYAB inhibits intestinal mucosal inflammatory responses and protects barrier integrity through suppressing IKKβ activity. *Mucosal Immunol*. 2019;12(6):1291-1303. doi:10.1038/s41385-019-0198-5

28. Mirsky R, Jessen KR, Schachner M, Goridis C. Distribution of the adhesion molecules N-CAM and L1 on peripheral neurons and glia in adult rats. *J Neurocytol*. 1986;15(6):799-

815. doi:10.1007/BF01625196

29. Valihrach L, Androvic P, Kubista M. Platforms for Single-Cell Collection and Analysis. *Int J Mol Sci*. 2018;19(3):807. doi:10.3390/ijms19030807

30. Lau ST, Li Z, Pui-Ling Lai F, et al. Activation of Hedgehog Signaling Promotes Development of Mouse and Human Enteric Neural Crest Cells, Based on Single-Cell Transcriptome Analyses. *Gastroenterology*. 2019;157(6):1556-1571.e5. doi:10.1053/j.gastro.2019.08.019

31. Strand AD, Aragaki AK, Baquet ZC, et al. Conservation of Regional Gene Expression in Mouse and Human Brain. Flint J, ed. *PLoS Genet*. 2007;3(4):e59. doi:10.1371/journal.pgen.0030059

32. Bonora E, Bianco F, Cordeddu L, et al. Mutations in RAD21 disrupt regulation of apob in patients with chronic intestinal pseudo-obstruction. *Gastroenterology*. 2015;148(4):771-782.e11. doi:10.1053/j.gastro.2014.12.034

33. Wright CM, Garifallou JP, Schneider S, et al. Dlx1/2 mice have abnormal enteric nervous system function. *JCI Insight*. 2020;5(4). doi:10.1172/jci.insight.131494

34. Videlock EJ, Mahurkar-Joshi S, Hoffman JM, et al. Sigmoid colon mucosal gene expression supports alterations of neuronal signaling in irritable bowel syndrome with constipation. *Am J Physiol Liver Physiol*. 2018;315(1):G140-G157. doi:10.1152/ajpgi.00288.2017

35. Kim M, Rosenbaum C, Schlegel N, et al. Obstructed defecation—an enteric neuropathy? An exploratory study of patient samples. *Int J Colorectal Dis*. September 2018:10-13. doi:10.1007/s00384-018-3160-1

36. Gianino S, Grider JR, Cresswell J, Enomoto H, Heuckeroth RO. GDNF availability determines enteric neuron number by controlling precursor proliferation. *Development*. 2003;130(10):2187-2198. doi:10.1242/dev.00433

37. Soret R, Schneider S, Bernas G, et al. Glial Cell-Derived Neurotrophic Factor Induces Enteric Neurogenesis and Improves Colon Structure and Function in Mouse Models of Hirschsprung Disease. *Gastroenterology*. 2020;159(5):1824-1838.e17. doi:10.1053/j.gastro.2020.07.018

38. Shen L, Pichel JG, Mayeli T, Sariola H, Lu B, Westphal H. Gdnf Haploinsufficiency Causes Hirschsprung-Like Intestinal Obstruction and Early-Onset Lethality in Mice. *Am J Hum Genet*. 2002;70(2):435-447. doi:10.1086/338712

39. Lopes L V., Marvin-Guy LF, Fuerholz A, et al. Maternal deprivation affects the neuromuscular protein profile of the rat colon in response to an acute stressor later in life. *J Proteomics*. 2008;71(1):80-88. doi:10.1016/j.jprot.2008.01.007

40. Roy-Carson S, Natukunda K, Chou H chao, et al. Defining the transcriptomic landscape of the developing enteric nervous system and its cellular environment. *BMC Genomics*. 2017;18(1):1-24. doi:10.1186/s12864-017-3653-2

41. Schürmann G, Bishop AE, Facer P, et al. Secretoneurin: A new peptide in the human

enteric nervous system. *Histochem Cell Biol*. 1995;104(1):11-19. doi:10.1007/BF01464781

42. Vohra BPS, Tsuji K, Nagashimada M, et al. Differential gene expression and functional analysis implicate novel mechanisms in enteric nervous system precursor migration and neuritogenesis. *Dev Biol*. 2006;298(1):259-271. doi:10.1016/j.ydbio.2006.06.033

43. Lasrado R, Boesmans W, Kleinjung J, et al. Lineage-dependent spatial and functional organization of the mammalian enteric nervous system. *Science (80-)*. 2017;356(6339):722-726. doi:10.1126/science.aam7511

44. McCann CJ, Alves MM, Brosens E, et al. Neuronal Development and Onset of Electrical Activity in the Human Enteric Nervous System. *Gastroenterology*. 2019;156(5):1483-1495.e6. doi:10.1053/j.gastro.2018.12.020

45. Gabanyi I, Muller PA, Feighery L, Oliveira TY, Costa-Pinto FA, Mucida D. Neuro-immune Interactions Drive Tissue Programming in Intestinal Macrophages. *Cell*. 2016;164(3):378-391. doi:10.1016/j.cell.2015.12.023

46. Matheis F, Muller PA, Graves CL, et al. Adrenergic Signaling in Muscularis Macrophages Limits Infection-Induced Neuronal Loss. *Cell*. 2020;180(1):64-78.e16. doi:10.1016/j.cell.2019.12.002

47. DiPatrizio N V. Endocannabinoids in the Gut. *Cannabis Cannabinoid Res*. 2016;1(1):67-77. doi:10.1089/can.2016.0001

48. Kienzl M, Storr M, Schicho R. Cannabinoids and Opioids in the Treatment of Inflammatory Bowel Diseases. *Clin Transl Gastroenterol*. 2020;11(1):e00120. doi:10.14309/ctg.0000000000000120

49. Sharma U, Olson RK, Erhart FN, et al. Prescription Opioids induce Gut Dysbiosis and Exacerbate Colitis in a Murine Model of Inflammatory Bowel Disease. *J Crohn's Colitis*. 2020;14(6):801-817. doi:10.1093/ecco-jcc/jjz188

50. Jarret A, Jackson R, Duizer C, et al. Enteric Nervous System-Derived IL-18 Orchestrates Mucosal Barrier Immunity. *Cell*. 2020;180(1):50-63.e12. doi:10.1016/j.cell.2019.12.016

51. Grubišić V, McClain JL, Fried DE, et al. Enteric Glia Modulate Macrophage Phenotype and Visceral Sensitivity following Inflammation. *Cell Rep*. 2020;32(10):108100. doi:10.1016/j.celrep.2020.108100

52. Chow AK, Grubišić V, Gulbransen BD. Enteric Glia Regulate Lymphocyte Activation via Autophagy-Mediated MHC-II Expression. *Cell Mol Gastroenterol Hepatol*. June 2021. doi:10.1016/j.jcmgh.2021.06.008

53. Delvalle NM, Dharshika C, Morales-Soto W, Fried DE, Gaudette L, Gulbransen BD. Communication Between Enteric Neurons, Glia, and Nociceptors Underlies the Effects of Tachykinins on Neuroinflammation. *Cell Mol Gastroenterol Hepatol*. 2018;6(3):321-344. doi:10.1016/j.jcmgh.2018.05.009

54. Liñán-Rico A, Turco F, Ochoa-Cortes F, et al. Molecular Signaling and Dysfunction of the Human Reactive Enteric Glial Cell Phenotype. *Inflamm Bowel Dis*. 2016;22(8):1812-

1834. doi:10.1097/MIB.0000000000000854

55. Rosenbaum C, Schick MA, Wollborn J, et al. Activation of myenteric glia during acute inflammation in vitro and in vivo. *PLoS One*. 2016;11(3):1-20. doi:10.1371/journal.pone.0151335

56. Al-Nedawi K, Mian MF, Hossain N, et al. Gut commensal microvesicles reproduce parent bacterial signals to host immune and enteric nervous systems. *FASEB J*. 2015;29(2):684-695. doi:10.1096/fj.14-259721

57. Esquerre N, Basso L, Defaye M, et al. Colitis-Induced Microbial Perturbation Promotes Postinflammatory Visceral Hypersensitivity. *Cmgh*. 2020;10(2):225-244. doi:10.1016/j.jcmgh.2020.04.003

58. Zhou XY, Li M, Li X, et al. Visceral hypersensitive rats share common dysbiosis features with irritable bowel syndrome patients. *World J Gastroenterol*. 2016;22(22):5211-5227. doi:10.3748/wjg.v22.i22.5211

59. De Palma G, Blennerhassett P, Lu J, et al. Microbiota and host determinants of behavioural phenotype in maternally separated mice. *Nat Commun*. 2015;6. doi:10.1038/ncomms8735

60. Long X, Li M, Li L-X, et al. Butyrate promotes visceral hypersensitivity in an IBS-like model via enteric glial cell-derived nerve growth factor. *Neurogastroenterol Motil*. 2018;30(4):e13227. doi:10.1111/nmo.13227

61. Hung LY, Boonma P, Unterweger P, et al. Neonatal Antibiotics Disrupt Motility and Enteric Neural Circuits in Mouse Colon. *Cell Mol Gastroenterol Hepatol*. 2019;8(2):298-300.e6. doi:10.1016/j.jcmgh.2019.04.009

62. Hung LY, Parathan P, Boonma P, et al. Antibiotic exposure postweaning disrupts the neurochemistry and function of enteric neurons mediating colonic motor activity. *Am J Physiol Liver Physiol*. 2020;318(6):G1042-G1053. doi:10.1152/ajpgi.00088.2020

63. Yarandi SS, Kulkarni S, Saha M, Sylvia KE, Sears CL, Pasricha PJ. Intestinal Bacteria Maintain Adult Enteric Nervous System and Nitrergic Neurons via Toll-like Receptor 2-induced Neurogenesis in Mice. *Gastroenterology*. 2020;159(1):200-213.e8. doi:10.1053/j.gastro.2020.03.050

64. De Palma G, Lynch MDJ, Lu J, et al. Transplantation of fecal microbiota from patients with irritable bowel syndrome alters gut function and behavior in recipient mice. *Sci Transl Med*. 2017;9(379):eaaf6397. doi:10.1126/scitranslmed.aaf6397

65. Ek WE, Reznichenko A, Ripke S, et al. Exploring the genetics of irritable bowel syndrome: a GWA study in the general population and replication in multinational case-control cohorts. *Gut*. 2015;64(11):1774-1782. doi:10.1136/gutjnl-2014-307997

66. Rui Q, Ni H, Li D, Gao R, Chen G. The Role of LRRK2 in Neurodegeneration of Parkinson Disease. *Curr Neuropharmacol*. 2018;16(9):1348-1357. doi:10.2174/1570159X16666180222165418

67. Hosie S, Ellis M, Swaminathan M, et al. Gastrointestinal dysfunction in patients and mice

expressing the autism-associated R451C mutation in neuroligin-3. *Autism Res*. 2019;12(7):1043-1056. doi:10.1002/aur.2127

68. Barrett JC, Hansoul S, Nicolae DL, et al. Genome-wide association defines more than 30 distinct susceptibility loci for Crohn's disease. *Nat Genet*. 2008;40(8):955-962. doi:10.1038/ng.175

69. Brant SR, Okou DT, Simpson CL, et al. Genome-Wide Association Study Identifies African-Specific Susceptibility Loci in African Americans With Inflammatory Bowel Disease. *Gastroenterology*. 2017;152(1):206-217.e2. doi:10.1053/j.gastro.2016.09.032

70. Rioux JD, Xavier RJ, Taylor KD, et al. Genome-wide association study identifies new susceptibility loci for Crohn disease and implicates autophagy in disease pathogenesis. *Nat Genet*. 2007;39(5):596-604. doi:10.1038/ng2032

71. Mirza AH, Kaur S, Brorsson CA, Pociot F. Effects of GWAS-associated genetic variants on lncRNAs within IBD and T1D candidate loci. *PLoS One*. 2014;9(8). doi:10.1371/journal.pone.0105723

72. Buhner S, Hahne H, Hartwig K, et al. Protease signaling through protease activated receptor 1 mediate nerve activation by mucosal supernatants from irritable bowel syndrome but not from ulcerative colitis patients. *PLoS One*. 2018;13(3):1-16. doi:10.1371/journal.pone.0193943

73. Perez-Riverol Y, Zorin A, Dass G, et al. Quantifying the impact of public omics data. *Nat Commun*. 2019;10(1):3512. doi:10.1038/s41467-019-11461-w

74. Srivastava D, Iyer A, Kumar V, Sengupta D. CellAtlasSearch: A scalable search engine for single cells. *Nucleic Acids Res*. 2018;46(W1):W141-W147. doi:10.1093/nar/gky421

CHAPTER TWO: ADAPTING GENETIC TECHNIQUES TO STUDY THE ENTERIC NERVOUS SYSTEM

ABSTRACT

The enteric nervous system is comprised on neurons and glia that regulate gastrointestinal functions including motility. Specialized genetic tools such as RiboTag RNA-sequencing allow investigators to capture cell-specific expression signatures from enteric neurons and glia in a multitude of complex physiologic and disease states. These data provide invaluable resources for understanding mechanisms of cellular communication and are supplemented by methods of visualizing gene expression *in situ* such as RNAscope. These genetic tools have been used by few researchers to study enteric neurons and already demonstrate their usefulness in highlighting novel biological patterns. The use of these methods by a larger community could provide exponential molecular insights about enteric nervous system function and particularly enteric glia that are relatively understudied. In this technical review we describe detailed methods for using RiboTag RNA-sequencing and RNAscope in the myenteric plexus of the enteric nervous system to study gene expression of enteric neurons and enteric glia. We supplement these detailed protocols with diagrams and representative data and discuss additional considerations for troubleshooting and optimizing these techniques. These methods are relatively simple and inexpensive to perform and we hope this information serves to further genetic research of the enteric nervous system and enteric glia that will provide further data and subsequent molecular insights by the scientific community.

INTRODUCTION

The enteric nervous system (ENS) consists of neurons and glia that contribute to essential gastrointestinal (GI) functions including motility, visceral sensation, secretion, absorption, neuroimmune communication, and permeability.[1,2] The ENS is comprised of two layers, the submucosal and myenteric plexus, which are nested within the connective tissue under the mucosa and between the intestinal muscle layers respectively (**Fig 2.1b**).[3] Enteric glia were historically believed to simply provide structural and metabolic support for enteric neurons. However there is continuously growing evidence supporting critical roles for enteric glia in regulating canonical functions of the ENS through communication with both enteric neurons and other cells types within the GI tract.[4–7] While many important mechanisms enteric glia utilize to regulate these functions in health and disease have been explored[8–19] there is still relatively little known about the molecular mediators utilized by enteric glia to modulate gut function. High-throughput "omics" research can efficiently gather molecular data on a large and comprehensive scale and therefore is highly appropriate for contributing novel information to our understanding of enteric glia.[20,21] Specialized "omics" tools have already begun to revolutionize our understanding of enteric neuronal genetic architecture in homeostatic and pathologic roles and additionally provided gene expression databases invaluable for future research directions and mechanistic insights.[22–26] However these types of studies rarely focus on enteric glia and as such there are relatively few enteric glial omics databases to date.[11,22,25,27] These resources are critical for advancing our knowledge of enteric glia and subsequently the ENS and therefore effective methods of generating these data are needed. One such method is the RiboTag model that uses a genetically encoded hemagglutinin (HA) tag to immunoprecipitate ribosomes from specific cells for downstream RNA-sequencing analysis.[28,29] Because this method is performed *in vivo* it is effective for understanding complex systems and/or disease models and applying this method in the ENS would be invaluable for generating relevant enteric glial omics data.

It is equally important to understand any generated omics data in biological context and this begins with validating expression *in situ*. Robust visualization tools are essential for this in the ENS as enteric neurons and glia are highly interconnected both mechanistically and physically[3,5] and therefore present unique challenges to teasing apart cell-specific information such as biomolecule localization. Immunolabeling is often useful for *in situ* visualization but can be difficult to interpret when localization is not distinct and proteins are expressed in enteric neuronal or glial cellular processes that are highly overlapped. RNAscope is an emerging tool for *in situ* visualization that has provided molecular validation in many cells across biological systems.[22,24,30–34] While typically for use in micro-sectioned tissue on slides or cell culture RNAscope has been adapted for specialized use in other tissues where these modalities would not be appropriate.[35–37] The ENS is difficult to visualize effectively on slides given its planar orientation (**Fig 2.1b**) and additionally challenging to study accurately and stably in culture.[5,38] Whole mount preparations are ideal for maintaining proper orientation and physiologic relevance of enteric neurons and glia.[39] Thus the ability to utilize RNAscope in whole mount tissue of the ENS is an important tool for placing genetic data in situationally-relevant context.

In the protocols section we provide specialized adaptations of RiboTag RNA-sequencing and RNAscope for effectively studying the ENS and enteric glia. We utilize simple methods to overcome the unique challenges of working with genetic material in the ENS that are relatively inexpensive and straightforward to use. Supplemental diagrams and example data for these protocols are presented in representative results. Finally in the considerations section we discuss additional challenges and our recommended solutions with relevant data such that these adaptations can be easily transferred to other similar conditions.

PROTOCOLS

RiboTag RNA-sequencing in the ENS

Dissecting the myenteric plexus for RNA

Typical dissections for functional analyses of whole-mount myenteric plexus involve cutting open the intestine alone the mesenteric border, pinning out the tissue flat either luminal- or serosal-side up, and removing the uppermost muscle layer to expose the myenteric plexus.[15] This is a time-consuming and delicate process that is used to produce small tissue preparations (approx. 0.5cmx0.5cm) at a time in order to preserve ganglionic morphology. While important for physiological studies harvesting tissue for RNA must be more expedient to preserve RNA integrity. Furthermore one challenge of RiboTag is relatively low RNA yield and therefore it is necessary to harvest as much myenteric tissue as possible in this time frame. To achieve this we adapted a dissection for ENS cell primary culture[40] that utilizes a plastic or glass rod with a tapered end. A diagram of our set-up for this dissection is represented in **Fig 2.1c**. The procedure for myenteric plexus rod dissection for RNA is as follows:

1. Nest a Sylgard-coated petri dish with insect pins (0.2mm diameter) that can fit the length of the dissection rod inside a larger dish. Fill this dish with dry ice and then dH_2O. See **Fig 2.1c** for details.
2. Fill the inner petri dish with cell culture media such as Dulbecco's Modified Eagle Medium (DMEM/F-12).
3. Euthanize the mouse in accordance with institutional protocols and remove the intestinal segment of interest. While not necessary, flushing luminal contents before placing tissue in the dissection dish will help keep cell media clear during dissection. Transfer intestinal tube to the petri dish surrounded by dry ice.
4. Under a dissection scope use forceps to gently stretch the intestinal tube around the dissection rod. Make sure the dissection rod was previously submerged in cell culture medium and not dry when doing this.

a. The appropriate size of this dissection rod is dependent on the age of mice used and the intestinal portion being harvested. For harvesting colon from 10-20 week-old mice a 3.2mm diameter rod is appropriate. Once mounted on the rod tissue should be taut enough that it will easily separate with minimal force (see step 9) but not so taut that this force causes mucosal tears.

5. Place the insect pins around both ends of the rod where there is no intestinal tissue. These should be close enough to the rod such that it does not move too much but not so close the rod cannot rotate.
6. Pull the mesentery gently with forceps until its connection with the intestine is visible. This is easily achieved by pulling towards the investigator and letting the rod rest against the forward insect pins. Cut away the mesentery from one side to the other using microdissection scissors.
7. Run the flat edge of angled forceps parallel against the mesenteric border to further loosen the connection. This should be done gently so as to preserve underlying additional circular muscle (see **Fig 2.1b** for orientation).
8. Using two cotton swabs gently begin to tease the myenteric plexus (and some surrounding longitudinal and circular muscle) away from the dissection rod and rest of the tissue. Position the mesenteric border opening upward. Use one cotton swab to stabilize the dissection rod against the insect pins and keep the intestinal tissue from rolling by gently pressing against the side of the intestine and rod.
9. Starting on either end of the intestine, with the other cotton swab gently swipe against the mesenteric opening parallel to the dish surface in the opposite direction of the applied stabilizing pressure. For instance, if stabilizing the intestine and rod by situating the first cotton swab on the side of the rod closest to the investigator, swipe with the second cotton swab in an away direction.

10. Continue this motion across the mesenteric opening until the other side of the intestine is reached. The stabilizing cotton swab may need to move in tandem with the dissecting swab in order to maintain appropriate tension in tissue to easily separate the myenteric plexus.
11. Once the myenteric plexus has been separate along the entire intestinal length rotate the rod so the new connection point is facing upward. For instance if following the positioning recommended in step 9, rotate the rod toward the investigator.
12. Repeat steps 9-11 until the full circumference of the myenteric plexus has been removed. Tissue can now be quickly placed in a labeled tube and snap-frozen in dry ice.
13. With practice this dissection should only take ~10mins. Most cell culture media will begin to freeze along the circumference of the petri dish as the dry ice solution is very cold and this may hinder turning the dissection rod. However this is only noted when media is in the dish for much longer time periods (over 30mins).

Homogenizing flash frozen tissue

While typical RiboTag methods utilize Dounce homogenization[28,41] prior to beginning the RiboTag procedure this is ineffective for colonic myenteric plexus and more aggressive methods are necessary. We utilized both a rotor-stator homogenizer and the CryoGrinder™ (OPS Diagnostics, Lebanon, NJ) mortar and pestle. While we were able to produce viable RNA for RNA-sequencing using both methods we had better overall results using the CryoGrinder™, with less variable RNA yield (**Fig 2.1d**, *left*) and higher RNA quality as measured by RNA integrity number/RIN ($P < 0.0001$; **Fig2.1d**, *right*). The increased effectiveness of the CryoGrinder™ is likely due to being designed for small amounts of tissue (<100mg) and ability to be submerged in liquid nitrogen to prevent RNAse activity. Furthermore there are supplementary products to assist in larger-scale batch sample processing. We utilized the CryoGrinder™ according the manufacturer's specifications. Briefly:

1. Wash the mortar and pestle with an RNAse removing detergent and rinse with RNase free water and/or dry heat sterilize at 200°C for 2h. Make sure the mortar and pestle are dry before use.
2. Keep mortar submerged in in liquid nitrogen in an appropriate cooler. The liquid nitrogen level should not be high enough that it leaks into the sample chamber. Keep the pestle in an RNase-free container submerged in liquid nitrogen as well, again ensuring the pestle head is not contaminated with liquid nitrogen.
3. Using RNase-free forceps remove flash frozen myenteric tissue from sample vial and place it in the mortar's sample chamber. Attach the pestle handle to the motorized handle (either the one sold with the kit or an automated screwdriver motor will provide appropriate RPMs) and grind the sample for 15-20s in one direction. Repeat in the opposite direction for additional sets of 15-20s if necessary. When sample is reduced to a fine white powder homogenization is sufficient.
4. Using an RNase-free spatula scrape sample powder into a RNase-free tube. Add the appropriate volume of supplemented homogenization buffer (see RiboTag protocols[28,29]) and pipet mix the sample into the buffer immediately.
5. Follow this with the RiboTag procedure. We will not discuss this here as it follows the indirect protocol supplied by the RiboTag creators[29] with minor alterations to the concentrations used in the supplemented homogenization buffer (as described in our prior RiboTag publication[11]) that are as follows: 20µL protease inhibitor (Sigma P8340), 10µL RNAse inhibitor (40U/µL), and 3mg/mL heparin.

RNAscope in the ENS *in situ*

Whole mount preparations of the ENS are preferred over longitudinal or cross-sectional cuts of the intestine. Whole mounts allow planar views of the largest dimension of ENS ganglia

whereas other orientations display only a very thin dimension of these sheet-like layers (**Fig 2.1b**). However slide thickness recommendations for RNAscope by the manufacturer (ACD Biosciences, Newark, CA) are 8-12μm can be upwards of 100μm in thickness in order to maintain enough surrounding musculature to support the ENS and preserve ganglionic morphology. Therefore standard RNAscope protocols do not readily work in whole mount myenteric plexus preparations and several adaptations are made in order to produce specific signaling. While others have utilized RNAscope in whole mount intestine previously[37] their particular protocol did not produce the best results for our tissue. This is perhaps due to differences in RNAscope kits where the previous investigators used the Fluorescent Multiplex Kit (ACD Biosciences, cat no. 320850) while we used the RED 2.5 HD Kit (ACD Biosciences, cat no. 322350). Regardless we used this protocol as a starting point that was tweaked to optimize for our tissue. This protocol works effectively in adult colonic tissue and can be followed with immunohistochemistry to co-label proteins.

Dissecting the myenteric plexus for RNA

Best results require removing as much muscle as possible from the myenteric plexus as these contribute to background in both the RNAscope channel and potentially in antibody channels if immunohistochemistry is performed afterward. Furthermore layers with higher connective tissue such as the submucosal plexus and serosa can display fibrous staining patterns that make interpreting results more difficult. Therefore we recommend using microdissection to remove the mucosa, submucosa, and as much circular muscle as possible in addition to the serosa and longitudinal muscle. This is accomplished by performing a longitudinal muscle-myenteric plexus dissection similar to previously described[15] and then flipping over the tissue gently remove the serosa and longitudinal muscle similar to the circular muscle-myenteric preparation previously described.[15] However rod dissections like those described for RNA-sequencing above are also satisfactory in for larger-scale processing if the target gene is highly

expressed (**Fig 2.5b**) and/or highly specific antibodies are used in conjunction. In this case tissue is pinned out and fixed after dissection 4% paraformaldehyde overnight (16-20h) at 4°C. These may be more difficult to use for certain targets as these preparations tend to have higher background in the RNAscope and immunohistochemistry channels.

1. Euthanize the mouse in accordance with institutional protocols and remove the colon. Luminal contents can be flushed with a syringe but is not necessary.
2. Transfer colon to a Sylgard-coated petri dish with insect pins (0.2mm diameter) containing ice-cold cell culture media such as DMEM/F-12.
    a. Since it is important to maintain RNA integrity here just as in our RNA-sequencing RiboTag dissection a similar schema utilized to keep cell culture media very cold can be used here by nesting the petri dish in a larger tray of dry ice and dH_2O (**Fig 2.1c**).
3. Pin the colon at the oral and aboral ends taughtly with the mesentery facing up. At this point the mesenteric can be cut away with microdissection scissors but this is not necessary.
4. Cut along the mesenteric border using microdissection scissors. Stretch and pin the colon taut and flat with the mucosa facing upwards with insect pins.
5. Fix tissue in 4% paraformaldehyde overnight (16-20h) at 4°C.
6. Rinse tissue 3x10mins on an orbital shaker with 1x phosphate buffered saline (1x PBS) at 20°C. Tissue can be stored in 1xPBS at 4°C until dissection. While we have not tested exactly how long RNA signal is preserved in fixed tissue, we recommend dissection the tissue and running the RNAscope protocol within 2-3 weeks at most.
7. Remove the mucosa and submucosal plexus using microdissection. This can be accomplished in many different ways including separating the layers from underlying circular muscles along the lateral edge and teasing back the layers across the colon width.

8. Remove as much circular muscle as possible with forceps by teasing away fibers at the lateral edge and pulling them across the colon width. Ideally as much circular muscle as possible should be removed so when nearly perpendicular light is applied to the tissue circular fibers are barely visible.
9. Cut the longitudinal muscle-myenteric plexus preparation away from the rest of the intestinal tissue. Cut the preparation slightly larger than desired as the tissue will be re-pinned along the border.
10. Flip the tissue over and re-pin flat. It is recommended to use smaller diameter pins for this part such as cut pieces of tungsten wire (0.075mm diameter) as the tissue is now much more delicate.
11. Remove the serosa and longitudinal muscle using a microdissection technique similar to that for circular muscle removal (step 9). This layer is much thinner (**Fig 2.1b**) so a cautious approach is recommended. As with circular muscle removal, muscle fibers lines should be barely perceivable by parallel light.
12. Cut around the pinned border areas to produce the final preparation. This can be stored again in 1x phosphate buffered saline (PBS) until starting the RNAscope protocol.

Performing RNAscope in whole mount ENS tissue

While this protocol is adapted from manufacturer and previous protocols in many ways one of the most important differences is adequate washing time and technique. As these preparations are much thicker than slides inadequate washing can lead to high background and false positive signal. Other modifications to the protocol additionally increased the signal-to-noise ratio and maintained specificity in our tissue. All RNAscope pretreatment, hybridization, and amplification steps are performed in a 96-well plate but the tissue is transferred to a 48-well plate for washes unless otherwise specified. During each wash step tissue is washed 3x5mins while

the 96-well plate is also washed 1x time with the same wash buffer used for the tissue. All steps at 20°C are performed with gentle rotation on an orbital shaker.

1. *Pretreatment:*
2. In a 48-well plate wash tissue for 5mins in 1x PBS with 0.1% Triton X-100 (PBS-T).
3. Dehydrate tissue using an ethanol gradient diluted in PBS-T for 5mins each using 25% ethanol, then 50% ethanol, then 75% ethanol, and finally 100% ethanol.
4. Exchange 100% ethanol for fresh 100% ethanol for 5mins. Then rehydrate tissue up the same gradient for 5mins each. After the 25% ethanol wash tissue in 1x PBS for 5mins.
5. Incubate tissue with H_2O_2 for 10mins and subsequently wash in 1x PBS.
6. Incubate tissue with Protease III (ACD Biosciences, cat no. 322337) for 45mins at 40°C and subsequently wash in 1x PBS at 20°C.
    a. The RNAscope manufacturer recommends their HybEZ™ II oven for all 40°C steps to maintain adequate humidity and prevent tissue drying. However this is not a high concern for whole mount tissue and any oven that maintains consistent temperature can be used. A tray or beaker of H_2O placed in the oven is sufficient to maintain humidity.
7. *Probe hybridization:*
8. Incubate tissue with RNAscope probe for 16-18h at 40°C and subsequently wash with 1x wash buffer from the RNAscope kit.
9. *Signal amplification:*
10. Perform amplification steps AMP1-AMP6 for times and temperatures recommended by the manufacturer in a 96-well plate. Wash tissue with 1x wash butter 3x5 mins between each step in a 48-well plate. Make sure to also wash the 96-well plate at least 1x with 1x wash buffer as well.
11. *Signal detection:*

12. During the wash step after the final amplification step (AMP6) create the fast RED working solution following manufacturer dilutions and incubate tissue in the dark for 10mins as recommended.
13. Immediately wash tissue at least 3x5mins in 1x PBS. Tissue will be red in color where intensity can indicate both high signal and high background.
14. Tissue can now be mounted flat with mounting media and a coverslip to visualize signal. Once RNAscope protocol is working correctly this can be followed with 1x PBST washes and immunohistochemistry steps as described previously.[15] The additional washes during immunohistochemistry steps can lighten the tissue red color and reduce background signal but not by a large amount, so it is not recommended to proceed with antibody labeling unless the signal-to-noise ratio is already acceptable.

REPRESENTATIVE RESULTS

Proper use of these techniques allows for assessment of RNA in enteric glia or neurons with high quality and specificity through sequencing and *in situ*. Specificity of our RiboTag models for enteric glia and neurons along with dissection diagrams and homogenization results are shown in **Fig 2.1**. Specificity and signal-to-noise of RNAscope in myenteric whole mounts with cell-specific genetic markers and manufacturer controls are shown in **Fig 2.2**. Details of RNAscope probes and antibodies used in this and the considerations sections are in **Table 2.1**.

Table 2.1 RNAscope probes and IHC antibodies used in Chapter 2.

RNAscope Probes			
Probe Target	*Vendor*	*Catalog Number*	*Channel*
DapB	ACD Bio-Techne	310043	C1
Ppib	ACD Bio-Techne	313911	C1
UBC	ACD Bio-Techne	310771	C1
Lpar1	ACD Bio-Techne	318591	C1
Tmem173 (Alt. name for *Sting1*)	ACD Bio-Techne	413321	C1
Immunohistochemistry (IHC) Antibodies			
Primary antibodies			
Target	*Vendor*	*Catalog Number*	*Dilution*
Chicken anti-GFAP	Abcam	ab4674	1:1000
Mouse anti-Peripherin	Santa Cruz	sc-377093	1:100
Rabbit anti-HA(C29F4)	Cell Signaling	3724	1:500
Rabbit anti-S100β	Abcam	ab52647	1:200
Secondary antibodies			
Goat anti-chicken Dylight 405	Jackson Laboratories	103-475-155	1:400
Donkey anti-mouse Alexa Fluor 488	Jackson Laboratories	715-545-150	1:400
Donkey anti-rabbit Alexa Fluor 594	Jackson Laboratories	711-585-152	1:400
Donkey anti-rabbit Alexa Fluor 647	Jackson Laboratories	711-605-152	1:400
Note: Images containing DAPI were mounted with DAPI Fluoromount-G (SouthernBiotech, Birmingham, AL; cat no. 0100-20)			

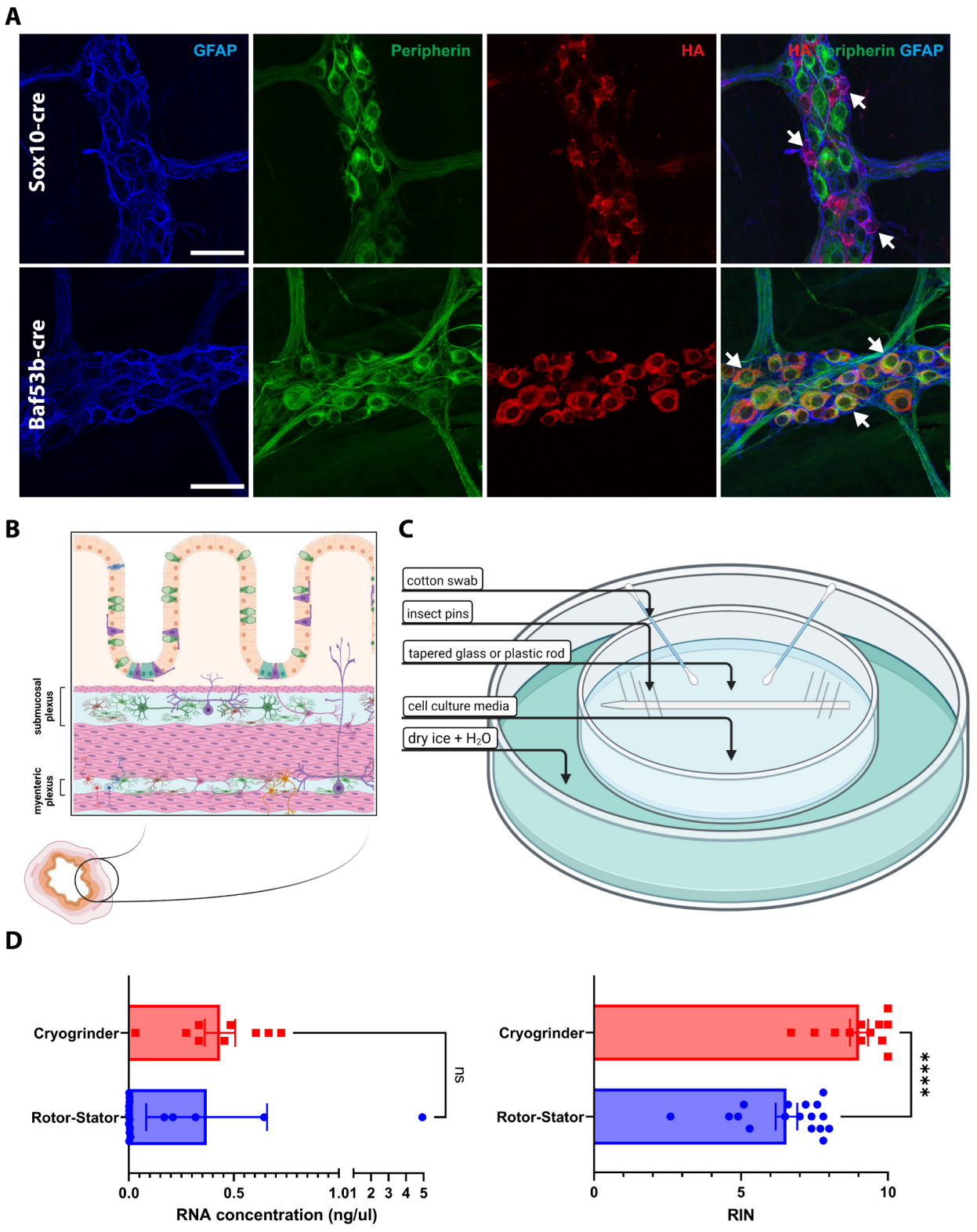

Figure 2.1 Preparing myenteric tissue for RiboTag: validation, dissection, and homogenization.

(A) Validation of our RiboTag floxed line for glial- and neuronal-specificity in with our Sox10-Cre and BAF53b-Cre driver lines, respectively. Immunolabeling demonstrates co-localization of the HA tag with either enteric glial cell bodies (as indicated by small cells enveloped by $GFAP^+$ processes) or $peripherin^+$ neuronal cell bodies. Representative cells are shown by arrows (glial in top panels and neuronal in bottom panels). Images representative of n= 2-3 mice and captured using a Zeiss LSM 880 NLO confocal system (Zeiss, Jena, Germany) using Zen Black software and a 20x objective (0.8 numerical aperture, Plan ApoChromat; Zeiss). Scale bar represents 50µm. **(B)** Diagram of the intestinal layers and relative location of the submucosal and myenteric plexus (created with Biorender.com). Gut lumen is oriented at the top of the diagram. **(C)** Diagram of the set-up used to dissect myenteric plexus for RNA protocols (created with Biorender.com). This is easiest used under a dissection scope. **(D)** Comparison of rotor-stator (blue) and CryoGrinder™ (red) homogenization methods for RNA yield (*left*) and quality (*right*). While RNA concentration does not differ significantly between methods variability is appreciably higher in rotor-stator samples. RNA integrity is higher using the CryoGrinder™ (****$P < 0.0001$). Data were analyzed using the student's T test in GraphPad Prism v9.2.0 (GraphPad Software, San Diego, CA) with n=9-17 mice/group and are represented as mean ± SEM.

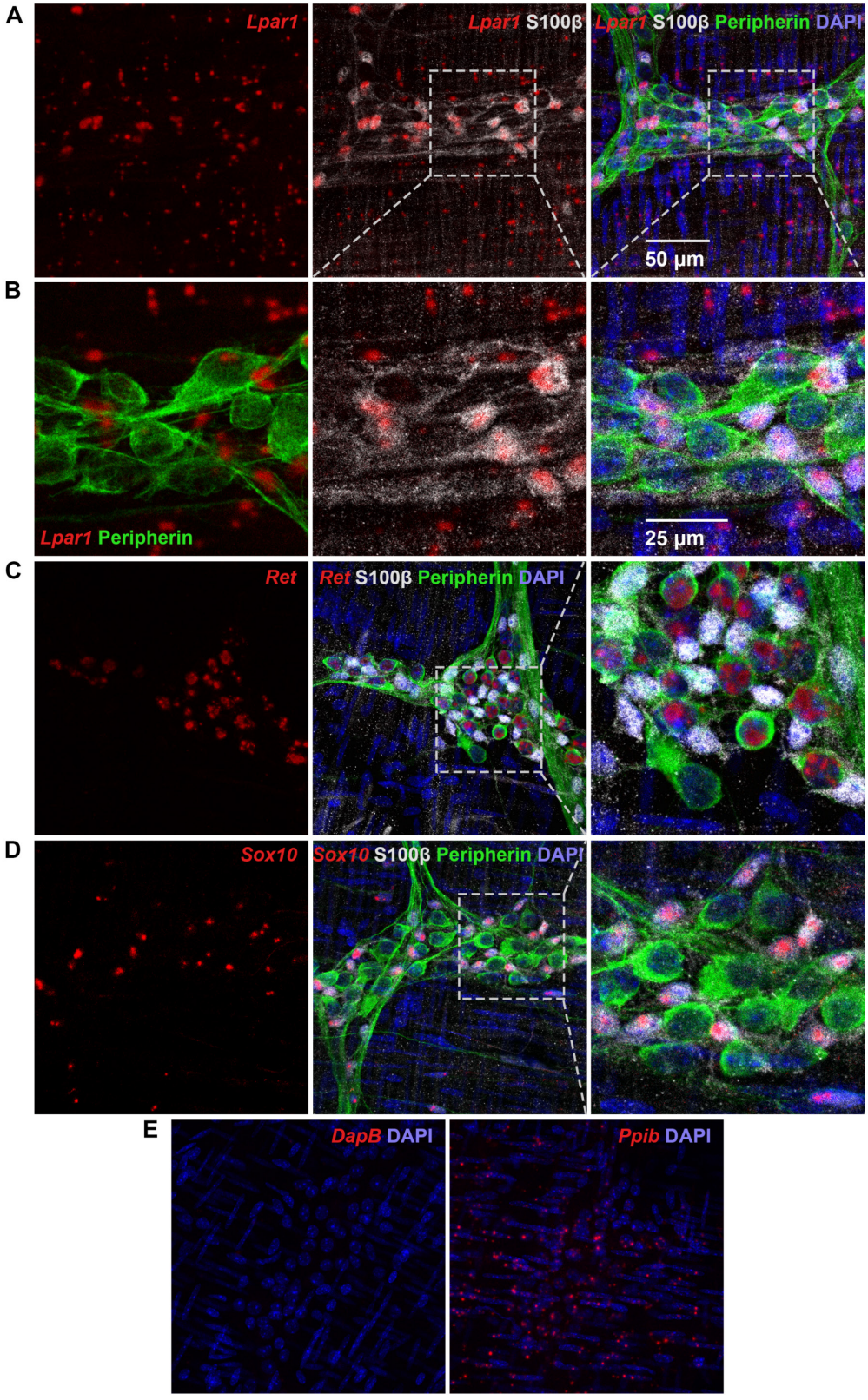

Figure 2.2 Specificity of RNAscope RED signal for enteric neurons and glia in the colonic myenteric plexus.

(A-E) adapted from Ahmadzai et al. (in review at *JCI*). **(A-B)** *Lpar1* is highly expressed in enteric glia while lowly expressed in enteric neurons (Ahmadzai et al.). This is visualized by the co-localization of RNAscope labeling for *Lpar1* in red mainly within enteric glia (S100β, white) and only in few enteric neurons (peripherin, green). Panels in **(B)** represent magnified inserts from panels in **(A)**. **(C-D)** RNAscope signal is specific for enteric neurons and glia with probes for canonical neuronal marker *Ret* **(C)** and glial marker *Sox10* **(D)** as measured by overlay with enteric neurons (peripherin, green) and enteric glia (S100β, white). **(E)** RNAscope expression of manufacturer negative control probe *DapB* and positive control probe *Ppib* in red demonstrate appropriate absence and presence of staining in myenteric plexus whole mount preparations, respectively. Images are representative of staining from 2-3 mice and captured on a Zeiss LSM 880 NLO confocal system (Zeiss, Jena, Germany) using Zen Black software and a 20x objective (0.8 numerical aperture, Plan ApoChromat; Zeiss).

ADDITIONAL CONSIDERATIONS

RiboTag RNA-sequencing in the ENS

Validating the RiboTag line for cell specificity

RiboTag (B6N.129-*Rpl22*$^{tm1.1Psam}$/J; Jackson Laboratories, stock number 011029) is a floxed line[28,29] and therefore can be crossed in a validated Cre-lox line to create a cell-specific signature. To capture enteric glial cells we crossed homozygous RiboTag mice with heterozygous *Sox10*^{CreERT2} mice (gifted by Dr. Vassilis Pachnis, The Francis Crick Institute, London, UK) to generate *Sox10::*$^{CreERT2+/-}$/*Rpl22*$^{fl/+}$ mice. RiboTag is commonly utilized as heterozygous as no difference in RNA yield or specificity has been noted.[28,29,41–43] To generate enteric neuronal-specific RiboTag mice we crossed homozygous BAF53b-Cre mice (Tg(Actl6b-Cre)4092Jiwu/J; Jackson Laboratories, stock number 027826) with homozygous RiboTag mice. The Sox10-Cre driver line has been previously validated and published using RiboTag by our lab[11,44,45] while the BAF53b-Cre line has been used to perform single-cell RNAs-sequencing from enteric neurons.[24] Regardless validating specificity of RiboTag expression in the ENS is important given the interconnectedness of these cell types. We visualized the specificity of both Sox10-RiboTag and BAF53b-RiboTag using immunohistochemistry for the HA tag (rabbit anti-HA C29F4; Cell Signaling cat no. 3724) combined with the glial marker GFAP (chicken anti-GFAP; Abcam, cat no. ab4674) or the neuronal marker peripherin (mouse-anti peripherin; Santa Cruz, cat no. sc-377093). Both our genetic lines demonstrate cell specificity *in situ* where Sox10-RiboTag mice only express HA in glia and not neurons while BAF53b-RiboTag mice only express HA in neurons and not glia (**Fig 2.1a**). Visualization of this specificity is useful for tissues with complex cellular architecture such as the ENS and therefore we recommend using this approach. It is also good to genetically validate your line with RNA measurements. This could be accomplished through PCR, RNA-sequencing, etc. We demonstrated high levels of glial-specific transcripts and low levels of neuronal and smooth muscle transcripts (see previous publication[11] and **Fig 3.1b**).

Preparing glial- or neuronal-RiboTag cDNA libraries

One potential challenge of using the RiboTag model is relatively low RNA yield and quality, due to the selection of cell-specific ribosome-associated mRNA only and the long processing procedure respectively. Additionally due to the nature of the protocol these samples likely have higher rRNA contents than bulk sequencing samples that must be removed to produce good mRNA libraries. There are several different cDNA library kits available that are designed to deal with these concerns. We utilized two different kits with two different methods of removing rRNA: ribosomal depletion and poly(A) selection. While ribosomal depletion is better at dealing with lower quality samples poly(A) selection is better at reducing the proportion of residual rRNA.[46] The SMART-Seq Stranded Kit (Takara Bio USA, Mountain View, CA) uses ribosomal depletion while the SMART-Seq v4 Ultra Low Input Kit (Takara Bio USA, Mountain View, CA) uses poly(A) selection. Consistent with other reports[47] the SMART-Seq v4 Ultra Low Input Kit works well with our RiboTag samples and produced lower duplicate reads ($P < 0.0001$; **Fig 2.3a**) and subsequently higher uniquely aligned reads in STAR v2.7.3a[48] (**Fig 2.3b**). This is likely due to the higher proportion of residual rRNA in data created with the SMART-Seq Stranded Kit, represented by a large percentage of sequences that map to multiple genomes in FastQ Screen (Babraham Bioinformatics; **Fig 2.3c**). Taken together these data suggest it is critical to make sure samples submitted for RNA-sequencing are of high quality RIN so a poly(A) selection library kit can be used. In particular the SMART-Seq v4 Ultra Low Input Kit provides comparatively high quality libraries for RiboTag when compared to other library kits (albeit not the SMART-Seq Stranded Kit in particular).[47]

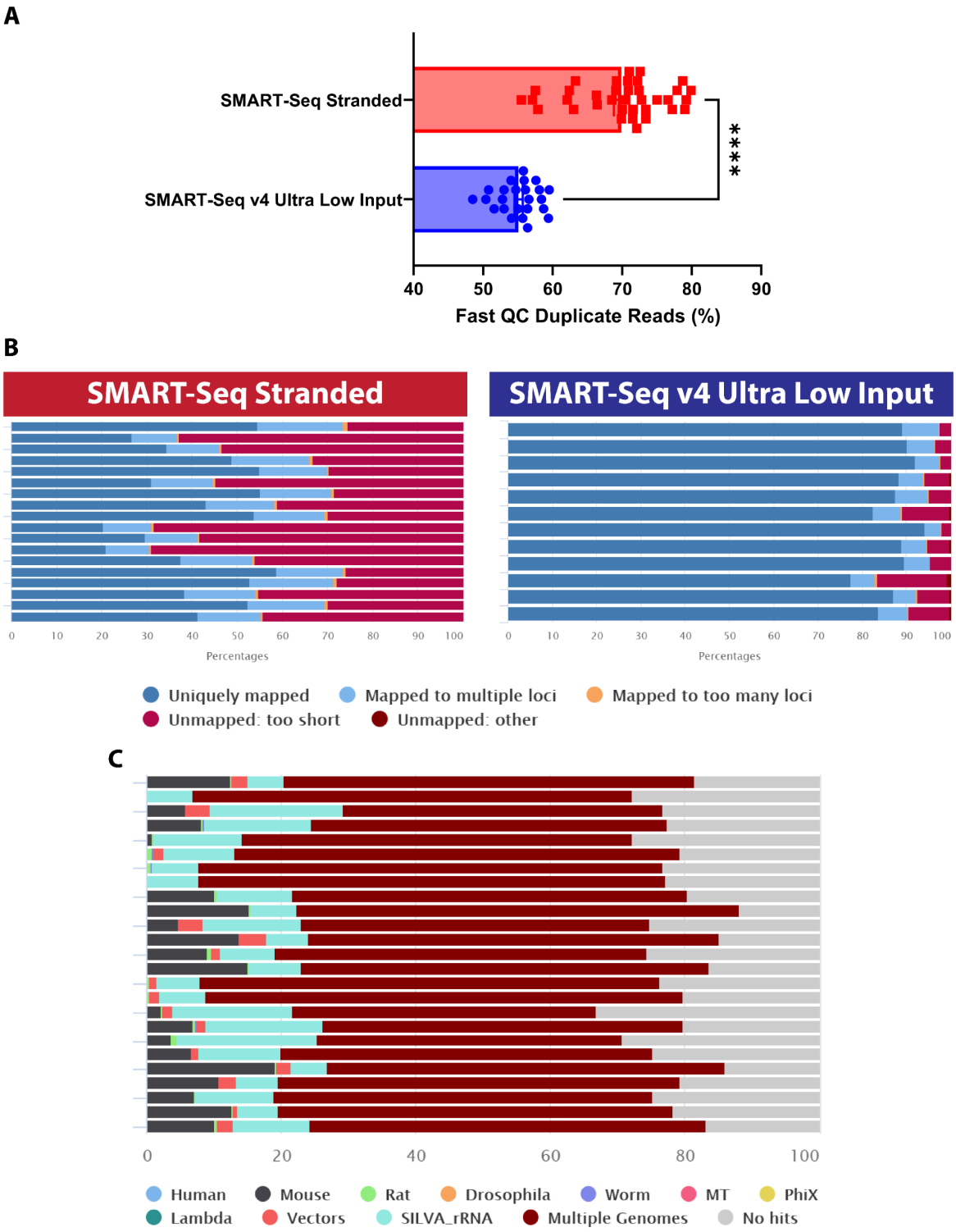

Figure 2.3 The SMART-Seq v4 Ultra Low Input Kit with poly(A) selection generates high quality cDNA libraries for RiboTag samples.

(A) The SMART-Seq Stranded cDNA library preparation kit that uses ribosomal depletion (red) produces higher duplicate reads in RiboTag samples compared to the SMART-Seq v4 Ultra Low Input kit that uses poly-A selection (****$P < 0.0001$). Data were analyzed by the student's T test in GraphPad Prism v9.2.0 with n=24-36 mice/group and are represented by mean ± SEM. **(B)** Libraries generated by the SMART-Seq v4 Ultra Low Input Kit have a higher percentage of uniquely mapped reads, indicated by the dark blue proportion of each sample column. This is indicative of higher mRNA exon content. **(C)** A high percentage of reads generated from the SMART-Seq Stranded libraries map to multiple genomes, represented by the maroon proportion of each sample column, and indicate high residual rRNA contamination. **(B-C)** Plots generated by MultiQC v1.8[49] and representative of n=12-25 mice/group.

Determining confounding variables to model in differential expression analysis

We also determined if any known metadata differing between our samples contributed to variation in our aligned read counts. While it is of course best practice to limit variables when possible and randomize samples as the next best solution,[46] there will be instances where neither of these are possible and whatever variation in metadata exists should be explored as a potentially confounding variable. In our experiment we are aware of three potential confounding variables in our metadata: tissue collection date (i.e. mouse litter), RiboTag protocol date, and RIN. We used DESeq2 v1.30.1[50] to process read count data and perform principal component analysis (PCA) for each of these variables while plotting this data using ggplot2 v3.3.3[51]. While collection date does not appear to cluster with any particular treatment group (**Fig 2.4a**), both RiboTag date (**Fig 2.4b**) and RIN (**Fig 2.4c**) do appear to relate to treatment group. However RiboTag date and RIN have similar patterns of association with treatment (representing semi-different portions of PC1 ranges on the x-axis) and RIN creates stronger separation between samples, therefore only RIN was accounted for in our differential expression model (see the differential expression results from this in Chapter 3). While investigating confounding variables to add to differential expression modeling is not a specialized practice for RiboTag and instead good practice for any RNA-sequencing experiment, this does not discount its importance in this method.

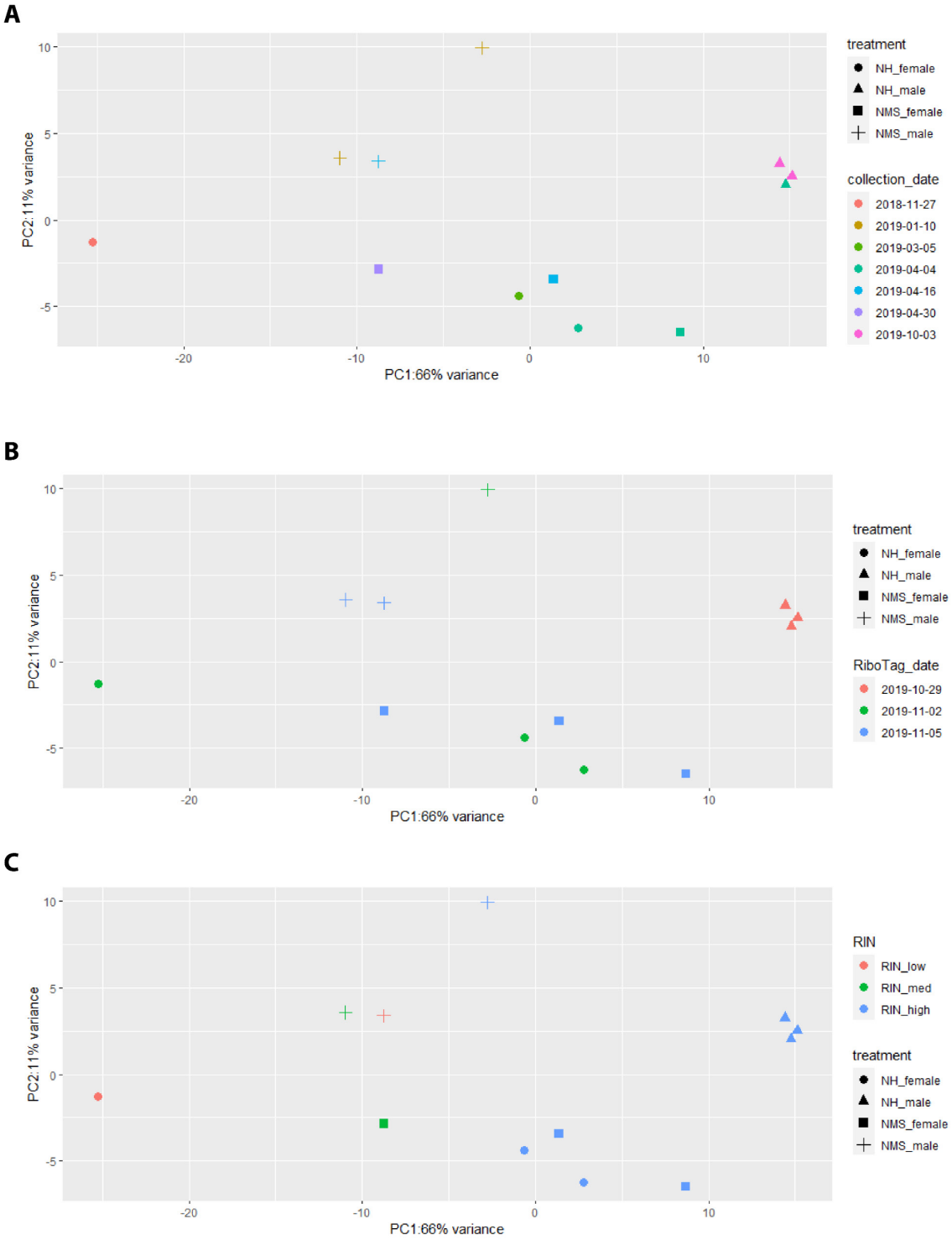

Figure 2.4 Principal component analysis including experimental metadata for RiboTag experiments.

PCAs of known metadata in RNA-sequencing to determine potential variables to include in differential expression modeling. **(A)** PCA of a glial RiboTag experiment (NMS Sox10-RiboTag; see Chapter 3) suggests no major association of tissue collection date (denoted by color) with treatment (denoted by shape). **(B)** PCA of NMS Sox10-RiboTag suggests a potential association of RiboTag date (denoted by color) with treatment (denoted by shape). However, this is better encapsulated by the PCA of the data with RIN date (denoted by color) and treatment (denoted by shape) **(C)** and thus suggests this is a better variable to include in the differential expression analysis model. Data representative of n=3 mice/group.

Selection of analysis pipeline software dramatically affects results

There are a multitude of different software to use at any particular point in the RNA-sequencing analysis pipeline and the options are no different for RiboTag data than any other sequencing dataset. While there could be some statistically appropriate reason to choose one over another for a particular dataset there is not great consensus amongst the field that one particular software is categorically better than another.[46] Decisions may be made based on traditional pipelines used in particular labs in order to best compare data between experiments or on how recently software was updated and how responsive the software creators are to the community. Regardless of the particular reasons it is important to note that these decisions can have a large impact on results. For instance, we compared an external analysis of our published RiboTag data[11] with a reanalysis performed with our lab's pipeline. The external analysis utilized Cutadapt v1.10[52] for read trimming and adapter removal, HISAT v2.0[53] for mapping reads to the genome, StringTie v1.3[54] for counting reads, and Ballgown[55] for performing differential expression analysis. Meanwhile our lab utilized TrimGalore v0.6.5 (Babraham Bioinformatics) for trimming, STAR v2.7.3a[48] for aligning reads, HTSeq v0.11.2[56] to count reads, and DESeq2 v1.30.1[50] to perform differential analysis. The difference in results between these two pipelines is dramatic. The external pipeline had only 8 differentially expressed genes significant at FDR < 0.1 and 680 differentially expressed genes at unadjusted $P < 0.005$ (**Fig 2.5a**). Meanwhile our pipeline detected 976 differentially expressed genes significant at FDR < 0.1 (**Fig 2.5b**). While we did not directly compare all the parameters used within these software for analysis it is unlikely that the software itself does not contribute to this profound difference. It is unclear which of these better represents the 'real' results, but there are some reports that DESeq2 is fairly conservative differential expression software[46,57] and therefore perhaps the external pipeline represents even more conservative results. Regardless this data demonstrates the importance of considering software choices and potentially analyzing RiboTag RNA-seq data with more than one analysis pipeline.

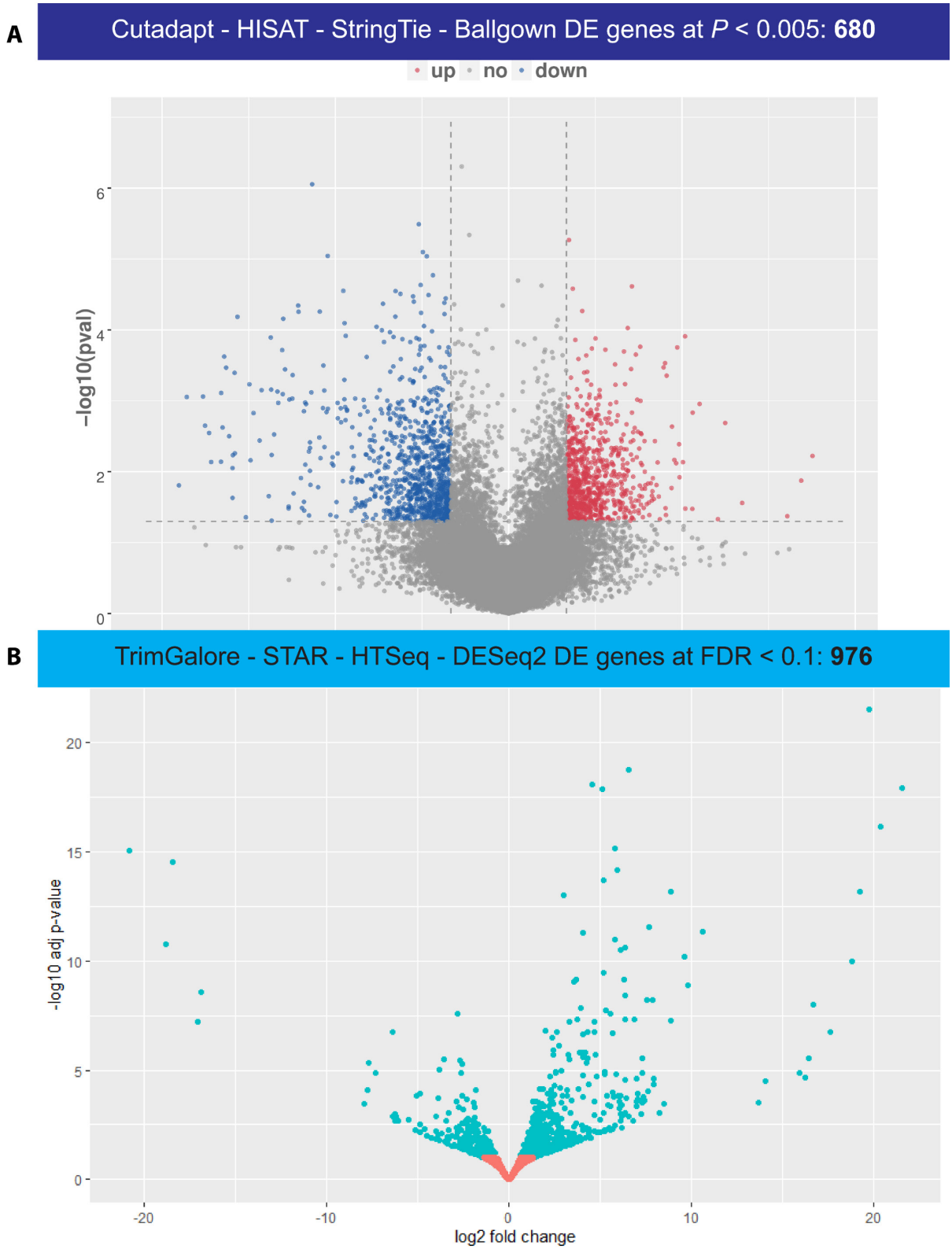

Figure 2.5 Analysis pipeline software dramatically influences results of Sox10-RiboTag data.

(A) Volcano plot of the RNA-sequencing analysis pipeline (Cutadapt, HISAT, StringTie, Ballgown) used by an external group on our published Sox10-RiboTag dataset[11] found 8 differentially expressed genes significant at FDR < 0.1 and 680 genes at $P < 0.005$. Unadjusted $-\log_{10}P$ value is measured on the y-axis and $\log_2$fold-change between treatment and control is measured on the x-axis. Upregulated genes significant at $P < 0.05$ are shown in red while downregulated genes significant at $P < 0.05$ are shown in blue. **(B)** Volcano plot of the same dataset analyzed through a different pipeline (TrimGalore, STAR, HTSeq, DESeq2) found 976 differentially expressed genes significant at FDR < 0.1. Adjusted $-\log_{10}P$ value (i.e. FDR) is measured on the y-axis and $\log_2$fold-change between treatment and control is on the x-axis. Differentially expressed genes significant at FDR < 0.1 are shown in cyan. Data representative of n=3 mice/group.

RNAscope of the ENS *in situ*

Optimizing fixation and dissection for RNAscope in myenteric plexus whole mounts

Recommended fixation times for whole mount RNAscope vary between tissues.[35–37] We tested three different 4% paraformaldehyde fixation conditions used in our lab for immunohistochemistry and assessed their efficacy of preserving RNAscope signal by using the manufacturer negative control probe *DapB* and positive control probe *Ppib* (**Fig 2.6a**). Fixation for 30mins at 20°C is not adequate for preserving RNAscope signal (*left panels*). While 2h at 20°C does stain for *Ppib* with minimal *DapB* staining (*middle panels*), fixation for 16h at 4°C provides the lowest background in muscle and highest *Ppib* signal while still maintaining negligible *DapB* signal. Using appropriate dissection methods before starting RNAscope are similarly important to optimizing results. Traditional longitudinal muscle-myenteric plexus preparations where the circular muscle (**Fig 2.6b**, CM in *top panels*) is removed produce signal but have higher background than when the serosa and longitudinal muscle (LM in *top panels*) are also removed. Thus if using probed with relatively low signal (such as *Sting1* pictured here) it is essential to reduce background as much as possible to visualize staining. Additionally the RNAscope protocol can lead to increased muscle staining by some antibodies (data not shown) and this dissection improves immunohistochemistry results as well. For larger batch processing using probes with high expression and antibodies maintain specificity after RNAscope the faster rod dissection method used for RiboTag RNA-sequencing can also be used for RNAscope as differences in staining between *DapB, Ppib,* and additional very high-expression manufacturer positive control probe *UBC* are appreciated after both the recommended pinned dissection (**Fig 2.6b**, *middle panels*) and the rod dissection (**Fig 2.6b**, *bottom panels*). However these dissections have higher background in both the RNAscope channel and with some immunohistochemistry antibodies and thus are not always appropriate.

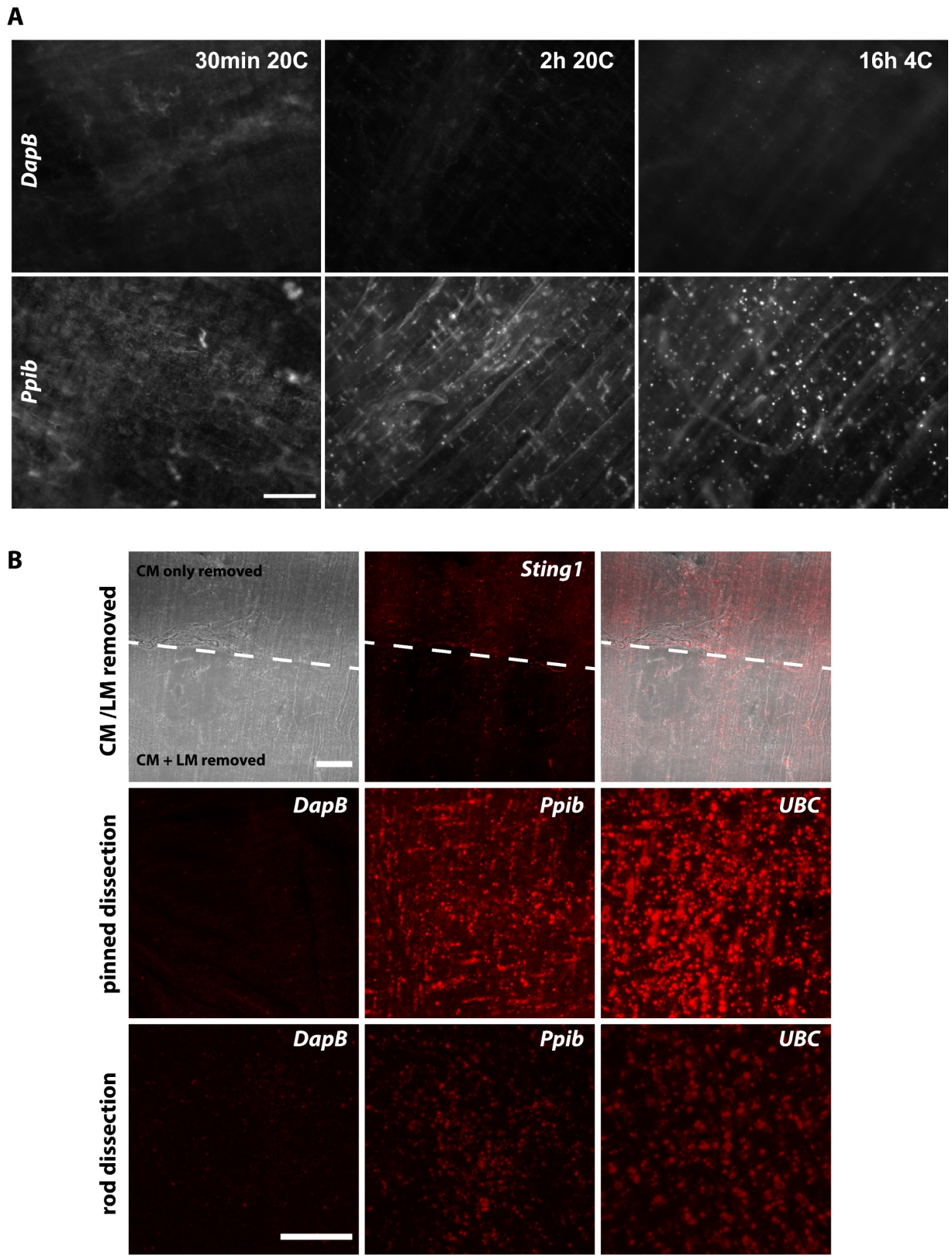

Figure 2.6 Optimizing fixation and dissection for RNAscope in myenteric plexus whole mounts.

(A) RNAscope staining of manufacturer negative control probe *DapB* and positive control probe *Ppib* in myenteric tissue fixed in 4% paraformaldehyde in three different conditions. While 2h at 20°C and 16h at 4°C both have acceptable negative and positive control staining, the latter has lower background staining in muscle and higher positive probe signal. Images were captured using the 40x objective (0.75 numerical aperture, Plan Fluor; Nikon) of an upright epifluorescence microscope (Nikon Eclipse Ni) with a Retiga 2000R camera (QImaging, Surrey, BC, Canada) controlled by QCapture Pro 7.0 (QImaging) software. **(B)** *Top panels:* in myenteric dissections, removing serosa and longitudinal muscle in addition to circular muscle further reduces background and is helpful for visualizing RNAscope signal when RNA expression is lower. *Middle panels:* While this recommended dissection provides the best signal based on expression of negative control probe *DapB,* positive control probe *Ppib*, and high-expression positive control probe *UBC*, using the much faster rod dissection method for myenteric plexus (*bottom panels*) also produces adequate results and can be helpful for large-scale processing when targeting genes with higher expression. Dissection images were captured on a Zeiss LSM 880 NLO confocal system (Zeiss, Jena, Germany) using Zen Black software and a 20x objective (0.8 numerical aperture, Plan ApoChromat; Zeiss). All images representative of n=2-3 mice. Scale bar = 50μm.

Optimizing tissue dehydration/rehydration and protease RNAscope pretreatments in myenteric plexus whole mounts

Similar to fixation times multiple methods of rehydration and dehydration are utilized in published whole mount RNAscope protocols.[35–37] We tested these different conditions in our tissue using negative control probe *DapB* and positive control probe *Ppib* and determined that ethanol dehydration and rehydration produced the best results (**Fig 2.7a**). Using only ethanol dehydration strongly reduced RNAscope signal while methanol dehydration and rehydration increased background. Ethanol dehydration and rehydration reduce background compared to no dehydration or rehydration. Additionally performing this step preserves protein morphology better after the RNAscope procedure than doing no dehydration and rehydration (data not shown.) While no whole mount protocols utilize the recommended manufacturer antigen retrieval step (15min in 100°C antigen retrieval buffer provided in the RNAscope kit) we also tried this in our tissue to see if it improved signal. This antigen retrieval visible altered our preparations and dramatically increased background and nonspecific ganglionic staining (**Fig 2.7b**, *left panels*). Finally we also compared two strengths of protease provided by ACD Biosciences. Protease III is stronger than the traditional Protease Plus that comes with RNAscope kits. Consistent with work in myenteric whole mounts[37] we found that Protease III further reduced background (**Fig 2.7b**, *right panels*) in our samples than Protease Plus treatment (**Fig 2.7b**, *middle panels*) while still maintaining cellular morphology in immunohistochemical staining (data not shown).

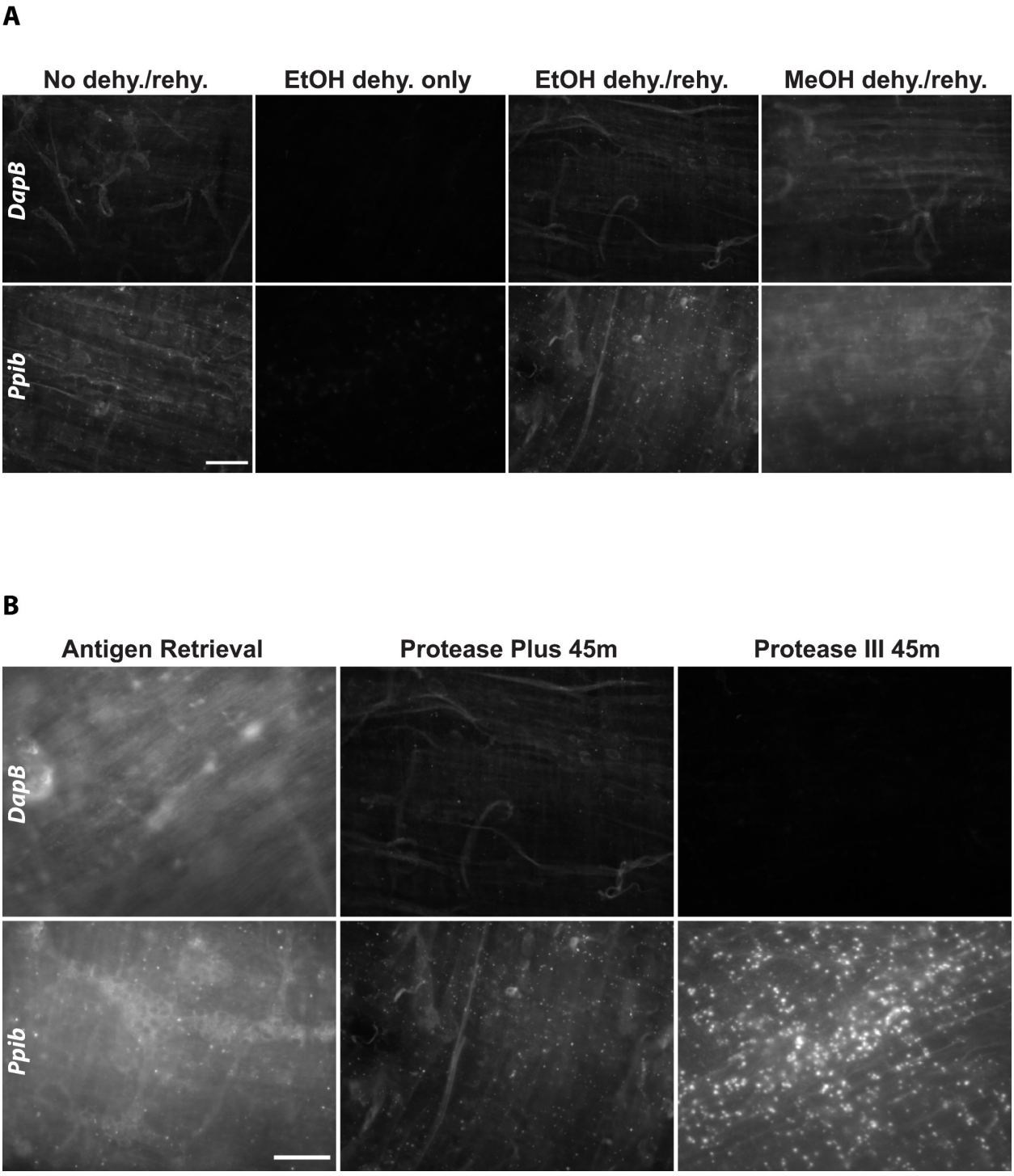

Figure 2.7 Optimizing pretreatment parameters for RNAscope in myenteric plexus whole mounts.

(A) Different conditions for tissue dehydration and rehydration were used in myenteric whole mounts and assessed by negative control probe *DapB* and positive control probe *Ppib* staining.

Ethanol dehydration and rehydration (third column) produced the highest *Ppib* signal while maintaining negligible *DapB* signal when compared with no dehydration/rehydration (first column), ethanol dehydration only (second column), and methanol dehydration/rehydration (last column). **(B)** *Left panels:* Antigen retrieval recommended by the manufacturer is not appropriate for RNAscope in whole mount myenteric tissue and results in high background and nonspecific ganglionic staining. Protease III (*right panels*) produces better signal-to-noise RNAscope results than the standard Protease Plus provided with RNAscope kits (*middle panels*). Images were captured using the 40x objective (0.75 numerical aperture, Plan Fluor; Nikon) of an upright epifluorescence microscope (Nikon Eclipse Ni) with a Retiga 2000R camera (QImaging, Surrey, BC, Canada) controlled by QCapture Pro 7.0 (QImaging) software and are representative of n=2-3 mice. Scale bar = 50μm.

DISCUSSION

In this technical review we provide detailed protocols for optimized preparation of myenteric plexus tissue for cell-specific RNA-sequencing and *in situ* RNA visualization through RNAscope. We additionally provide representative diagrams and results for these protocols and other considerations for troubleshooting and applying our methods to similar tissues and/or conditions. Genetic techniques such as RNA-sequencing are ideal for understanding molecular expression patterns especially in complex disease states and assessing this in specific cell types is easily achieved in conjunction with RiboTag.[28,29,58] Furthermore supplementing cell-specific RNA-sequencing with RNAscope enables expressional validation *in situ* and begins placing computational data into a biological context. While some studies have utilized these techniques to study the ENS[22,24,37,43,59] their methods are relatively brief and therefore difficult to recapitulate or apply to future research. By providing the methodological details and additional troubleshooting steps we used for these genetic methods in the ENS here we hope this becomes a valuable resource for further study of ENS gene expression.

REFERENCES

REFERENCES

1. Furness JB. *The Enteric Nervous System*. (Furness JB, ed.). Malden, Massachusetts, USA: Blackwell Publishing; 2006. doi:10.1002/9780470988756

2. Furness JB. The enteric nervous system and neurogastroenterology. *Nat Rev Gastroenterol Hepatol*. 2012;9(5):286-294. doi:10.1038/nrgastro.2012.32

3. Furness J. Types of neurons in the enteric nervous system. *J Auton Nerv Syst*. 2000;81(1-3):87-96. doi:10.1016/S0165-1838(00)00127-2

4. Grubišić V, Gulbransen BD. Enteric glia: the most alimentary of all glia. *J Physiol*. 2017;595(2):557-570. doi:10.1113/JP271021

5. Gulbransen BD. Enteric Glia. *Colloq Ser Neuroglia Biol Med From Physiol to Dis*. 2014;1(2):1-70. doi:10.4199/C00113ED1V01Y201407NGL002

6. Chow AK, Gulbransen BD. Potential roles of enteric glia in bridging neuroimmune communication in the gut. *Am J Physiol - Gastrointest Liver Physiol*. 2017;312(2):G145-G152. doi:10.1152/ajpgi.00384.2016

7. Morales-Soto W, Gulbransen BD. Enteric Glia: A New Player in Abdominal Pain. *Cell Mol Gastroenterol Hepatol*. 2018. doi:10.1016/j.jcmgh.2018.11.005

8. Grubišić V, McClain JL, Fried DE, et al. Enteric Glia Modulate Macrophage Phenotype and Visceral Sensitivity following Inflammation. *Cell Rep*. 2020;32(10):108100. doi:10.1016/j.celrep.2020.108100

9. Brown IAM, Gulbransen BD. The antioxidant glutathione protects against enteric neuron death in situ, but its depletion is protective during colitis. *Am J Physiol Liver Physiol*. 2017;314(1):G39-G52. doi:10.1152/ajpgi.00165.2017

10. Delvalle NM, Fried DE, Rivera-Lopez G, Gaudette L, Gulbransen BD. Cholinergic activation of enteric glia is a physiological mechanism that contributes to the regulation of gastrointestinal motility. *Am J Physiol - Gastrointest Liver Physiol*. 2018;315(4):G473-G483. doi:10.1152/ajpgi.00155.2018

11. Delvalle NM, Dharshika C, Morales-Soto W, Fried DE, Gaudette L, Gulbransen BD. Communication Between Enteric Neurons, Glia, and Nociceptors Underlies the Effects of Tachykinins on Neuroinflammation. *Cell Mol Gastroenterol Hepatol*. 2018;6(3):321-344. doi:10.1016/j.jcmgh.2018.05.009

12. Gulbransen BD, Sharkey KA. Novel functional roles for enteric glia in the gastrointestinal tract. *Nat Rev Gastroenterol Hepatol*. 2012;9(11):625-632. doi:10.1038/nrgastro.2012.138

13. McClain JL, Grubišić V, Fried D, et al. Ca 2+ responses in enteric glia are mediated by connexin-43 hemichannels and modulate colonic transit in mice. *Gastroenterology*. 2014;146(2):497-507. doi:10.1053/j.gastro.2013.10.061

14. McClain JL, Fried DE, Gulbransen BD. Agonist-Evoked Ca2+ Signaling in Enteric Glia Drives Neural Programs That Regulate Intestinal Motility in Mice. *Cell Mol Gastroenterol Hepatol*. 2015;1(6):631-645. doi:10.1016/j.jcmgh.2015.08.004

15. McClain JL, Mazzotta EA, Maradiaga N, et al. Histamine-dependent interactions between mast cells, glia, and neurons are altered following early-life adversity in mice and humans. *Am J Physiol Liver Physiol*. 2020;319(6):G655-G668. doi:10.1152/ajpgi.00041.2020

16. Chow AK, Grubišić V, Gulbransen BD. Enteric Glia Regulate Lymphocyte Activation via Autophagy-Mediated MHC-II Expression. *Cell Mol Gastroenterol Hepatol*. June 2021. doi:10.1016/j.jcmgh.2021.06.008

17. Hernandez S, Fried DE, Grubišić V, McClain JL, Gulbransen BD. Gastrointestinal neuroimmune disruption in a mouse model of Gulf War illness. *FASEB J*. 2019;(1):fj.201802572R. doi:10.1096/fj.201802572R

18. Brown IAMM, McClain JL, Watson RE, Patel BA, Gulbransen BD. Enteric Glia Mediate Neuron Death in Colitis Through Purinergic Pathways That Require Connexin-43 and Nitric Oxide. *Cell Mol Gastroenterol Hepatol*. 2016;2(1):77-91. doi:10.1016/j.jcmgh.2015.08.007

19. Grubišić V, Gulbransen BD. Enteric glial activity regulates secretomotor function in the mouse colon but does not acutely affect gut permeability. *J Physiol*. 2017;595(11):3409-3424. doi:10.1113/JP273492

20. Hasin Y, Seldin M, Lusis A. Multi-omics approaches to disease. *Genome Biol*. 2017;18(1):83. doi:10.1186/s13059-017-1215-1

21. Misra BB, Langefeld C, Olivier M, Cox LA. Integrated omics: tools, advances and future approaches. *J Mol Endocrinol*. 2019;62(1):R21-R45. doi:10.1530/JME-18-0055

22. Drokhlyansky E, Smillie CS, Van Wittenberghe N, et al. The Human and Mouse Enteric Nervous System at Single-Cell Resolution. *Cell*. September 2020:1-17. doi:10.1016/j.cell.2020.08.003

23. May-Zhang AA, Tycksen E, Southard-Smith AN, et al. Combinatorial transcriptional profiling of mouse and human enteric neurons identifies shared and disparate subtypes in situ. *Gastroenterology*. 2020;160(3):1-16. doi:10.1053/j.gastro.2020.09.032

24. Morarach K, Mikhailova A, Knoflach V, et al. Diversification of molecularly defined myenteric neuron classes revealed by single-cell RNA sequencing. *Nat Neurosci*. December 2020. doi:10.1038/s41593-020-00736-x

25. Wright CM, Schneider S, Smith-Edwards KM, et al. scRNA-sequencing reveals new enteric nervous system roles for GDNF, NRTN, and TBX3. *Cell Mol Gastroenterol Hepatol*. January 2021:140981. doi:10.1016/j.jcmgh.2020.12.014

26. Zeisel A, Hochgerner H, Lönnerberg P, et al. Molecular Architecture of the Mouse Nervous System. *Cell*. 2018;174(4):999-1014.e22. doi:10.1016/j.cell.2018.06.021

27. Rao M, Nelms BD, Dong L, et al. Enteric glia express proteolipid protein 1 and are a

transcriptionally unique population of glia in the mammalian nervous system. *Glia*. 2015;63(11):2040-2057. doi:10.1002/glia.22876

28. Sanz E, Yang L, Su T, Morris DR, McKnight GS, Amieux PS. Cell-type-specific isolation of ribosome-associated mRNA from complex tissues. *Proc Natl Acad Sci*. 2009;106(33):13939-13944. doi:10.1073/pnas.0907143106

29. Sanz E, Bean JC, Carey DP, Quintana A, McKnight GS. RiboTag: Ribosomal Tagging Strategy to Analyze Cell-Type-Specific mRNA Expression In Vivo. *Curr Protoc Neurosci*. 2019;88(1):1-19. doi:10.1002/cpns.77

30. Kupari J, Häring M, Agirre E, Castelo-Branco G, Ernfors P. An Atlas of Vagal Sensory Neurons and Their Molecular Specialization. *Cell Rep*. 2019;27(8):2508-2523.e4. doi:10.1016/j.celrep.2019.04.096

31. Park J-E, Botting RA, Conde CD, et al. A cell atlas of human thymic development defines T cell repertoire formation. *bioRxiv*. 2020;(February):2020.01.28.911115. doi:10.1101/2020.01.28.911115

32. Lanfranco MF, Loane D, Mocchetti I, Burns M, Villapol S. Combination of Fluorescent in situ Hybridization (FISH) and Immunofluorescence Imaging for Detection of Cytokine Expression in Microglia/Macrophage Cells. *BIO-PROTOCOL*. 2017;7(22):139-148. doi:10.21769/BioProtoc.2608

33. Grabinski TM, Kneynsberg A, Manfredsson FP, Kanaan NM. A method for combining rnascope in situ hybridization with immunohistochemistry in thick free-floating brain sections and primary neuronal cultures. *PLoS One*. 2015;10(3):1-19. doi:10.1371/journal.pone.0120120

34. Wang F, Flanagan J, Su N, et al. RNAscope: A novel in situ RNA analysis platform for formalin-fixed, paraffin-embedded tissues. *J Mol Diagnostics*. 2012;14(1):22-29. doi:10.1016/j.jmoldx.2011.08.002

35. Gross-Thebing T, Paksa A, Raz E. Simultaneous high-resolution detection of multiple transcripts combined with localization of proteins in whole-mount embryos. *BMC Biol*. 2014;12(1):55. doi:10.1186/s12915-014-0055-7

36. Morrison JA, McKinney MC, Kulesa PM. Resolving in vivo gene expression during collective cell migration using an integrated RNAscope, immunohistochemistry and tissue clearing method. *Mech Dev*. 2017;148:100-106. doi:10.1016/j.mod.2017.06.004

37. Obata Y, Castaño Á, Boeing S, et al. Neuronal programming by microbiota regulates intestinal physiology. *Nature*. 2020;578(7794):284-289. doi:10.1038/s41586-020-1975-8

38. Joseph NM, He S, Quintana E, Kim Y, Núñez G, Morrison SJ. Enteric glia are multipotent in culture but primarily form glia in the adult rodent gut. *J Clin Invest*. 2011;121(9):3398-3411. doi:10.1172/JCI58186

39. Fried DE, Gulbransen BD. In Situ Ca^{2+} Imaging of the Enteric Nervous System. *J Vis Exp*. 2015;(95):1-7. doi:10.3791/52506

40. Smith TH, Ngwainmbi J, Grider JR, Dewey WL, Akbarali HI. An In-vitro

Preparation of Isolated Enteric Neurons and Glia from the Myenteric Plexus of the Adult Mouse. *J Vis Exp*. 2013;(78):1-7. doi:10.3791/50688

41. Gabanyi I, Muller PA, Feighery L, Oliveira TY, Costa-Pinto FA, Mucida D. Neuro-immune Interactions Drive Tissue Programming in Intestinal Macrophages. *Cell*. 2016;164(3):378-391. doi:10.1016/j.cell.2015.12.023

42. Haimon Z, Volaski A, Orthgiess J, et al. Re-evaluating microglia expression profiles using RiboTag and cell isolation strategies. *Nat Immunol*. 2018;19(6):636-644. doi:10.1038/s41590-018-0110-6

43. Matheis F, Muller PA, Graves CL, et al. Adrenergic Signaling in Muscularis Macrophages Limits Infection-Induced Neuronal Loss. *Cell*. 2020;180(1):64-78.e16. doi:10.1016/j.cell.2019.12.002

44. McClain JL, Gulbransen BD. The acute inhibition of enteric glial metabolism with fluoroacetate alters calcium signaling, hemichannel function, and the expression of key proteins. *J Neurophysiol*. 2017;117(1):365-375. doi:10.1152/jn.00507.2016

45. Memic F, Knoflach V, Morarach K, et al. Transcription and Signaling Regulators in Developing Neuronal Subtypes of Mouse and Human Enteric Nervous System. *Gastroenterology*. 2018;154(3):624-636. doi:10.1053/j.gastro.2017.10.005

46. Conesa A, Madrigal P, Tarazona S, et al. A survey of best practices for RNA-seq data analysis. *Genome Biol*. 2016;17(1). doi:10.1186/s13059-016-0881-8

47. Song Y, Milon B, Ott S, et al. A comparative analysis of library prep approaches for sequencing low input translatome samples. *BMC Genomics*. 2018;19(1):696. doi:10.1186/s12864-018-5066-2

48. Dobin A, Davis CA, Schlesinger F, et al. STAR: ultrafast universal RNA-seq aligner. *Bioinformatics*. 2013;29(1):15-21. doi:10.1093/bioinformatics/bts635

49. Ewels P, Magnusson M, Lundin S, Käller M. MultiQC: summarize analysis results for multiple tools and samples in a single report. *Bioinformatics*. 2016;32(19):3047-3048. doi:10.1093/bioinformatics/btw354

50. Love MI, Huber W, Anders S. Moderated estimation of fold change and dispersion for RNA-seq data with DESeq2. *Genome Biol*. 2014;15(12):550. doi:10.1186/s13059-014-0550-8

51. Wickham H, Chang W, Henry L, et al. ggplot2: Create Elegant Data Visualisations Using the Grammar of Graphics. 2020. https://cran.r-project.org/package=ggplot2.

52. Martin M. Cutadapt removes adapter sequences from high-throughput sequencing reads. *EMBnet.journal*. 2011;17(1):10. doi:10.14806/ej.17.1.200

53. Kim D, Langmead B, Salzberg SL. HISAT: A fast spliced aligner with low memory requirements. *Nat Methods*. 2015;12(4):357-360. doi:10.1038/nmeth.3317

54. Pertea M, Pertea GM, Antonescu CM, Chang T-C, Mendell JT, Salzberg SL. StringTie enables improved reconstruction of a transcriptome from RNA-seq reads. *Nat Biotechnol*. 2015;33(3):290-295. doi:10.1038/nbt.3122

55. Frazee AC, Pertea G, Jaffe AE, Langmead B, Salzberg SL, Leek JT. Ballgown bridges the gap between transcriptome assembly and expression analysis. *Nat Biotechnol*. 2015;33(3):243-246. doi:10.1038/nbt.3172

56. Anders S, Pyl PT, Huber W. HTSeq--a Python framework to work with high-throughput sequencing data. *Bioinformatics*. 2015;31(2):166-169. doi:10.1093/bioinformatics/btu638

57. Seyednasrollah F, Laiho A, Elo LL. Comparison of software packages for detecting differential expression in RNA-seq studies. *Brief Bioinform*. 2015;16(1):59-70. doi:10.1093/bib/bbt086

58. Sanz E, Evanoff R, Quintana A, et al. RiboTag Analysis of Actively Translated mRNAs in Sertoli and Leydig Cells In Vivo. Schlatt S, ed. *PLoS One*. 2013;8(6):e66179. doi:10.1371/journal.pone.0066179

59. Muller PA, Matheis F, Schneeberger M, Kerner Z, Jové V, Mucida D. Microbiota-modulated CART + enteric neurons autonomously regulate blood glucose. *Science (80-)*. 2020;6176(August):eabd6176. doi:10.1126/science.abd6176

CHAPTER THREE: EARLY LIFE STRESS PROMOTES ‘FEMINIZATION’ OF ENTERIC GLIA IN MALE MICE

ABSTRACT

Both early life stress (ELS) and sex are risk factors for development of gastrointestinal disorders of the gut-brain axis including irritable bowel syndrome (IBS). The enteric nervous system and enteric glia are altered in IBS but the molecular changes in enteric glia following ELS that contribute to disease pathogenesis are unknown. Here we investigated molecular contributions to altered signaling pathways in the neonatal maternal separation (NMS) model for ELS using RNA-sequencing. Functional changes in enteric glia are supported by differential gene expression and pathway analysis and select genes were validated *in situ* with RNAscope. These data uncovered physiologic differences in enteric glia between male and female mice in addition to sex-specific responses to ELS. Enteric glia from NMS male mice upregulate many of the same genes that are increased in females compared with males suggesting that enteric glia from male mice 'feminize' following ELS. These shared differentially expressed genes are within pathways implicated in GI and neurological disease and aspects of type I interferon (IFN) signaling. G protein-coupled receptor (GPCR) signaling is also differentially regulated in males and females and in females following ELS. These data support novel molecular differences between enteric glia from male and female mice and suggest potential mechanisms that may contribute to sexually dimorphic gastrointestinal disease presentation. We anticipate that the dataset presented here will be valuable for understanding the molecular basis of gastrointestinal disorders and for understanding basic roles of enteric glia in health and disease.

INTRODUCTION

Physical and psychosocial stress is associated with many common GI disorders and predisposes individuals to developing some diseases and exacerbates symptoms in others.[1–3] Stress dysregulates communication along the gut-brain axis such as hypothalamic-pituitary-adrenal signaling to exacerbate gut inflammation and alter functions such as colonic motility and visceral hypersensitivity. These ultimately contribute to the symptoms of GI disorders including abdominal pain and altered bowel habits.[1–4] Early life stress (ELS) in particular influences the host during critical developmental periods for many organ systems and is a major risk factor for persistent gastrointestinal (GI) disease in adulthood. ELS specifically contributes to developing disorders of the gut-brain axis (previously categorized as functional bowel disorders)[5] such as irritable bowel syndrome (IBS).[4,6–17] Indeed childhood histories including poor socioeconomic status, physical trauma, and emotional or sexual abuse are significantly associated with IBS and symptoms of recurrent functional abdominal pain into adulthood.[10,13] This is recapitulated in animal models of ELS where neonates exposed to psychological stressors develop persistent increased pain responsiveness and bowel transit into adulthood.[9,15,17] Collectively these findings highlight the importance of biopsychosocial factors in GI dysfunction.[12,16]

This relationship is complicated by sex, where both GI disease prevalence and the impact of ELS on GI disease vary between sexes and suggest sex-specific underlying mechanisms.[9–13,15,17] Disorders of the brain-gut axis such as IBS are more prevalent in females and the impact of ELS on IBS diagnosis is identified primarily in female patients.[10,12,16] Similarly females animals are more likely to have increased visceral hypersensitivity, mucosal permeability, and diarrhea following ELS.[9,11,15,18] Taken together these data suggest the impact of ELS on GI disorders is clearer in females than males. However evidence still supports a role for ELS in males that may be more context-dependent. Specific emotional stressors including feeling alone or insignificant correlated with IBS in males even though general physical, emotional, and sexual abuse did not.[10] Furthermore, IBS symptom severity is associated with perceived athletic or physical competence

in males while associated with social competence in females.[19] This is further supported in rodents where different ELS models affect males differently and specific models increase visceral hypersensitivity in males while others do not.[17] Collectively these studies highlight the importance and also complexity of sex in the relationship between ELS and GI disorders but how ELS alters mechanisms differently between males and females to contribute to disease is unknown. Studying these sex-specific differences is essential for understanding mechanisms of GI pathogenesis and developing patient-targeted therapies.[12,16]

The enteric nervous system (ENS) is the vast neural network housed within the digestive tract and is a critical component of brain-gut communication.[2,20] The ENS consists of neurons and glia that help regulate many GI functions including motility, visceral sensation, secretion, absorption, immune communication, and mucosal permeability.[20,21] The postnatal early life period is critical in ENS development during which ganglia form and neurons functionally differentiate to establish appropriate neurocircuitry.[22,23] This developing framework is not only affected by cell growth but also cell death and pruning to maintain the appropriate balance to coordinate complex ENS functions,[24–26] requiring important timing and integration of molecular signatures in the ENS microenvironment.[21,27–29] Perturbations during this critical period lead to altered ENS composition and function in adulthood. Increased proportions of cholinergic neurons, subsequent cholinergic activity,[9,30] and mast cell infiltration occur in adult animals following ELS.[15,31] These compositional changes likely contribute to ENS-driven pathologies including secretomotor function but the specific mechanisms that link ENS changes to altered function after ELS are poorly understood.

Even less is known about the impact of ELS on enteric glia than is known about enteric neurons. Glia in the central nervous system are key players in stress response and integrate molecular stress signals to modulate neuroinflammation that ultimately determines the physiologic outcomes of acute and chronic stress.[32,33] Enteric glia are important in regulating canonical functions of the ENS through communication with both enteric neurons and other cells types within the GI tract including coordinating secretomotor reflexes and modulating neuronal

survival.[34–40] They also communicate with extrinsic sensory neurons and immune cells to regulate visceral hypersensitivity and neuroinflammation.[40–43] Enteric glia are morphologically altered in IBS[31,41,44–46] but the specific contribution of enteric glia to developing functional disease are unclear. Furthermore how underlying sex differences affect these mechanisms and contribute to disease susceptibility are completely unknown. Characterizing sex-specific mechanisms in critical cells of gut-brain axis communication such as enteric glia is essential for understanding the underpinnings of sexually dimorphic GI disease development and creating appropriate targeted therapies.[12,16]

The goal of this work was to study how changes to the molecular structure of enteric glia contribute to gastrointestinal pathophysiology caused by ELS and identify molecular differences in glia from males and females that may underlie these changes. We hypothesized that enteric glial gene expression patterns are sexually dimorphic and determine sex-specific disease responses. We tested this hypothesis using the neonatal maternal separation plus early weaning (NMS + EW) model for ELS in male and female RiboTag mice that genetically express the HA tag on enteric glial ribosomes. From these mice we immunoprecipitated glial transcripts and performed RNA-sequencing to capture glial-specific gene expression profiles. Our results show that enteric glia exhibit distinct transcriptional profiles in male and female mice. Unexpectedly, exposure to ELS shifts enteric glial expression patterns to become more similar between males and females. This is driven in large part by ‘feminization’ of enteric glia from male mice where these expression profiles become more female-like. Sex-dependent shifts highlight important differences in canonical glial signaling through g protein-coupled receptors (GPCRs) and immune communication through interferons (IFNs). These data provide the first database for sex-dependent enteric glial expression with and without early life stress and additionally suggest potential mechanisms enteric glia contribute to GI dysfunction following ELS.

MATERIALS AND METHODS

Animal use

All experimental protocols were approved by the Michigan State University Institutional Animal Care and Use Committee (IACUC) in facilities accredited by the Association for Assessment and Accreditation for Laboratory Care (AAALAC) International. Adult male and female C57BL/6 mice 10-16 weeks of age were used for all experiments unless stated otherwise. Mice were maintained in specific pathogen-free conditions and a temperature-controlled environment (Optimice cage system; Animal Care Systems, Centennial, CO) on a 12:12hr light-dark cycle with *ad libitum* access to water and minimal phytoestrogen diet (Diet Number 2919; Envigo, Indianapolis, IN).

Sox10$^{CreERT2+/-}$;*Rpl22tm1.1Psam*/J mice were generated as described previously[44] to express the hemagglutinin (HA) tag on ribosomes within enteric glial cells upon tamoxifen administration. This line was maintained as hemizygous for both Cre (*Sox10*$^{CreERT2+/-}$; a gift from Dr. Vassilis Pachnis, The Francis Crick Institute, London, England) and the floxed allele (*Rpl22*$^{tm1.1Psam}$/J; RRID:IMSR_JAX:011029; The Jackson Laboratory, Bay Harbor, ME). Mice were genotyped by Transnetyx (Cordova, TN) and fed tamoxifen citrate (400mg/kg) for 2 wks to induce HA expression. Specificity of HA expression for enteric glia was confirmed by immunofluorescence labeling and RNA-sequencing in previously work.[44]

Neonatal maternal separation and early weaning model of early life stress

NMS was conducted as previously described[31] and represented in **Fig 3.1a** (created with Biorender.com). Briefly, C57BL/6 pregnant nulliparous dams were isolated before giving birth. The first day pups were observed was denoted *postnatal day 0* (PN0). For control/normally handled (NH) groups, pups were raised under standard protocols and undisturbed in home cages until weaning at PN21-PN28. For the NMS +EW model mice were subjected to 3 hours of isolation (Zeitgeber + 3–6) from PN1-PN16 and weaned early at PN17. This separation was accomplished

by placing each pup in individual plastic cups containing small amounts of their own bedding. These cups were housed in another cage with 4-5 cups/cage. NMS mothers were also placed in a separate clean cage with access to food and water *ad libitum*. After the 3h separation both dams and pups were returned to their home cage with standard food, water, bedding, and day/night cycling and undisturbed until the next morning of separation.

Myenteric plexus isolation

Distal colonic myenteric plexus was dissected as previously described[44] to maintain RNA integrity. Briefly, mice were euthanized by cervical dislocation and subsequent decapitation. The distal half of colonic tissue from male and female NH and NMS *Sox10*$^{CreERT2+/-;Rpl22tm1.1Psam/J}$ mice was removed and placed in a petri dish containing ice-cold Dulbecco's Modified Eagle Medium (DMEM/F-12) surrounded by dry ice. Luminal contents were flushed with a syringe and a plastic rod (~3.2mm diameter) was inserted into the lumen. The longitudinal muscle-myenteric plexus (LMMP) was isolated by gently removing the mesenteric border and teasing away the LMMP from the underlying circular muscle using cotton swabs. For RNA-seq, LMMP samples were flash frozen in 1.5mL tubes in liquid nitrogen immediately and stored at -80°C until further processing. For RNAscope and immunohistochemistry, LMMPs were pinned flat in a sylgard-coated petri dish and fixed overnight in 4% paraformaldehyde (PFA) at 4°C. Fixed tissue was washed 3x10mins with 1x phosphate-buffered saline (PBS) and stored in 1x PBS at 4°C until further processing.

RiboTag procedure and RNA processing

Flash frozen distal colon LMMPs from *Sox10*$^{CreERT2+/-;Rpl22tm1.1Psam/J}$ mice were homogenized using a CryoGrinder™ (OPS Diagnostics, Lebanon, NJ) mortar and pestle cooled using liquid nitrogen. Samples were ground into a fine powder for 20-30s and transferred to an ice-cold 1.5mL tube. RiboTag isolation was performed on these homogenized samples as previously described with solution adjustments for gastrointestinal tissue.[47,48] Briefly, 1mL of

supplemented homogenization buffer (50mM Tris, pH 7.4, 100mM KCl, 12mM $MgCl_2$, 1% Nonidet P-40, 1mM DTT, 10mg sodium deoxycholate, 100µg/mL cyclohexamide, 20µL protease inhibitor (Sigma P8340), 10µL RNAse inhibitor (40U/µL), and 3mg/mL heparin in RNAse-free water) were added to each sample vial and mixed vigorously by pipetting. Samples were then centrifuged at 10,000*g* for 10mins and ~800µL of supernatant was transferred to a clean 1.5mL vial with 5µL HA antibody (Covance, MMS-101R). Samples were gently rotated on an Eppendorf tube rotator (Rotoflex R2000, Argos Technologies) for 4hr at 4°C. Samples were then added to 200µL Protein A/G beads (ThermoFisher) and gently rotated overnight at 4°C. The following day sample supernatants were removed using a magnetic stand on ice and sample beads were washed 3 x 10mins at 4°C with high salt buffer (50 mM Tris, pH 7.5, 300 mM KCl, 12 mM MgCl2, 1% Nonidet P-40, 1 mM DTT, 100 µg/mL cycloheximide)[49] and subsequently eluted with 350µL RLT Plus lysis buffer (Qiagen RNeasy Plus Micro Kit) with DTT.

Eluted mRNA was purified using the RNeasy Micro Kit Plus (Qiagen) and quantified using the Quant-IT™ RiboGreen® RNA Assay Kit (ThermoFisher) using the low range standards according to the manufacturers' protocols. RNA integrity number (RIN) was assessed using a 2100 Bioanalyzer and the Eukaryote Total RNA 6000 Pico chip (Aglient, Santa Clara, CA) and samples with RIN > 6.5 were used for sequencing.

RNA library preparation and sequencing

Libraries were prepared by the Van Andel Genomics Core (Grand Rapids, MI) from 1 ng of total RNA using Takara SMART-Seq Stranded Kit (Takara Bio USA, Mountain View, CA) per the manufacturer's protocol. In brief, RNA was sheared to 300-400 bp, after which dsDNA was generated using a template switching mechanism and unique dual indexed adapters were added to each sample. Ribosomal cDNA was degraded by scZapR and scrRNA probes and libraries amplified with 12 cycles of PCR. Quality and quantity of the finished libraries were assessed using a combination of Agilent DNA High Sensitivity chip (Agilent, Santa Clara, CA), QuantiFluor®

dsDNA System (Promega Corp., Madison, WI), and Kapa Illumina Library Quantification qPCR assays (Kapa Biosystems). Individually indexed libraries were pooled and 100 bp, single-end sequencing was performed on an Illumina NovaSeq6000 sequencer (Illumina Inc., San Diego, CA), to return a minimum read depth of 30M read pairs per library. Base calling was done by Illumina RTA3 and output of NCS was demultiplexed and converted to FastQ format with Illumina Bcl2fastq v1.9.0.

To increase read depth and power the same libraries were re-sequenced to achieve a minimum aligned read depth of 30M read pairs per sample. Technical replicates were combined after generating read counts using the 'CollapseReplicates' in DESeq2.[50] FastQ files for both technical replicates will be available at the NCBI Gene Expression Omnibus upon publication.

RNA-sequencing analysis

RNA-sequencing (RNA-seq) analysis from FastQ to count files was supported through computational resources provided by the Institute for Cyber-Enabled Research at Michigan State University. Quality control of RNA-seq data was performed using FastQC v0.11.7 (Babraham Bioinformatics) and compiled using MultiQC v1.7.[51] Low-quality bases and adapters were trimmed using TrimGalore v0.6.5 (Babraham Bioinformatics). Reads were aligned to the GRCm38 (mm10) mouse genome using STAR v2.7.3a[52] and reads were counted using HTSeq v0.11.2.[53]

Count visualization, normalization, and differential expression analysis were performed in R v4.0.5[54] and utilized packages dplyr v.1.0.5,[55] tidyverse v1.3.0,[56] and readr v1.4.0[57] to organize data. Low-expression read counts were filtered from DESeq2[50] normalized counts tables (median of ratios method) using zFPKM v1.12.0[58] and excluded from analysis. For normal handled (NH) comparisons between males and females BioMart[59] was used to generate chromosome X and Y annotations to remove these genes from analysis. Principal component analyses (PCA) and volcano plots were generated in DESeq2 v1.30.1[60] and visualized using ggplot2 v3.3.3[61] with ggforce v0.3.3[62] and ggrepel 0.9.1.[63] Hierarchical clustering heatmaps were generated in DESeq2

v1.30.1[60] and visualized using pheatmap v1.0.12.[64] Count normalization and differential expression was performed in DESeq2 v1.30.1[60] where modeling adjusted for RIN and results shrunk using ashr v2.2-47.[65] Gene symbol and other identifying information were determined from Ensembl ID using AnnotationDbi v1.52.0[66] and org.Mm.eg.db v3.12.0.[67] Knitr v.1.31[68] was used to export R package citations. Pathway analyses were performed using Gene Set Enrichment Analysis (GSEA) v4.1.0[69,70] and Ingenuity Pathway Analysis (IPA) (QIAGEN Inc., https://www.qiagenbioinformatics.com/products/ingenuity-pathway-analysis). Scripts and code utilized in this analysis are available upon request.

RNAscope in whole mount LMMP

RNAscope in whole mount myenteric plexus LMMP tissue was adapted from previous protocols[71] using the RNAscope™ 2.5 HD Assay – RED (ACD Biosciences, Newark, CA; cat no. 322350) according to manufacturer instructions with the following adjustments for colonic LMMP tissue. Tissue was dehydrated and subsequently rehydrated by a serial ethanol gradient (25%, 50%, 75%, 100% in 1x PBS with 0.1% Triton X-100) prior to H_2O_2 treatment. Tissue was then digested with Protease III for 45 mins and incubated with RNAscope probes overnight at 40°C. Tissue was washed 3x5mins between each step with 1x PBS after protease and FastRED steps and 1x RNAscope™ wash buffer after probe and amplification steps. All RNAscope steps were performed in a 96-well place while wash steps were performed in a 48-well plate. Following completion of the RNAscope protocol immunohistochemistry and tissue mounting was performed as described below. Specificity of RNAscope labeling was determined by manufacturer negative and positive control probes and probes for enteric neuronal and enteric glial-specific transcripts combined with immunolabeling of enteric neurons and glia (see Chapter 2, **Fig 2.2** and Ahmadzai et al., in review at JCI). RNAscope probe details are provided in **Table 3.1**.

Immunohistochemistry in whole mount LMMP

Immunohistochemistry (IHC) was performed as described previously.[31,44] Primary and secondary antibody details are provided in **Table 3.1**. Briefly, LMMP preparations were washed 3x10mins in PBS with 0.1% Triton X-100 followed by 45min incubation in blocking solution (4% normal donkey serum, 0.4% Triton X-100, and 1% bovine serum albumin) at 20°C. Primary antibodies were diluted in blocking solution and incubated with tissue for 24-48hrs at 4°C. Primary antibodies were removed and tissue was washed 3x10mins in 1x PBS and incubated with secondary antibodies diluted in blocking solution for 2hrs at 20°C. LMMP preparations were then rinsed 2x10mins in 1xPBS followed by 1x10mins in 0.1M phosphate buffer. Tissue was then mounted on slides with Fluoromount-G mounting medium with or without DAPI (Southern Biotech, Birmingham, AL). Specificity for antibodies used were previously validated.[31,36,40,44]

Imaging

All RNAscope and IHC imaging was performed on a Zeiss LSM 880 NLO confocal system (Zeiss, Jena, Germany) using Zen Black software and a 20x objective (0.8 numerical aperture, Plan ApoChromat; Zeiss). 40x images were achieved using digital zoom within the software.

Statistical Analysis

Statistical analysis of RNA-seq was performed by DESeq2[50] where a false discovery rate (FDR) < 0.1 was considered significant. FDR < 0.1 and $\log_2$fold-change > 0.58 were used to perform IPA. Data from these analyses were visualized as bar graphs using GraphPad Prism v9.2.0 (GraphPad Software, San Diego, CA).

Table 3.1 RNAscope probes and IHC antibodies used in Chapter 3.

RNAscope Probes			
Probe Target	*Vendor*	*Catalog Number*	*Channel*
Ifit1	ACD Bio-Techne	500071	C1
Oasl2	ACD Bio-Techne	534501	C1
Rgs5	ACD Bio-Techne	430181	C1
Xist	ACD Bio-Techne	454231	C1
Immunohistochemistry (IHC) Antibodies			
Primary antibodies			
Target	*Vendor*	*Catalog Number*	*Dilution*
Chicken anti-GFAP	Abcam	ab4674	1:1000
Rabbit anti-HA(C29F4)	Cell Signaling	3724	1:500
Mouse anti-Peripherin	Santa Cruz	sc-377093	1:100
Rabbit anti-S100β	Abcam	ab52647	1:200
Secondary antibodies			
Goat anti-chicken Dylight 405	Jackson Laboratories	103-475-155	1:400
Donkey anti-mouse Alexa Fluor 488	Jackson Laboratories	715-545-150	1:400
Donkey anti-rabbit Alexa Fluor 594	Jackson Laboratories	711-585-152	1:400
Donkey anti-rabbit Alexa Fluor 647	Jackson Laboratories	711-605-152	1:400

RESULTS

Enteric glia regulate homeostasis within enteric neurocircuits and changes in how glia function are thought to contribute to the pathophysiology of gut-brain axis disorders.[31,41,44–46] Early life stress predisposes individuals to developing a gut-brain axis disorder, but it is not clear how glia might contribute to the lasting effects of early life stress on gut functions. Moreover, the molecular toolkit that enteric glia use to carry out their diverse roles, how these may differ between males and females, and how they are affected by exposure to early life stress is not understood. We performed RNA-sequencing (RNA-seq) to study the molecular structure of enteric glia in colon myenteric plexus of male and female mice glia-specific RiboTag mice (*Sox10*$^{CreERT2+/-}$;*Rpl22tm1.1Psam/J*, referred to here as Sox10-RiboTag) and studied glial changes that occur following early life stress using the neonatal maternal separation and early weaning (NMS + EW, referred to here as NMS) mouse model. Immediately after birth (on day PN1) Sox10-RiboTag litters underwent NMS or normal handling and weaning (NH) (**Fig 3.1a**). Mice were euthanized in adulthood and distal colon longitudinal muscle-myenteric plexus (LMMP) was collected and processed for RNA-seq. Immunoprecipitation of the HA tag on glial-specific ribosomes (RiboTag) was effective at enriching glial cell-specific transcripts compared to canonical markers of other LMMP cells including enteric neurons and smooth muscle cells (**Fig 3.1b**).[72–75] Immunolabeling also demonstrated that the HA tag was localized to glia in the myenteric plexus and not the surrounding enteric neurons or smooth muscle cells (**Fig 3.1c**).

Enteric glial gene expression is sex-dependent and more variable in female mice

We performed RNA-seq on four different groups (NH males, NH females, NMS males, and NMS females) to investigate baseline sex differences and sex-specific responses to ELS in enteric glia. Principal component analysis (PCA) of these data show distinct expression patterns among enteric glia isolated from males and females (**Fig 3.1d**) even when sex chromosome genes are removed (**Fig 3.1d'**). This is further supported by the large overlap of top genes

contributing to PCA axes 1 and 2 (**Fig 3.1e-e'**). Furthermore control (NH) male glial expression patterns are less variable than females. Sex differences in glial expression are unknown as there are very few enteric glia-specific transcriptional studies to date and these do not sex-stratify their data.[44,72,76] In our RNA-seq analysis we first compared glial transcripts between control (NH) male and female mice to determine physiologic sex differences. Many genes are differentially expressed between enteric glia from NH male and NH female mice and the majority of these genes are located on somatic chromosomes (log_2fold-change > ± 0.58, FDR < 0.1; **Fig 3.2a**), suggesting that X and Y chromosome genes do not reflect relatively large differences in enteric glial gene expression between male and female mice. These include genes involved in immune regulation like genes for the lymphotoxin beta receptor (*Ltbr*) that is increased in females and complement proteins (*C3* and *C4b*) that are decreased in females. Enteric glia from females also express 14 solute carrier genes higher than enteric glia from males including *Slc4a8, Slc24a3, Slc6a17,* and *Slc33a19*. These genes code for transport proteins that mediate the influx and efflux of several metabolic molecules across cell membranes and are linked to several metabolic diseases.[77]

The majority of these differentially expressed genes are located on somatic chromosomes and suggest fundamental differences in expression profiles of enteric glia between male and female mice independent of sex chromosomes. This includes genes important for PCA axes (**Fig 3.1e-e'**) that are increased in females such as genes involved in metabolism including ATP binding cassette *Abcg5*, cobalamin binding intrinsic factor (*Cblif*), and proline dehydrogenase 2 (*Prodh2*) and genes regulating cellular division like meiotic division factor *Rmnd1*. Since many of the genes contributing to PCA are differentially expressed between control (NH) male and female mice sex is an important contributor to variation in glial gene expression. Interestingly enteric glia from female mice primarily have increased gene expression compared to enteric glia from male mice (**Figs 3.2a** in red, **3.2b-b'** and **3.2c-c'**) and only 42-50 genes decreased in females compared to males (**Fig 3.2a**). These include genes involved in regulating gene expression like

transcription factor high mobility group protein B1 (*Hmgb1*) and microRNA containing gene (*Mirg*) and genes involved in inflammatory and immune response such as glutathione S transferase alpha 4 (*Gsta4*), superoxide dismutase 3 (*Sod3*), transforming growth factor beta 2 (*Tgfb2*), and major histocompatibility complex genes (*H2-T23, H2-Q4, H2-K1,* and *H2-D1*). Additional genes decreased in females are involved in cellular structure and adhesion such as metallopeptidases (*Adamts10* and *Adam33*), collagens (*Col12a1* and *Col16a1*), integrins (*Itga1*), and protocadherins (*Pcdhga6*). We then visualized differential expression of some genes in the myenteric plexus using RNAscope, where gene transcripts are visible as punctae and cell-specific expression is assessed by immunofluorescence labeling and co-localization with the glial cell marker S100β. We first demonstrated the viability of this method by examining expression of X chromosome gene X-inactive specific transcript (*Xist*) in the myenteric plexus of control (NH) males and females. As supported by our RNA-seq data (**Fig 3.2c**) *Xist* is much more highly expressed in myenteric plexus and enteric glia from female mice compared to male mice (**Fig 3.2d**). This is demonstrated by lack of *Xist* signaling in NH male myenteric plexus and additionally overlap of *Xist* signal with $S100\beta^+$ enteric glial cell bodies. Taken together these data support fundamental signaling differences in enteric glia between male and female mice.

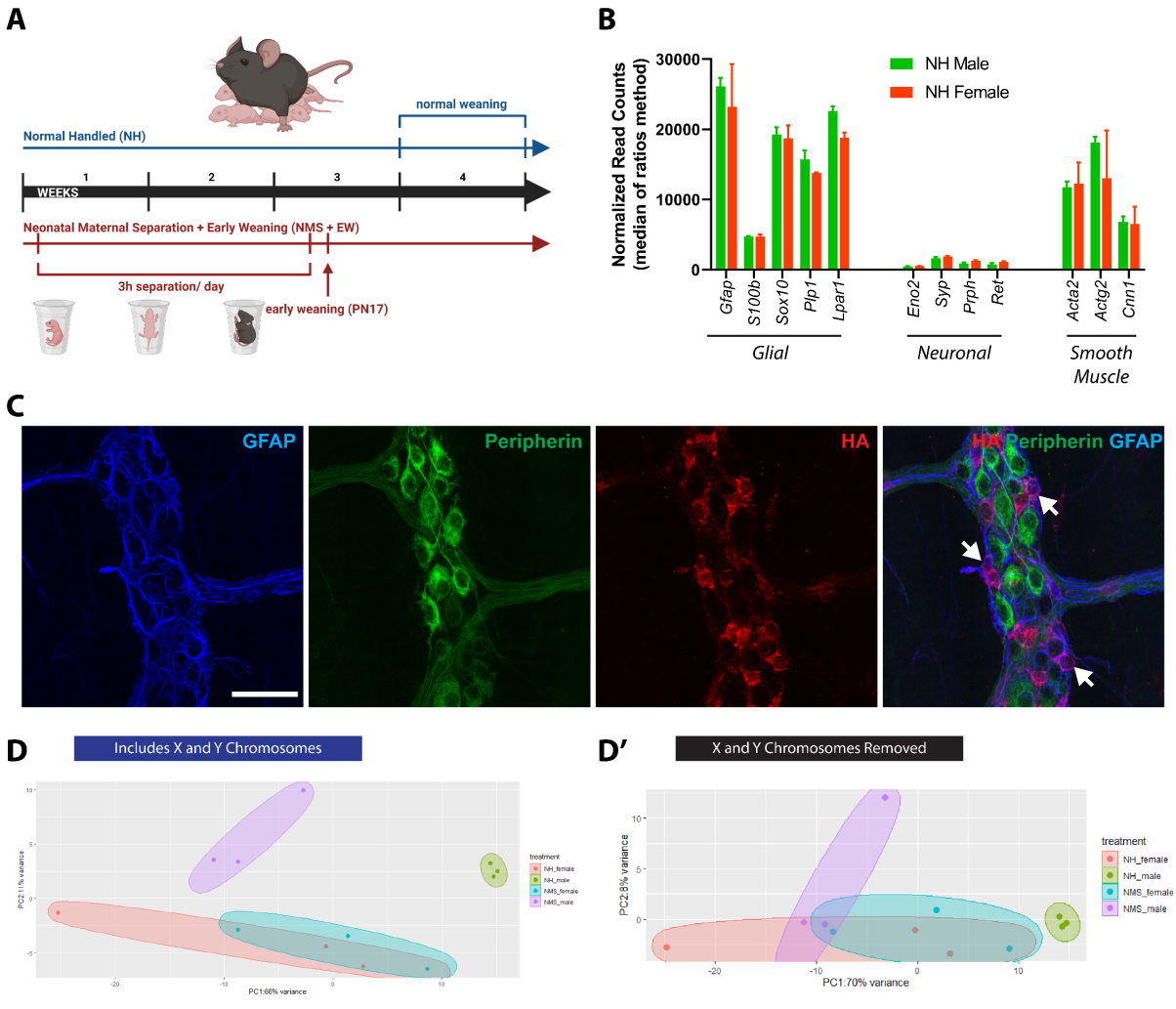

E

PC1 Genes		PC2 Genes	
Gene Symbol	Loading Score	Gene Symbol	Loading Score
Abcg5	-0.10733	*Xist*	0.2193
Ebpl	-0.09587	*Ddx3y*	-0.18631
Cblif	-0.09169	*Tcaf3*	-0.14932
Ttll11	-0.09165	*Uty*	-0.11033
Prodh2	-0.0916	*Kdm5d*	-0.10774
LOC115488869	-0.09038	*9530053A07Rik*	-0.09803
Dnah1	-0.08724	*Eif2s3y*	-0.07964
Rmnd1	-0.08624	*Rgs5*	0.066193
Vmn1r193	-0.08311	*Hspb7*	0.062225
Olfr474	-0.08199	*Rpph1*	0.058134
Baiap2l2	-0.08113	*Top2a*	0.054539
Dio3os	-0.08092	*Ciart*	-0.05001
Vmn1r217	-0.07991	*Apod*	-0.0499
Snrpg	-0.07917	*Mki67*	0.048437
Olfr592	-0.0753	*Cenpf*	0.048173
Rasd1	-0.07355	*Thbs1*	0.047847
Vwc2l	-0.07343	*Zbtb16*	0.047724
Mrpl11	-0.07262	*Pigr*	-0.04759
Msh5	-0.07226	*Fbxl22*	0.045139
Hoxaas3	-0.06903	*Prc1*	0.044364

E'

PC1 Genes		PC2 Genes	
Gene Symbol	Loading Score	Gene Symbol	Loading Score
Abcg5	-0.10868	*Tcaf3*	0.097206
Gm16072	-0.10846	*Snord34*	-0.06114
Ebpl	-0.09713	*Snord87*	-0.05901
Ttll11	-0.0928	*Gm16072*	0.058877
Cblif	-0.09279	*Car3*	-0.05798
Prodh2	-0.09266	*Gm25935*	0.056692
Gm25935	-0.09157	*Prodh2*	0.054327
Dnah1	-0.08835	*Myh4*	0.053908
Rmnd1	-0.08697	*Snord55*	-0.05382
Vmn1r193	-0.08409	*9530053A07Rik*	0.053011
Olfr474	-0.08311	*Gm24494*	0.054539
Baiap2l2	-0.08212	*Rny3*	-0.05267
Dio3os	-0.08199	*Abcg5*	0.051636
Vmn1r217	-0.08092	*Ttll11*	0.051091
Snrpg	-0.08019	*Snord104*	0.050506
Olfr592	-0.07615	*Fabp4*	-0.04886
Rasd1	-0.07448	*Vmn1r193*	-0.04662
Vwc2l	-0.07435	*Serpina3m*	0.045177
Mrpl11	-0.0736	*Ebpl*	0.044923
Msh5	-0.07318	*Lypd8*	-0.04382

Figure 3.1 Enteric glia have sex-specific expression patterns physiologically and in response to early life stress.

(A) Schema of the neonatal maternal separation and early weaning (NMS + EW) model (created with Biorender.com). NH control mice are handled as normal until weaning at PN21-28 while NMS mice are isolated for 3 hours/day from PN1-16 and weaned early at PN17. **(B)** RNA-seq of myenteric plexus from *Sox10*$^{CreERT2+/-;}$*Rpl22tm1.1Psam*/J (Sox10-RiboTag) mice are enriched for glial gene markers compared to neuronal or smooth muscle gene markers in both males and females (n=3 mice/group). **(C)** The HA tag in Sox10-RiboTag mice is specific for enteric glia as determined by overlap of HA signal (red) with enteric glial cell bodies (small cells within the ganglia surrounded by GFAP^{+} blue processes) and not enteric neurons (peripherin, green). Representative locations of HA within glial cell bodies are denoted by white arrows. Images representative of data from n=3 mice. Scale bar represents 50µm. **(D-D')** Principal component analysis (PCA) including **(D)** and without **(D')** sex chromosomes X and Y. NH males are indicated in green, NH females in salmon, NMS males in purple, and NMS females in blue. Enteric glia differ between male and female NH mice and are less variable in NH male mice than all three other groups. **(E-E')** Top genes determining PCA axes for PC1 and PC2 including **(E)** and without **(E')** sex chromosomes demonstrate overlap of several genes that contribute to PCA variation in both analyses.

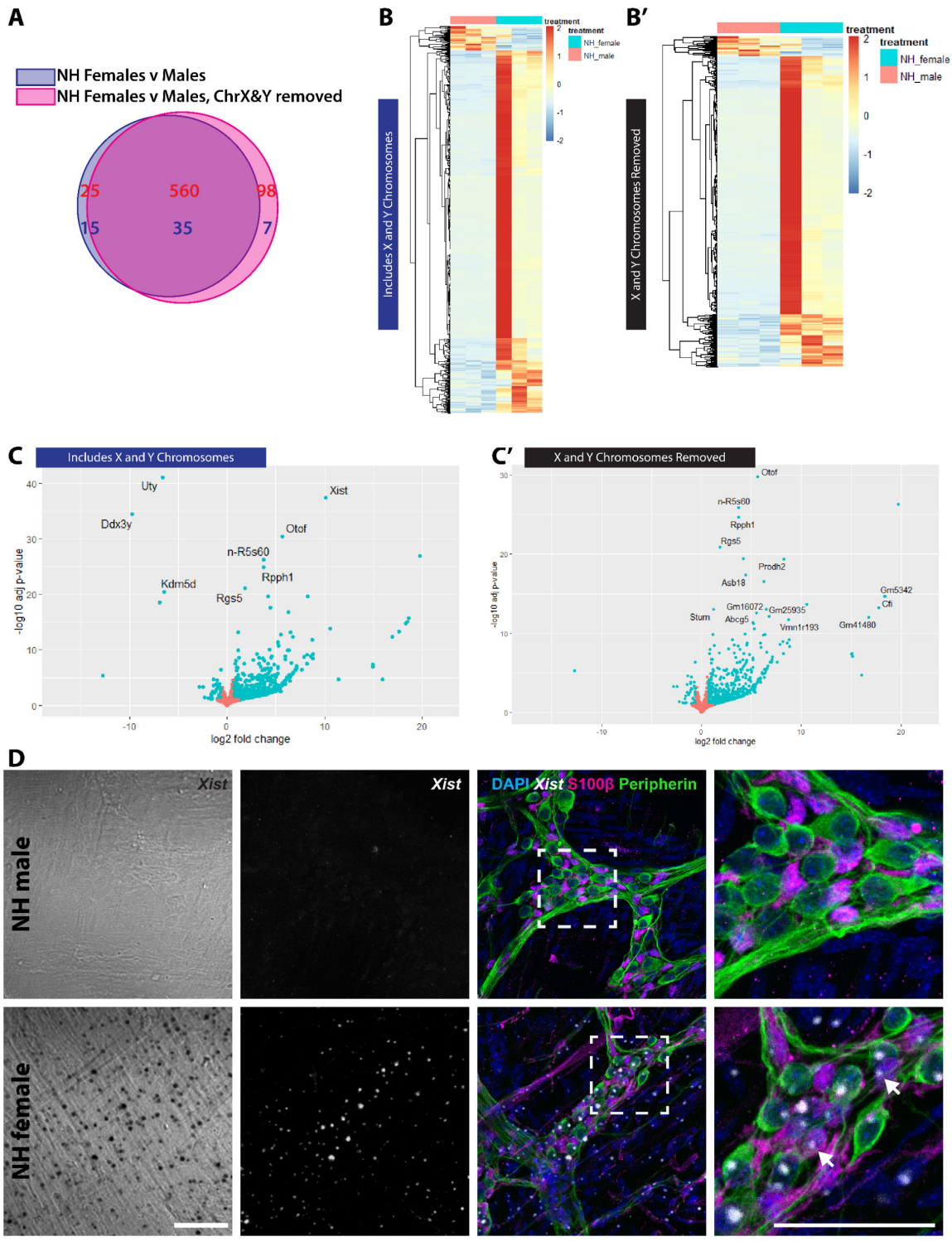

Figure 3.2 Enteric glia have higher expression of differentially expressed genes in females compared males.

(A) Venn diagram illustrating differential gene expression between enteric glia from male and female mice. Many of these differentially expressed genes are from somatic chromosomes and indicate fundamental sex-differences in enteric glial gene expression, as demonstrated by the high degree of overlap between analyses with and without sex chromosomes (overlap of blue and pink circles). Numbers in red represent genes with increased expression in NH females while numbers in blue represent genes with decreased expression in NH females (log_2fold-change > ± 0.58 and FDR < 0.1, n=3mice/group). **(B-B')** Hierarchical clustering and heatmaps of NH female (columns with blue color in treatment) and NH male (columns with salmon color in treatment) relative gene expression with **(B)** and without **(B')** sex chromosomes. Genes relatively increased in NH males or females are red while genes relative decreased are in blue. **(C-C')** Volcano plots of NH female compared to NH male enteric glial gene expression with **(C)** and without **(C')** sex chromosomes. Gene with significant differential expression (FDR < 0.1) are represented by blue dots. All data are restricted by log_2fold-change > ± 0.58 and FDR < 0.1 (n=3mice/group). **(D)** *Xist* (demonstrated in brightfield and fluorescence, first and second column respectively) RNA expression is higher in myenteric ganglia and enteric glia from NH female mice than NH males. Panels in final column represent magnified images within white dotted boxes of previous column. Glial cell bodies are represented by S100β in magenta and neurons by peripherin in green. Enteric glial *Xist* expression is highlighted by white arrows. Images representative of n=2 mice/group. Scale bars represent 50μm.

Early life stress promotes 'feminization' of enteric glial expression patterns in male mice

NMS alters glial morphology in both male and female mice in addition to increasing histamine$^+$ cells in the myenteric ganglia of male mice.[31] However, the specific molecular and sex-dependent changes that occur in enteric glia following NMS are unknown. We analyzed sex-specific responses to early life stress by comparing NMS males to NH males and NMS females to NH females. Interestingly, differential gene expression patterns of enteric glia in response to early life stress are sex-specific and differentially expressed genes in males are completely different from those in females where < 1% of differentially expressed genes are altered in both males and females in response to ELS (**Fig 3.3a**). Gene expression patterns in enteric glia from male mice shift more dramatically than those from female mice in response to ELS both in the number of differentially expressed genes and the magnitude of expressional changes as the $\log_2$fold-change values of differentially expressed genes in male mice are as high as 20 while in the 2.5 range in females (**Fig 3.3c-c'**) Furthermore, enteric glia from males predominantly increase gene expression in response to ELS while female glia tend to downregulate genes. This is visualized by heatmaps of different expression (**Fig 3.3b-b'**) where males upregulate most differentially expressed genes following ELS (**Fig 3.3b**, *salmon/pink left three columns*) while females downregulate most genes following ELS (**Fig 3.3b'**, *salmon/pink left three columns*). Taken together these data suggest that the molecular response of enteric glia following ELS is highly sex-specific.

Early life stress can promote feminization in male rats indicated by increased serum estradiol and decreased anogenital distance.[78] Similarly, male enteric glial gene expression patterns became more similar to females following ELS (**Figs 3.1d-d'** and **3.4a**). Almost half of differentially expressed genes between NH female or NMS males compared to NH males are shared and similarly up- or downregulated. This overlap supports the concept of 'feminization' of enteric glia from male mice in response to ELS. Many genes for olfactory receptors are upregulated in both NH females and NMS males including *Olfr474, Olfr592,* and *Olfr967*. Only 1

of the 15 olfactory receptors, *Olfr1042*, significantly differentially expressed in males following ELS is not differentially expressed in control (NH) females Interestingly X chromosome gene *Xist* is also slightly increased in males following ELS (**Fig 3.4b**). The function of *Xist* expression in males is unknown[79]; however, it is a canonically female-specific gene and its increased expression in NMS males may be indicative of female-like molecular changes in enteric glia. Additionally several genes upregulated in NH females compared to males that contributed to PCA variation are similarly upregulated in NMS mice compared to NH mice and further support them as important sources of variation between sexes and in males following ELS. These include *Ebpl, Abcg5, Ttll11, Otof,* and *Prodh2* that are both top genes for determining PCA axes 1 and 2 (**Fig 3.1e-e'**) and differentially expressed genes in control (NH) females compared to males (**Fig 3.2c-c'**). Strikingly even the magnitude of log_2fold-change of these genes is similar between males and females (**Fig 3.4b**) and further supports 'feminization' of these processes. 2',5'-oligoadenylate synthase-like protein 2 (*Oasl2*) is one of the few genes decreased in both NMS males and NH females compared to NH males. *Oasl2* plays a role in antiviral immunity and cancer and is expressed in cultured glia and neurons[80–83] but its expression and role in enteric glia is unknown. In situ hybridization data show that *Oasl2* is expressed by enteric neurons and glia in the myenteric plexus and that *Oasl2* expression in enteric glia tends to decrease following ELS (**Fig 3.4c**), as represented by decreased co-localization of RNAscope signal with S100β$^+$ cell bodies Collectively these data highlight sexually dimorphic responses to early life stress in enteric glia that partially 'feminize' enteric glia from male mice.

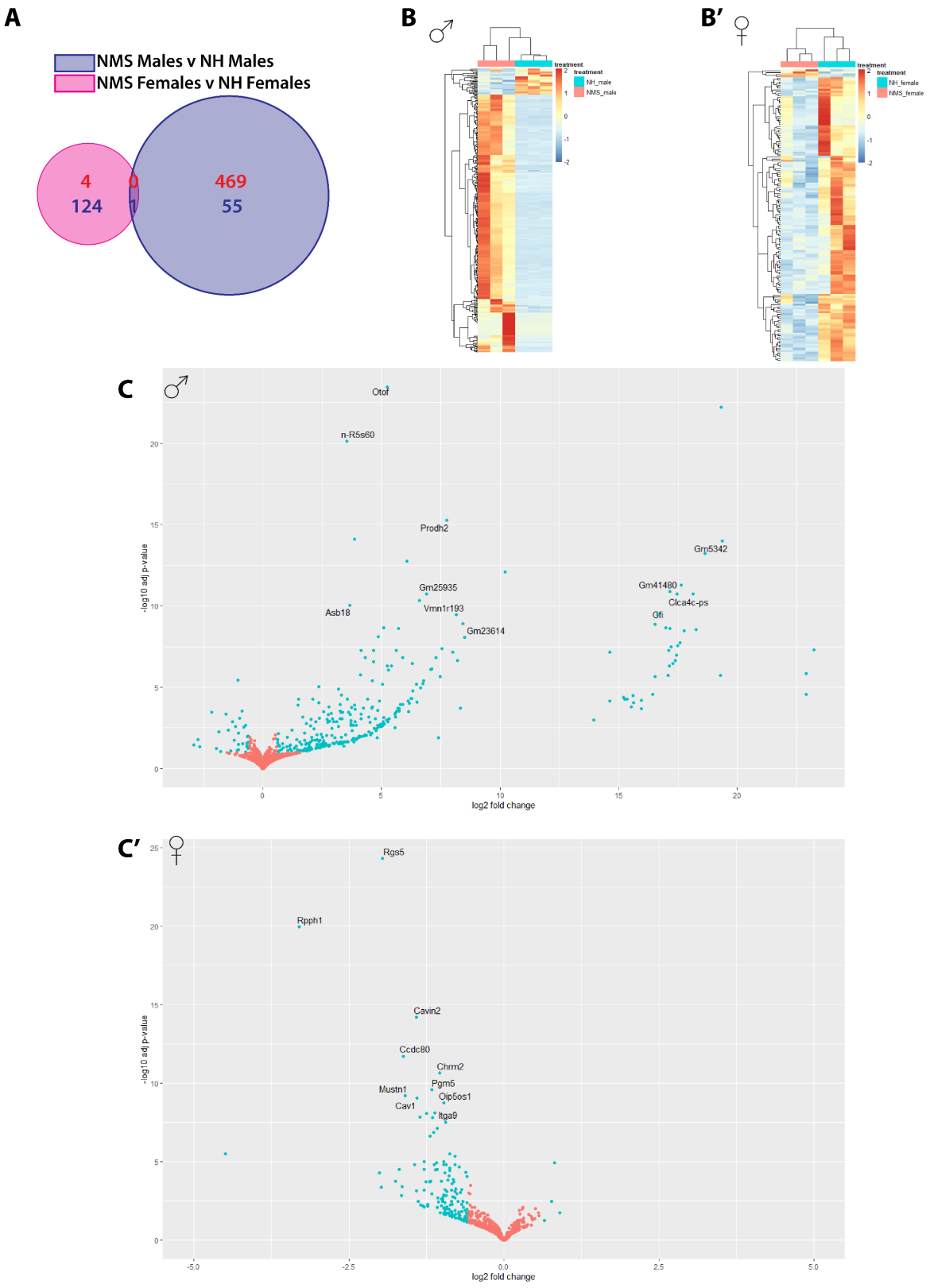

Figure 3.3 Differential gene expression in enteric glia following early life stress is sexually dimorphic.

(A) Venn diagram of shared and exclusive differentially expressed genes in enteric glia from male and female mice with ELS. Genes differentially expressed in males following ELS are in the blue circle while genes differentially expressed in females following ELS are in the pink circle. Upregulated gene numbers are written in red while downregulated gene numbers are written in blue. **(B-B')** Hierarchical clustering and heatmaps of differential expression following ELS in males **(B)** and females **(B')** demonstrating predominantly upregulated genes following ELS in males (**B**, *salmon/pink left three columns*) and downregulated genes following ELS in females (**B'**, *salmon/pink left three columns*). Genes with relatively increased gene expression following ELS are red while genes relatively decreased are blue. **(C-C')** Volcano plots of differential expression following ELS in males **(C)** and females **(C')** compared to NH control males and females, respectively. Genes with significant differential expression (FDR < 0.1) are represented by blue dots. All data are restricted by $\log_2$fold-change > ± 0.58 and FDR < 0.1 (n=3mice/group).

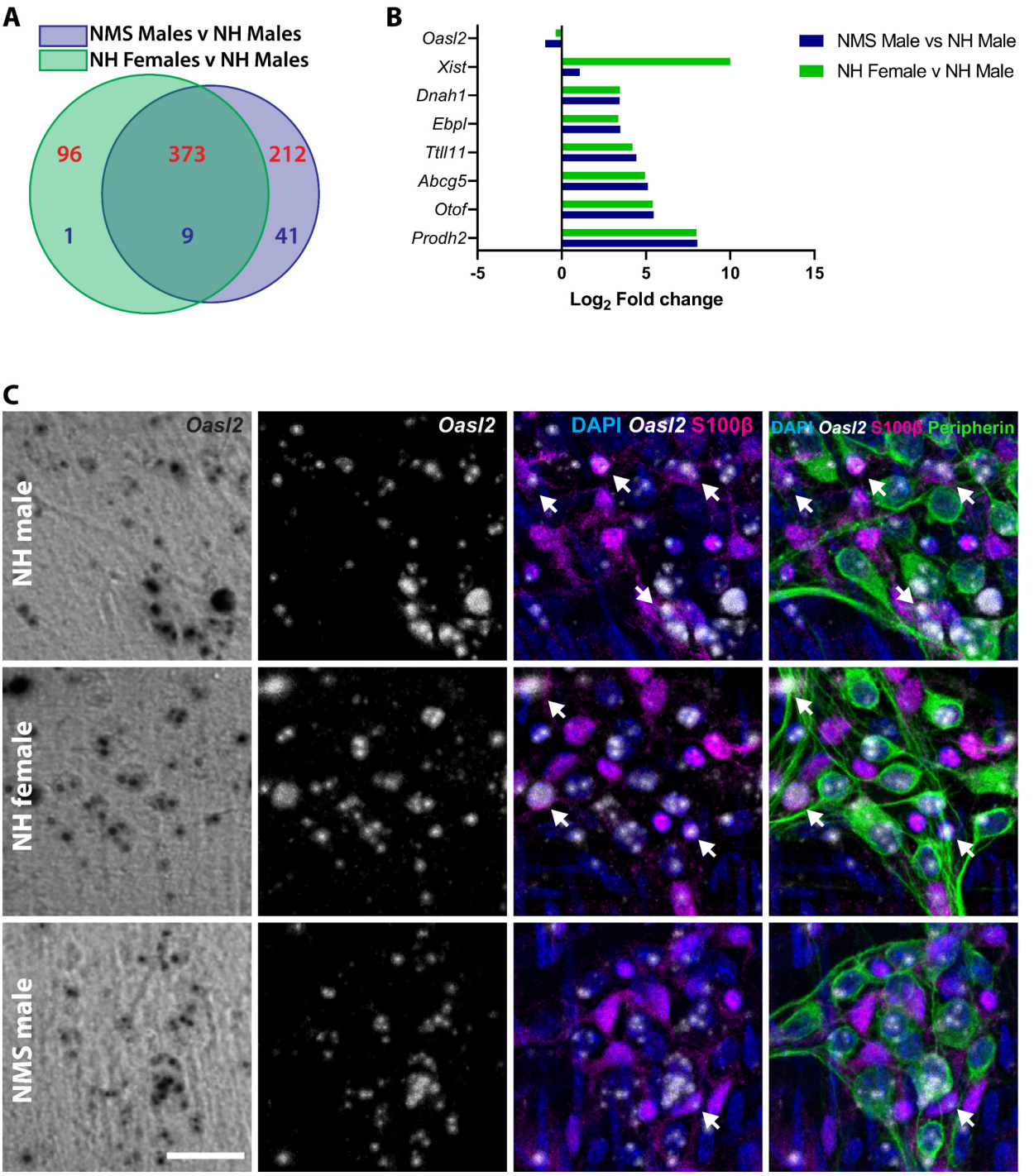

Figure 3.4 Enteric glial gene expression patterns in male mice are 'feminized' in response to early life stress.

(A) Venn diagram highlighting shared and exclusive differential expression patterns in males following ELS compared to NH males (blue circle) and NH females compared to NH males (green circle). The number of upregulated genes are written in red while downregulated genes are written

in blue. Differential expression patterns between these two groups are highly (~50%) shared as signified by the high overlap of blue and green circles. **(B)** Several differentially expressed genes and their log_2fold-changes are shared in comparisons between NMS males and NH males and between NH females and NH males. This includes *Oasl2*, which is downregulated in both NMS males and NH females in comparison to NH males. All data are restricted by log_2fold-change > ± 0.58 and FDR < 0.1 (n=3mice/group). **(C)** *In situ* RNA expression of *Oasl2* in the myenteric plexus using RNAscope (demonstrated in brightfield and fluorescence, first and second column respectively) is primarily expressed in enteric neurons (peripherin immunolabeling, green) but is also expressed in enteric glia (S100β immunolabeling, magenta). Enteric glial *Oasl2* expression is signified by co-localization of *Oasl2* with S100β and highlighted by white arrows. Glial *Oasl2* expression appears slightly lower in NH females (*middle row panels*) and moderately lower in NMS males (*bottom row panels*) compared to NH males (*top row panels*), similar to RNA-seq findings. Images representative of n=2 mice/group. Scale bar represents 25μm.

Early life stress and female sex alter expression pathways related to metabolic, gastrointestinal, and neurological disease in enteric glia

Gastrointestinal diseases like FBDs are more prevalent in females and the link between ELS and GI disease is clearer in females as well.[9–13,15,17] We performed pathway analysis on our RNA-seq data to determine if the enteric glial differential expression patterns we observed highlighted potentially shared functions as well. We first utilized Ingenuity Pathway Analysis (IPA) and uncovered several shared pathways altered in both NMS males and NH females when compared to NH males including interesting pathways in their 'Canonical Signaling' and 'Diseases & Functions' section (**Fig 3.5a**). Interestingly many of the differentially expressed genes are associated with gastrointestinal and neurological diseases in IPA's 'Diseases & Functions' analysis and suggest relevance to local GI and ENS function, respectively. Interestingly while the number of significant genes in each category is mostly similar between the two analyses, enteric glia from NH females appear to differentially express almost 3x more genes specifically related to GI disease (60 genes related to this pathway in NMS males and 273 in NH females when compared to NH males) suggests a stronger role for enteric glia in GI disease in females. Meanwhile differential immune response in both groups is suggested by the pathways 'Inflammatory Disease,' 'Inflammatory Response,' and 'Immunological Disease' while altered metabolism is suggested by 'Metabolic Disease' and 'Endocrine Disorders.' Taken together these data suggest that the genes that 'feminize' in enteric glia from males following ELS affect metabolism and glial-immune signaling. ELS and sex also affect gene expression related to neurologic and ENS function as suggested by shared pathways in the 'Canonical Pathways' section. These included pathways related to neuronal signaling like 'Endocannabinoid Neuronal Synapse Pathway,' 'CREB Signaling in Neurons,' and 'Synaptic Long Term Depression.' They also included pathways for G protein-coupled receptors (GPCRs) and calcium signaling that are fundamentally important for glial-neuronal communication.[37,39] We also assessed pathway-level changes using Gene Set Enrichment Analysis (GSEA) with our datasets. GSEA utilizes ranked

expression of genes to determine pathways instead of statistical cut-offs and therefore may provide different nuances in results. Representative rankings of gene expression generated for analysis within the Gene Ontology database are depicted in **Fig 3.5b** and highlight the top 50 most highly and lowly ranked genes that contribute to pathway findings. Overall this analysis found similar shared mechanisms between NH females and NMS males including metabolism, inflammation, and neurological function. However GSEA also provided more specified putative pathways including oxidative phosphorylation (**Fig 3.5c***, top panels*) and IFN-γ responses (**Fig3.5c**, *second panels*) from the Hallmark gene database. These are both enriched in NH males compares to NH females or NMS males suggesting parallel changes in energy regulation and immune function. Altered glial-neuronal signaling is suggested by enrichment of Gene Ontology pathways involved in detection of chemical and/or sensory stimuli (**Fig 3.5c**, *third and final panels*). These are enriched in NH females and NMS males and suggest alternate communication with neurons. Taken together these data suggest that the 'feminization' of enteric glial gene expression patterns in males following ELS alters intercellular metabolism in addition to communication with neurons and immune cells.

Similar to differential gene expression, pathways highlighted in enteric glia from females following ELS were largely different to those identified in control (NH) females and males following ELS (data not shown). This included predicted downregulation of the STAT3 pathways as indicated by decreased growth factor gene receptors *Egfr, Fgfr2, Flt4, and Igf1* and altered GPCR inhibitory signaling (Gαi signaling) indicated by decreased expression of adenylate cyclase 5 (*Adcy5*), caveolin 1 (*Cav1*), and prostaglandin E receptor 3 (*Ptger3*). Many of the top 'Diseases & Functions' pathways IPA predicted were altered in NMS females suggest altered developmental mechanisms as represented by significant predictions for the groups 'Organismal Development,' 'Cellular Development,' 'Tissue Development,' 'Organ Development,' 'Digestive System Development and Function,' and 'Embryonic Development.' These are additionally recapitulated on the cellular level by significant predictions for 'Cellular Movement,' 'Cellular Assembly and

Organization,' 'Cell-to-Cell Signaling and Interaction,' and 'Cellular Growth and Proliferation.' Taken together these data suggest important alterations in fundamental cellular processes occur in enteric glial from female mice following ELS.

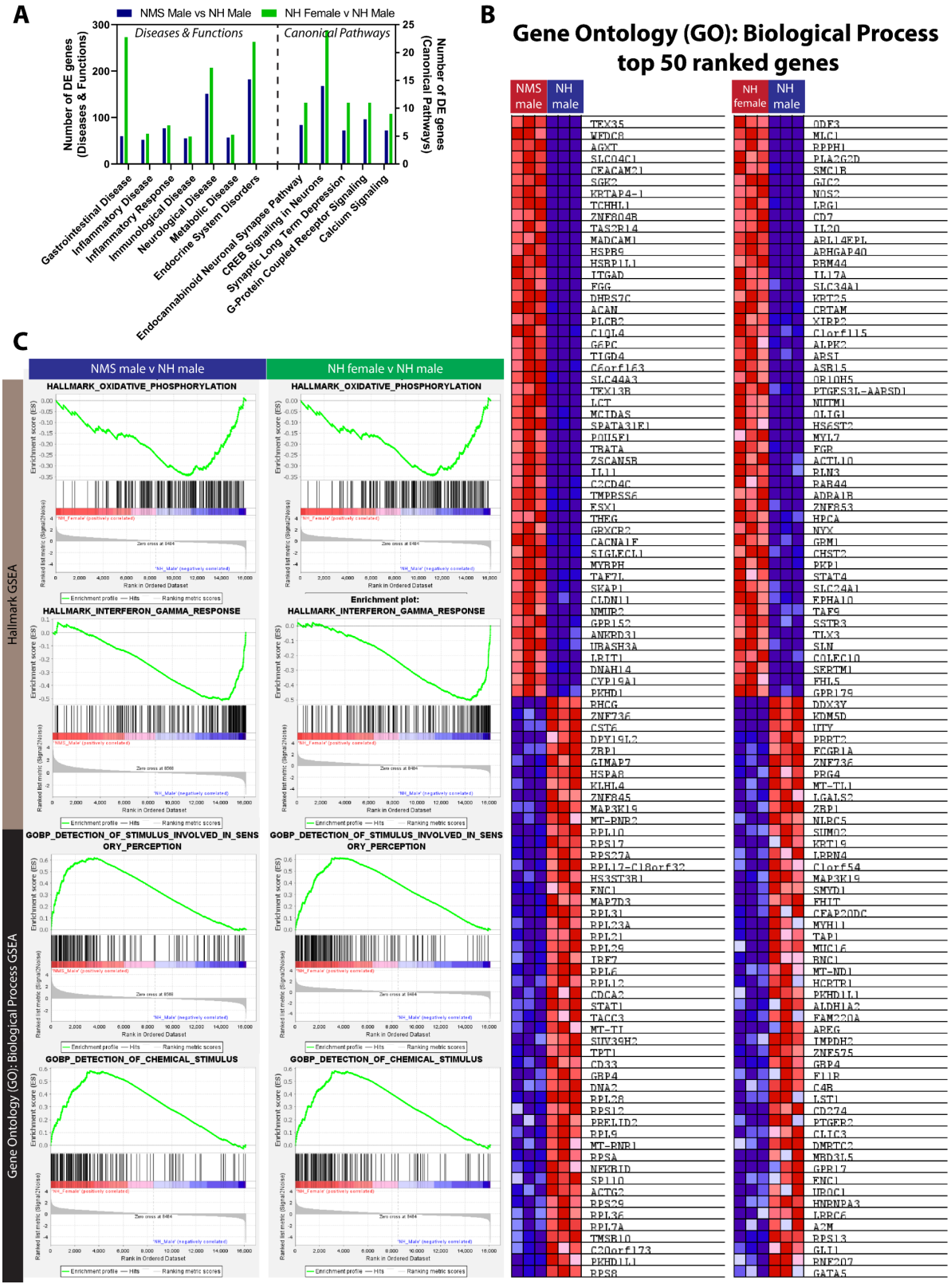

Figure 3.5 Early life stress in males and female sex share functional signatures in enteric glia.

(A) Number of differentially expressed genes in NMS males (blue) or NH females (green) compared to NH males in significant pathways from IPA. 'Diseases & Functions' including GI, neurological, and inflammatory disease are measured on the left y-axis while 'Canonical Pathways' including ENS signaling are measured on the right y-axis. Genes submitted to IPA analysis were restricted to $\log_2$fold-change > ± 0.58 and FDR < 0.1 (n=3 mice/group). **(B)** Top 50 genes in GSEA ranking for Gene Ontology (GO) biological process gene sets that contributed to defining putative pathways with differential regulation between NMS males and NH males (*left*) and NH females and NH males (*right*). Relative gene expression in NH males is represented in columns with a blue header while NMS males or NH females are in columns with a red header. Genes with relatively increased expression in one group are red while genes with relatively decreased expression are in blue. **(C)** *Top two columns:* GSEA enrichment plots from the Hallmark database that are enriched in NH males (right side of each graph) compared to NMS males (left side of left graphs) and NH females (left side of right graphs). Enrichment is indicated by increased density of black bars on the NH male (right side) of each graph and suggest differential regulation of oxidative phosphorylation and IFN-γ response. *Bottom two columns:* GSEA enrichment plots for select gene sets from Gene Ontology significantly enriched in both NMS males (left side of left graphs) and NH females (left side of right graphs) compared to NH males (right side of each graph). Enrichment is indicated by increased density of black bars on the NMS male or NH female (left side) of each graph and suggest differential regulation of neuronal sensing of stimuli. GSEA pathways are significant at FDR <0.05 (n=3 mice/group).

GPCR signaling is altered in enteric glia by female sex and early life stress

GPCR signaling is important in glial-neuronal communication and disruption of this signaling contributes to GI dysfunction.[36,37,39] Pathway analysis supports differences in enteric glial GPCR signaling between control (NH) males and females and following ELS. GPCR signaling and cAMP-dependent signaling are enriched in NMS males and NH females compared to NH males by GSEA in the Reactome database (**Fig 3.5a**). Enteric glia have the highest expression of cAMP in the myenteric plexus of the ENS but the significance of this expression and cAMP-related signaling in glial intercellular communication is unclear.[37] However cultured enteric glia express adenosine receptors that signal through cAMP[84] and together these data suggest cAMP signaling likely has an important role. Similarly IPA's Canonical Pathway 'G protein-coupled receptor signaling' (**Fig 3.5a**) is significantly increased in enteric glia from both NMS males and NH females compared to NH males (**Fig 3.6b**). Interestingly the specific genes that contribute to altered GPCR signaling in this pathway are different between NMS males and NH females. While both share differential expression of phospholipase C beta 2 (*Plcb2*), dopamine receptor 1 (*Drd1*), glutamate metabotropic receptor *Grm4*, and vasoactive intestinal peptide receptor *Vipr1*, NMS males have increased expression of adrenoreceptor alpha 1B (*Adra1b*), opioid receptor mu 1 (*Oprm1*), and Ras-related dexamethasone gene *Rasd1*. Meanwhile control (NH) females have increased expression of adenylate cyclase 5 (*Adcy5*), ES cell expressed Ras (*Eras*), and phosphodiesterase 11A (*Pde11a*), suggesting that the specific mechanisms by which GPCR signaling is altered in NH females or NMS males are different. Additionally many of these genes code for neurotransmitter receptors and while neurotransmitter receptors for norepinephrine, glutamate, and acetylcholine are expressed on enteric glia[39] their functional significance it still unclear.

Sex-dependent regulation of GPCR signaling is further exemplified by regulator of G Protein Signaling 5 (*Rgs5*) which is differentially expressed in enteric glia from female mice compared to male mice (**Fig 3.2c-c'**) but also decreases in females following ELS (**Fig 3.6b**). This

suggests differences in *Rgs5* expression contribute to altered GPCR signaling in enteric glia from females. *Rgs5* is primarily expressed in brain and heart tissue but is also highest in the glial-heavy regions of these tissues and suggestive of glial expression in these organs.[85,86] Furthermore *Rgs5* expression modulates Gα and Gq signaling activity in arteriole smooth muscle cells to promote cell division and growth.[87] Gq GPCR signaling is better characterized than other signaling mechanisms in enteric glia[37,39] and they utilize Gq signaling to regulate neuroinflammation and gastrointestinal motility.[34–36] Therefore if this gene is differentially expressed in enteric glia it may have important implications for GI function. We examined *Rgs5* expression in the ENS using RNAscope (**Fig 3.6c**). Consistent with our RNA-seq data *Rgs5* appears to be more highly expressed in control (NH) females than males as determined by the increased size of *Rgs5* punctae within S100β$^+$ enteric glia in addition to the number of cells co-labeling for *Rgs5* and S100β. More notably however is the decrease in *Rgs5* expression in the ENS of females following ELS (**Fig 3.6c**, *bottom panels*). These data ultimately suggest sexually dimorphic differences in GPCR signaling within enteric glia in response to ELS.

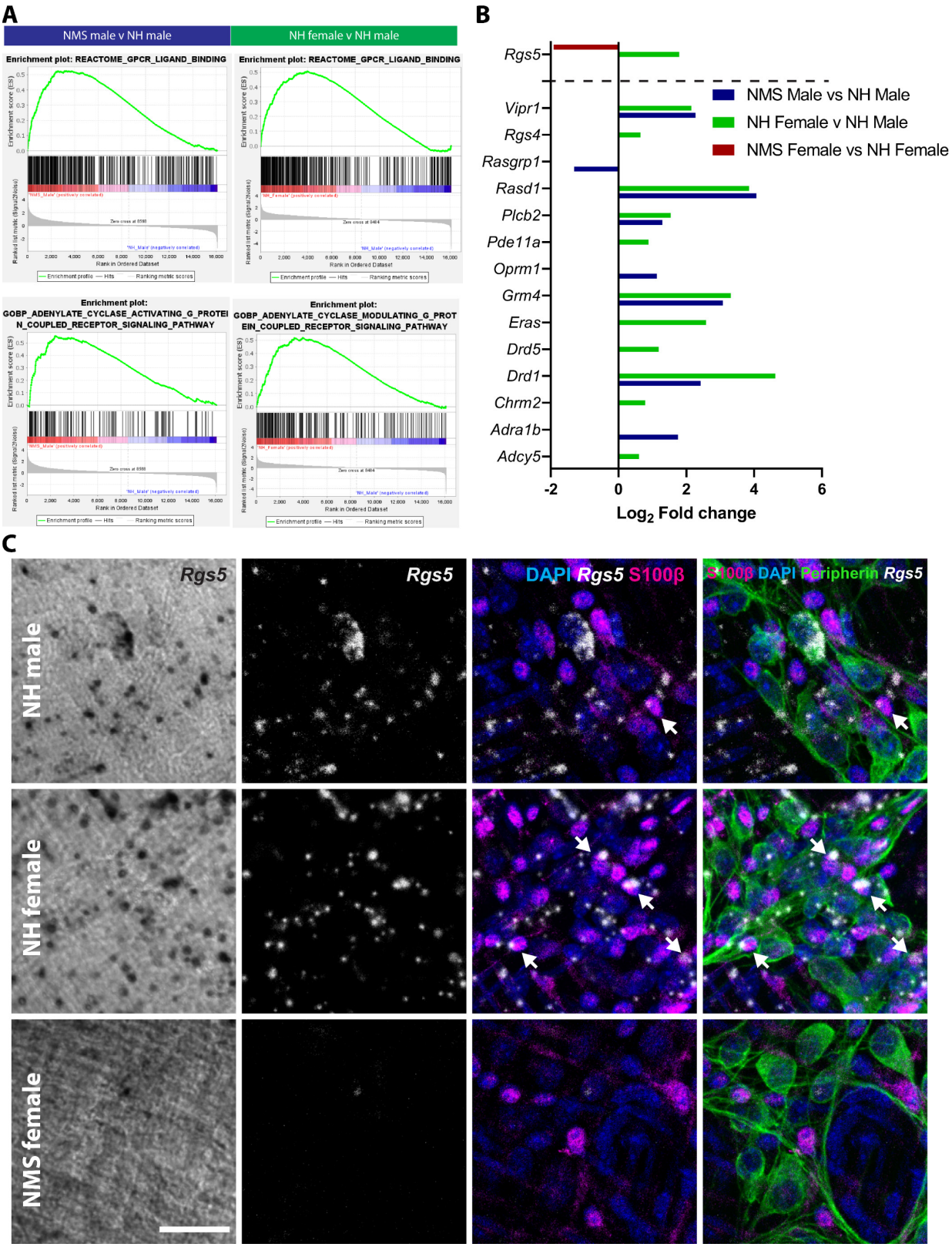

Figure 3.6 Enteric glia have sexually dimorphic alterations to GPCR signaling following ELS.

(A) Altered GPCR and specifically cAMP-dependent signaling in NMS males (*left panels*) and NH females (*right panels*) compared to NH males are suggested by GSEA in the Reactome and GO biological process gene sets, respectively, as demonstrated by the higher density of black bars on the left side of each graph (NMS males in left panels and NH females in right panels). GSEA pathways are significant at FDR <0.05. **(B)** Log_2fold-changes of genes implicated in IPA's Canonical Pathway 'G protein-coupled receptor signaling' in comparisons between NH males and NH females (green), NMS males and NH males (blue), and NMS females and NH females (red). *Rgs5* is not in this set but was a top differentially expressed gene in NH females compared to NMS females and thus also included here. Genes differentially expressed by NH females (green) and NMS males (blue) compared to NH males have some overlap (where genes have both green and blue columns present). However several genes are only differentially expressed in NMS males or NH females compared to NH males and suggest different regulatory mechanisms or responses. Genes submitted to IPA analysis were restricted to log_2fold-change > ± 0.58 and FDR < 0.1 (n=3mice/group). **(C)** RNA expression *in situ* of the GPCR-related gene *Rgs5* was visualized using RNAscope in the myenteric plexus (demonstrated in brightfield and fluorescence, first and second column respectively) and its expression in enteric glia determined by co-localization with S100β (magenta) and highlighted by white arrows. Enteric glial *Rgs5* expression appears higher in NH females (*middle row panels*) compared to NH males (*top row panels*) and NMS females (*bottom row panels*). Enteric neurons (labeled by peripherin in green) also express *Rgs5.* Images representative of n=2 mice/group. Scale bar represents 25μm.

IFN signaling in enteric glia is sex-dependent and altered following ELS

Interferon (IFN) signaling and type I IFN signaling in particular is active in neurons and glia and important for antiviral defense and modulating neuroinflammation in the brain.[80,81,88,89] However the role of type I IFNs in enteric neurons and glia is unknown. IFN and type I IFN signaling-related genes are expressed at lower levels in NH female glia and NMS male glia compared to NH male glia (**Fig 3.7a**). Differentially expressed genes were related to IFN induction and included IFN-induced GTPases (*Irgm1, Irgm2,* and *Igtp*), guanylate binding proteins (*Gbp1* and *Gbp3*), transmembrane protein *Ifitm3*, and homologous genes *Ifit1* and *Ifit3*. Altered type I IFN signaling was supported in IPA's 'Upstream Regulators' section due to these differentially expressed genes. Upstream signaling molecules potentially altered in enteric glia included proteins such as IFN alpha and beta receptor (Ifnar), Tbk1, Irf3, Ifnb1 and general Ifnα/β group signaling. Altered Ifnar signaling is supported through the differential expression of several downstream genes in both NMS males and NH females however the functional change in type I IFN signaling that results from these expression patterns is appears more complex than strict up- or downregulated (**Fig3.7b**). Both NMS males and NH females express IFN-γ at lower levels (signified by blue coloration in the pathway) than NH males but express IL-1β at higher levels (signified by orange coloration in the pathway). Synergistic down- and upregulation of downstream signaling molecules for IFN-γ and IL-1β respectively further support differential changes in the signaling patterns of these mediators and further support complex differences in enteric glial immune signaling in these mice.

IFN signaling is also significant in GSEA analysis where IFN genes are enriched in NH males compared to NMS males and NH females (**Fig 3.7c**). Enrichment of these genes in the Reactome database recapitulates IPA data and supports alterations in general and type I IFN signaling. Of the differently expressed IFN-related genes (**Fig 3.7a**) IFN-induced with tetratricopeptide repeats (*Ifit1*) is only differentially expressed in NMS males and not NH females and may suggest subtle sex-dependent differences in IFN regulation. CNS and cultured glia

express *Ifit1* but the circumstances that induce expression of this gene are unclear.[80,90] Furthermore the role of *Ifit1* as a promoter or silencer of inflammation, IFN signaling, and antimicrobial response is complex.[91] To see if *Ifit1* is expressed in enteric glia *in situ* we visualized its expression in the ENS using RNAscope. *Ifit1* co-localizes with S100β^{+} enteric glia within ENS ganglia and decreases in enteric glia of NMS males (**Fig 3.7d**). Furthermore *Ifit1* expression in the ENS appears to be higher in enteric glia than enteric neurons. This suggests that within myenteric ganglia *Ifit1* is primarily expressed in enteric glial cells in contrast to other *in situ* expression we visualized where expression appeared relatively similar (**Fig 3.2d**, *Xist*; and **Fig 3.6c**, *Rgs5*) or higher in neurons (**Fig 3.4c**, *Oasl2*).

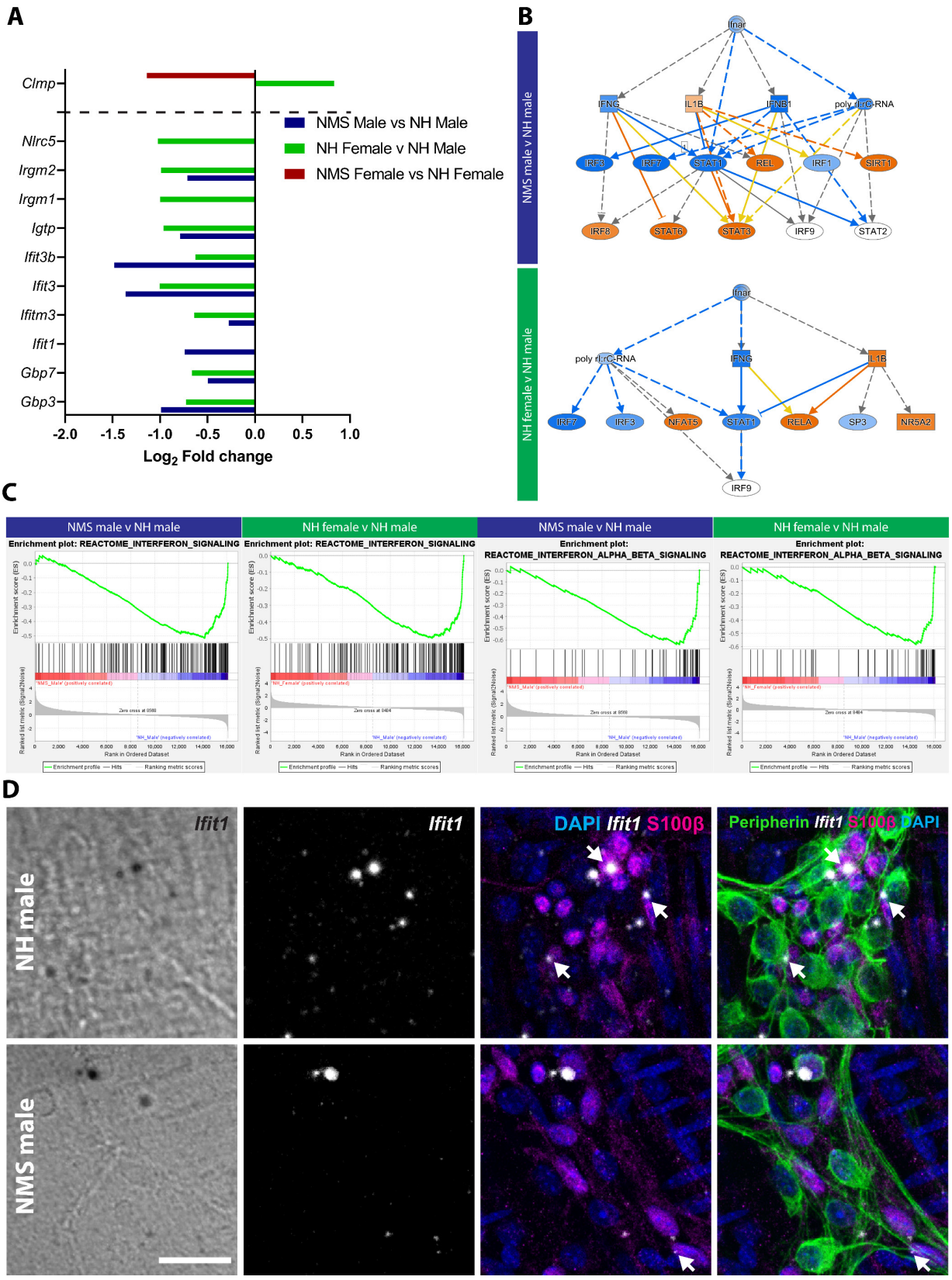

Figure 3.7 IFN expression in enteric glia differs between sexes and following ELS.

(A) Log_2fold-changes of IFN-induced genes between NMS males and NH males and between NH females and NH males support significantly different IFN regulation in NMS male and NH female enteric glia. These differentially expressed genes contributed to putative altered IFN signaling regulation in IPA's 'Upstream Regulators' analysis. **(B)** In particular, altered Ifnar signaling is highlighted in both NMS males (*top*) and NH females (*bottom*) compared to NH males by IPA in 'Upstream Regulators'. Genes and arrows in orange suggest activation based on findings in literature while those in blue suggest inhibition. Yellow arrows indicate unclear findings and/or relationships. Genes submitted to IPA analysis were restricted to log_2fold-change > ± 0.58 and FDR < 0.1 (n=3 mice/group). **(C)** GSEA enrichment graphs for IFN and type I IFN pathways supports similar findings in Reactome gene sets and suggest IFN signaling is enriched in NH males compared to NH females (blue headers) or NMS males (green headers). NH males are on the right side of each graph while NMS males or NH females are on the left side. Enrichment in NH males is visualized by increased density of black bars on the right side of each graph. GSEA pathways are significant at FDR <0.05. **(D)** *Ifit1* RNA expression using RNAscope (demonstrated in brightfield and fluorescence, first and second column respectively) in the myenteric plexus co-localizes with enteric glia (S100β, magenta) and decreases in response to ELS in males (*bottom panels*) compared to NH males (*top panels*). Furthermore, *Ifit1* expression is higher in glia than enteric neurons (labeled by peripherin, green). Enteric glial *Ifit1* expression is highlighted by white arrows. Images representative of n=2 mice/group. Scale bar represents 25μm.

DISCUSSION

Early life stress and sex are risk factors for GI disease including disorders of the gut-brain axis.[9–13,15,17,18] The intersection of sex and early life stress on GI disease pathogenesis is likely even more complex in where only certain ELS models and potential types of stressors in humans increase male disease risk.[10,17] We hypothesized that enteric glia have sex-specific expression patterns and exhibit sexually dimorphic responses to ELS. We characterized glial-specific expression patterns with RNA-sequencing and discovered differential expression in enteric glia between males and females and their responses to ELS. Female enteric glia have more varied individual expression patterns than males and higher expression of several genes involved in metabolism and immune regulation. Altered enteric glial gene expression following ELS is sexually dimorphic where female enteric glia alter expression of fewer genes than males. Meanwhile male glia upregulate several genes in response to ELS that are more highly expressed in control (NH) females and therefore suggest 'feminization' of enteric glia from males in key pathways. These pathways suggest altered signaling mechanisms with neurons and immune cells to modulate neurological and gastrointestinal disease. Specifically GPCR and IFN signaling-related differential gene expression following ELS is sexually dimorphic and may underlie key differences in intercellular signaling and stress response between sexes. These data highlight novel fundamental differences in gene regulation between male and female enteric glia and support sex-dependent responses to ELS that feminize expression profiles in male enteric glia.

Sex differences in enteric glia are poorly understood and our dataset provides an invaluable resource for characterizing baseline differences between males and females. Expression patterns in female enteric glia are more variable than male enteric glia (**Fig 3.1d-d'**) and have higher expression of hundreds of genes (**Fig 3.2b-b'**). The majority of these genes are located on somatic chromosomes and therefore support that these dynamic expression patterns are due to more than sex chromosomal differences. Key differences in metabolic, neurological, and inflammatory disease pathways are supported by our findings and could underlie sex-specific

mechanisms of disease susceptibility and pathogenesis. For instance female enteric glia have higher expression of several solute carrier genes. These transporters regulate influx and efflux of a wide variety of biomolecules including ions, proteins, lipids, and carbohydrates and additionally regulate intestinal permeability. Many solute carriers are linked to metabolic diseases like obesity and type II diabetes in addition to being risk factors for intestinal disorders like inflammatory bowel disease.[77,92] While sex differences in solute carriers are not well characterized there is some evidence of sex-specific epigenetic regulation of the genes and impacts on blood brain barrier and kidney function.[93–95] What these expression patterns mean for cellular transport in female enteric glia is unclear but could support sex-specific mechanisms of altered intestinal permeability in GI disease. Enteric glia from female mice also have higher expression of complement proteins than males. Central neuroglia produce complement proteins that exacerbate neuroinflammation and synapse degeneration in Alzheimer's disease.[96,97] Complement signaling may also be a means of aberrant synaptic pruning in the ENS and increased complement signaling in females could contribute to increased neuroinflammation and degeneration in females. Together these data highlight sexually dimorphic signaling mechanisms in enteric glia and support the need for sex-stratified research in the ENS to truly capture accurate signaling mechanisms.

Gene expression patterns in male enteric glia 'feminize' following ELS (**Figs 3.1d-d'** and **3.4a**). This phenomenon is observed in rats hormonally and morphologically, where male rats following ELS had increased estradiol and decreased anogenital distance[78] and in humans where male testosterone is impaired into adulthood in response to prenatal stress.[98] It is interesting to see that enteric glia recapitulate this phenomenon on a molecular level. However what this means functionally remains to be seen. This shift could be protective and contribute to lower disease risk in males. This is supported by the reduction of IFN-related pathways in NMS males (**Fig 3.7**) as this could reflect inhibition of inflammatory responses. However since similar genes are also downregulated in NH females compared to NH males interpretation is more complex. It is possible that subtleties in sex-dependent IFN signaling ultimately create a paradoxical response in males

or females as this occurs in intestinal epithelium during viral infection.[99] However, it is also possible that our findings demonstrate an important risk factor for male disease pathogenesis. Male animals in addition to females develop GI symptoms in the NMS model[17,100] and perhaps that is why we also find differences in males here. Perhaps NMS provides the specific types of stress-induced molecular changes required to produce disease in males and subsequently in enteric glia. Especially since these glia shift toward the profile of females, the higher-risk sex, it is logical that this could highlight increased disease susceptibility. Further research in the functional implication of altered IFN signaling could resolve the effect of these differentially expressed genes and determine whether these changes support disease risk or protection.

It is equally interesting that our data supports more subtle changes in females following ELS compared to males. Additionally most of these genes are downregulated in contrast to the predominant upregulation seen in males after ELS (**Fig 3.3**). However due to the relatively lower number of differentially expressed genes it is difficult to hypothesize the functional role of their downregulation. Instead those genes that are differentially expressed in this dataset may highlight key regulators of disease response in females that lead to variable gene expression presentation between individuals downstream. This is supported by significant genes including growth factor receptors that may have more widespread downstream effects. The caveolin *Cav1* is also increased in female enteric glia following ELS and caveolin signaling in glia throughout other organs modifies cell growth, reactive gliosis, and calcium signaling[101,102] and therefore may alter these responses in female enteric glia as well. Another reason relatively few genes are differentially expressed in females following early life stress could be that the immediate postnatal time period is not as critical for enteric glia in females as it is in males. CNS neurons in female mice but not male mice were altered after social isolation during pre-adolescence (approximately 5wks old)[103] suggesting that critical timing for pathophysiology is sex-specific. Thus it is possible that stress during the neonatal time period has more robust effects on male enteric glia than in females.

Still alterations in some GPCR-related genes can be found across all groups and support GPCR signaling in enteric glia as a potentially important source of variation. Enteric glia utilize GPCR signaling to produce a wide variety of effects from modulating local neuronal health to altering gastrointestinal function[34,36,37] and differential expression of GPCR genes between males and females and their changes during ELS may signify fundamental differences in glial intercellular communication that underpin a wide range local and regional effects in the gut. Sex differences in glial GPCR signaling and excitability are supported by recent findings that glia exhibit sex-dependent Ca^{++} responses to ascending vs. descending stimuli (Ahmadzai et al. 2021, *accepted at PNAS*). Perhaps differential expression of GPCR-related genes we identified here contribute to this phenomenon and functional testing involving the proteins encoded by these genes could identify the particular mechanistic differences these genes confer. Since *Rgs5* expression is dramatically reduced *in situ* in females following ELS (**Fig 3.6c**) this may underlie signaling changes that promote disease susceptibility in females. This is further supported by the ability of *Rgs5* to alter Gα and Gq signaling in other cell types that underpin altered intercellular communication and subsequent cell growth.[87]

Limitations in our study include the use of genetic data to characterize mechanistic underpinnings. Transcript expression is not necessarily the same as protein expression and even protein expression may not correlate to altered function or effect. However this study represents the first investigation of sex differences in enteric glia and responses to ELS and therefore large-scale 'omics' technology is ideal for capturing both pathway-level changes and linking these to potential molecular regulators. Furthermore using the RiboTag model specifically captures mRNA being actively translated by ribosomes[49] and therefore is likely more reflective of protein expression than other cell-specific RNA capturing techniques. Other potential limitations in our study involve characterizing female gene expression patterns. We did not stage the estrus cycle in females and this variation could underlie the gene expression variability seen in female glia. However, female variability in expression patterns in other cell types is estrus-independent[104] and

therefore may also be so here. Another potential limitation in our characterization of female glia is that due to this higher variability our experiment is underpowered to detect some differential expression. In future work we plan to add additional cohorts to this group to further identify female differentially expressed genes. However this does not discredit significant data we did generate that still provides novel functional insights particularly in sex-differences in enteric glial GPCR signaling. An additional limitation is with *in situ* validation of glial specificity using RNAscope. Enteric neurons and glia are highly intertwined and overlapping and are sometimes difficult to differentiate within myenteric ganglia. Thus while RNAscope preliminarily supports our RNA-seq analysis in enteric glia, labeling in additional samples or with immunofluorescence could help validate the consistency of the changes seen here. Future research investigating enteric neuronal expression could compare gene expression between the two cells to also help resolve these issues. Finally further study of pathways highlighted here in functional contexts would also serve as validation in addition to determining the role of altered gene expression in ENS and GI disease.

In this study we provide the first look at expression differences in enteric glia between sexes and following ELS. This research provides novel and important insights on physiologic differences in enteric glia between males and females and in response to early life stress. These findings suggest key differences in glial intercellular communication with neurons and immune cells that impact neurological and gastrointestinal function through pathways including inflammatory signaling and metabolic alterations. The specific mechanisms that contribute to these differences will require future work but the contrasting expression patterns between males and females and the ‘feminization’ of males following early life stress suggest a completely new framework for enteric glial function between sexes and how stress alters these to regulate sexually dimorphic disease presentation. Some of the findings presented in this data could reflect important mechanisms within enteric glia that protect males from IBS or alternatively contribute to increased disease susceptibility after specific contexts of stressors. In addition to these findings we generated several datasets that provide a valuable research tool for continuing to uncover

complexities and sex-dependent heterogeneity in gastrointestinal disease. Future research can build on this by investigating enteric neurons in a similar context and synergizing these findings to support mechanistic differences in neuron-glia communication in the ENS between sexes and following ELS.

REFERENCES

REFERENCES

1. MAYER EA. The neurobiology of stress and gastrointestinal disease. *Gut*. 2000;47(6):861-869. doi:10.1136/gut.47.6.861

2. BHATIA V, TANDON RK. Stress and the gastrointestinal tract. *J Gastroenterol Hepatol*. 2005;20(3):332-339. doi:10.1111/j.1440-1746.2004.03508.x

3. Mönnikes H, Tebbe JJ, Hildebrandt M, et al. Role of Stress in Functional Gastrointestinal Disorders. *Dig Dis*. 2001;19(3):201-211. doi:10.1159/000050681

4. Pohl CS, Medland JE, Moeser AJ. Early-life stress origins of gastrointestinal disease: animal models, intestinal pathophysiology, and translational implications. *Am J Physiol Liver Physiol*. 2015;309(12):G927-G941. doi:10.1152/ajpgi.00206.2015

5. Drossman DA, Hasler WL. Rome IV—Functional GI Disorders: Disorders of Gut-Brain Interaction. *Gastroenterology*. 2016;150(6):1257-1261. doi:10.1053/j.gastro.2016.03.035

6. Agostini A, Rizzello F, Ravegnani G, et al. Adult Attachment and Early Parental Experiences in Patients With Crohn's Disease. *Psychosomatics*. 2010;51(3):208-215. doi:10.1176/appi.psy.51.3.208

7. Riba A, Olier M, Lacroix-Lamandé S, et al. Early life stress in mice is a suitable model for Irritable Bowel Syndrome but does not predispose to colitis nor increase susceptibility to enteric infections. *Brain Behav Immun*. 2018;73:403-415. doi:10.1016/j.bbi.2018.05.024

8. Talley NJ, Fett SL, Zinsmeister AR, Melton LJ. Gastrointestinal tract symptoms and self-reported abuse: A population-based study. *Gastroenterology*. 1994;107(4):1040-1049. doi:10.1016/0016-5085(94)90228-3

9. Medland JE, Pohl CS, Edwards LL, et al. Early life adversity in piglets induces long-term upregulation of the enteric cholinergic nervous system and heightened, sex-specific secretomotor neuron responses. *Neurogastroenterol Motil*. 2016;28(9):1317-1329. doi:10.1111/nmo.12828

10. Bradford K, Shih W, Videlock EJ, et al. Association Between Early Adverse Life Events and Irritable Bowel Syndrome. *Clin Gastroenterol Hepatol*. 2012;10(4):385-390.e3. doi:10.1016/j.cgh.2011.12.018

11. Chaloner A, Greenwood-Van Meerveld B. Sexually Dimorphic Effects of Unpredictable Early Life Adversity on Visceral Pain Behavior in a Rodent Model. *J Pain*. 2013;14(3):270-280. doi:10.1016/j.jpain.2012.11.008

12. Chang L, Di Lorenzo C, Farrugia G, et al. Functional Bowel Disorders: A Roadmap to Guide the Next Generation of Research. *Gastroenterology*. 2018;154(3):723-735. doi:10.1053/j.gastro.2017.12.010

13. Chitkara DK, van Tilburg MAL, Blois-Martin N, Whitehead WE. Early Life Risk Factors That Contribute to Irritable Bowel Syndrome in Adults: A Systematic Review. *Am J Gastroenterol*. 2008;103(3):765-774. doi:10.1111/j.1572-0241.2007.01722.x

14. Drossman DA. Sexual and Physical Abuse in Women with Functional or Organic Gastrointestinal Disorders. *Ann Intern Med*. 1990;113(11):828. doi:10.7326/0003-4819-113-11-828

15. Pohl CS, Medland JE, Mackey E, et al. Early weaning stress induces chronic functional diarrhea, intestinal barrier defects, and increased mast cell activity in a porcine model of early life adversity. *Neurogastroenterol Motil*. 2017;29(11):e13118. doi:10.1111/nmo.13118

16. Prusator DK, Andrews A, Greenwood-Van Meerveld B. Neurobiology of early life stress and visceral pain: translational relevance from animal models to patient care. *Neurogastroenterol Motil*. 2016;28(9):1290-1305. doi:10.1111/nmo.12862

17. Prusator DK, Greenwood-Van Meerveld B. Sex-related differences in pain behaviors following three early life stress paradigms. *Biol Sex Differ*. 2016;7(1):29. doi:10.1186/s13293-016-0082-x

18. Rosztóczy A, Fioramonti J, Jármay K, Barreau F, Wittmann T, Buéno L. Influence of sex and experimental protocol on the effect of maternal deprivation on rectal sensitivity to distension in the adult rat. *Neurogastroenterol Motil*. 2003;15(6):679-686. doi:10.1046/J.1350-1925.2003.00451.X

19. Claar R. Functional disability in adolescents and young adults with symptoms of irritable bowel syndrome: the role of academic, social, and athletic competence. *J Pediatr Psychol*. 1999;24(3):271-280. doi:10.1093/jpepsy/24.3.271

20. Furness JB. *The Enteric Nervous System*. (Furness JB, ed.). Malden, Massachusetts, USA: Blackwell Publishing; 2006. doi:10.1002/9780470988756

21. Furness JB. The enteric nervous system and neurogastroenterology. *Nat Rev Gastroenterol Hepatol*. 2012;9(5):286-294. doi:10.1038/nrgastro.2012.32

22. Lake JI, Heuckeroth RO. Enteric nervous system development: migration, differentiation, and disease. *Am J Physiol Liver Physiol*. 2013;305(1):G1-G24. doi:10.1152/ajpgi.00452.2012

23. Sasselli V, Pachnis V, Burns AJ. The enteric nervous system. *Dev Biol*. 2012;366(1):64-73. doi:10.1016/j.ydbio.2012.01.012

24. Gabella G. *Neuron Size and Number in the Myenteric Plexus of the Newborn and Adult Rat*. Vol 109.; 1971.

25. Schäfer K-H, Hänsgen A, Mestres P. Morphological changes of the myenteric plexus during early postnatal development of the rat. *Anat Rec*. 1999;256(1):20-28. doi:10.1002/(SICI)1097-0185(19990901)256:1<20::AID-AR4>3.0.CO;2-8

26. Wester T, O'Briain DS, Puri P. Notable postnatal alterations in the myenteric plexus of normal human bowel. *Gut*. 1999;44(5):666-674. doi:10.1136/gut.44.5.666

27. Hao MM, Bornstein JC, Young HM. Development of myenteric cholinergic neurons in ChAT-Cre;R26R-YFP mice. *J Comp Neurol*. 2013;521(14):3358-3370. doi:10.1002/cne.23354

28. Furness J. Types of neurons in the enteric nervous system. *J Auton Nerv Syst*. 2000;81(1-3):87-96. doi:10.1016/S0165-1838(00)00127-2

29. de Vries P, Soret R, Suply E, Heloury Y, Neunlist M. Postnatal development of myenteric neurochemical phenotype and impact on neuromuscular transmission in the rat colon. *Am J Physiol Liver Physiol*. 2010;299(2):G539-G547. doi:10.1152/ajpgi.00092.2010

30. Hyland NP, O'Mahony SM, O'Malley D, O'Mahony CM, Dinan TG, Cryan JF. Early-life stress selectively affects gastrointestinal but not behavioral responses in a genetic model of brain-gut axis dysfunction. *Neurogastroenterol Motil*. 2015;27(1):105-113. doi:10.1111/nmo.12486

31. McClain JL, Mazzotta EA, Maradiaga N, et al. Histamine-dependent interactions between mast cells, glia, and neurons are altered following early-life adversity in mice and humans. *Am J Physiol Liver Physiol*. 2020;319(6):G655-G668. doi:10.1152/ajpgi.00041.2020

32. Pearson-Leary J, Osborne DM, McNay EC. Role of Glia in Stress-Induced Enhancement and Impairment of Memory. *Front Integr Neurosci*. 2016;9(JAN2016):63. doi:10.3389/fnint.2015.00063

33. Jauregui-Huerta F, Ruvalcaba-Delgadillo Y, Gonzalez-Perez O, Gonzalez-Castaneda R, Garcia-Estrada J, Luquin S. Responses of Glial Cells to Stress and Glucocorticoids. *Curr Immunol Rev*. 2010;6(3):195-204. doi:10.2174/157339510791823790

34. Brown IAMM, McClain JL, Watson RE, Patel BA, Gulbransen BD. Enteric Glia Mediate Neuron Death in Colitis Through Purinergic Pathways That Require Connexin-43 and Nitric Oxide. *Cell Mol Gastroenterol Hepatol*. 2016;2(1):77-91. doi:10.1016/j.jcmgh.2015.08.007

35. McClain JL, Grubišić V, Fried D, et al. Ca 2+ responses in enteric glia are mediated by connexin-43 hemichannels and modulate colonic transit in mice. *Gastroenterology*. 2014;146(2):497-507. doi:10.1053/j.gastro.2013.10.061

36. McClain JL, Fried DE, Gulbransen BD. Agonist-Evoked Ca2+ Signaling in Enteric Glia Drives Neural Programs That Regulate Intestinal Motility in Mice. *Cell Mol Gastroenterol Hepatol*. 2015;1(6):631-645. doi:10.1016/j.jcmgh.2015.08.004

37. Grubišić V, Gulbransen BD. Enteric glia: the most alimentary of all glia. *J Physiol*. 2017;595(2):557-570. doi:10.1113/JP271021

38. Grubišić V, Gulbransen BD. Enteric glial activity regulates secretomotor function in the mouse colon but does not acutely affect gut permeability. *J Physiol*. 2017;595(11):3409-3424. doi:10.1113/JP273492

39. Gulbransen BD. Enteric Glia. *Colloq Ser Neuroglia Biol Med From Physiol to Dis*. 2014;1(2):1-70. doi:10.4199/C00113ED1V01Y201407NGL002

40. Chow AK, Grubišić V, Gulbransen BD. Enteric Glia Regulate Lymphocyte Activation via Autophagy-Mediated MHC-II Expression. *Cell Mol Gastroenterol Hepatol*. June 2021. doi:10.1016/j.jcmgh.2021.06.008

41. Morales-Soto W, Gulbransen BD. Enteric Glia: A New Player in Abdominal Pain. *Cell Mol Gastroenterol Hepatol*. 2018. doi:10.1016/j.jcmgh.2018.11.005

42. Wang P, Du C, Chen F-X, et al. BDNF contributes to IBS-like colonic hypersensitivity via activating the enteroglia-nerve unit. *Sci Rep*. 2016;6(1):20320. doi:10.1038/srep20320

43. Grubišić V, McClain JL, Fried DE, et al. Enteric Glia Modulate Macrophage Phenotype and Visceral Sensitivity following Inflammation. *Cell Rep*. 2020;32(10):108100. doi:10.1016/j.celrep.2020.108100

44. Delvalle NM, Dharshika C, Morales-Soto W, Fried DE, Gaudette L, Gulbransen BD. Communication Between Enteric Neurons, Glia, and Nociceptors Underlies the Effects of Tachykinins on Neuroinflammation. *Cell Mol Gastroenterol Hepatol*. 2018;6(3):321-344. doi:10.1016/j.jcmgh.2018.05.009

45. Fujikawa Y, Tominaga K, Tanaka F, et al. Enteric glial cells are associated with stress-induced colonic hyper-contraction in maternally separated rats. *Neurogastroenterol Motil*. 2015;27(7):1010-1023. doi:10.1111/nmo.12577

46. Lilli NL, Quénéhervé L, Haddara S, et al. Glioplasticity in irritable bowel syndrome. *Neurogastroenterol Motil*. 2018;30(4):e13232. doi:10.1111/nmo.13232

47. Sanz E, Bean JC, Carey DP, Quintana A, McKnight GS. RiboTag: Ribosomal Tagging Strategy to Analyze Cell-Type-Specific mRNA Expression In Vivo. *Curr Protoc Neurosci*. 2019;88(1):1-19. doi:10.1002/cpns.77

48. Gabanyi I, Muller PA, Feighery L, Oliveira TY, Costa-Pinto FA, Mucida D. Neuro-immune Interactions Drive Tissue Programming in Intestinal Macrophages. *Cell*. 2016;164(3):378-391. doi:10.1016/j.cell.2015.12.023

49. Sanz E, Yang L, Su T, Morris DR, McKnight GS, Amieux PS. Cell-type-specific isolation of ribosome-associated mRNA from complex tissues. *Proc Natl Acad Sci*. 2009;106(33):13939-13944. doi:10.1073/pnas.0907143106

50. Love MI, Huber W, Anders S. Moderated estimation of fold change and dispersion for RNA-seq data with DESeq2. *Genome Biol*. 2014;15(12):550. doi:10.1186/s13059-014-0550-8

51. Ewels P, Magnusson M, Lundin S, Käller M. MultiQC: summarize analysis results for multiple tools and samples in a single report. *Bioinformatics*. 2016;32(19):3047-3048. doi:10.1093/bioinformatics/btw354

52. Dobin A, Davis CA, Schlesinger F, et al. STAR: ultrafast universal RNA-seq aligner. *Bioinformatics*. 2013;29(1):15-21. doi:10.1093/bioinformatics/bts635

53. Anders S, Pyl PT, Huber W. HTSeq--a Python framework to work with high-throughput sequencing data. *Bioinformatics*. 2015;31(2):166-169. doi:10.1093/bioinformatics/btu638

54. Team RC. R: A Language and Environment for Statistical Computing. 2021. https://www.r-project.org/.

55. Wickham H, François R, Henry L, Müller K. dplyr: A Grammar of Data Manipulation. 2021. https://cran.r-project.org/package=dplyr.

56. Wickham H. tidyverse: Easily Install and Load the Tidyverse. 2019. https://cran.r-project.org/package=tidyverse.

57. Wickham H, Hester J. readr: Read Rectangular Text Data. 2020. https://cran.r-project.org/package=readr.

58. Ammar R, Thompson J. zFPKM: A suite of functions to facilitate zFPKM transformations. 2020. https://github.com/ronammar/zFPKM/.

59. Smedley D, Haider S, Durinck S, et al. The BioMart community portal: an innovative alternative to large, centralized data repositories. *W590 Nucleic Acids Res*. 2015;43. doi:10.1093/nar/gkv350

60. Love M, Anders S, Huber W. DESeq2: Differential gene expression analysis based on the negative binomial distribution. 2021. https://github.com/mikelove/DESeq2.

61. Wickham H, Chang W, Henry L, et al. ggplot2: Create Elegant Data Visualisations Using the Grammar of Graphics. 2020. https://cran.r-project.org/package=ggplot2.

62. Pedersen TL. ggforce: Accelerating ggplot2. 2021. https://cran.r-project.org/package=ggforce.

63. Slowikowski K. ggrepel: Automatically Position Non-Overlapping Text Labels with ggplot2. 2021. https://github.com/slowkow/ggrepel.

64. Kolde R. pheatmap: Pretty Heatmaps. 2019. https://cran.r-project.org/package=pheatmap.

65. Stephens M, Carbonetto P, Gerard D, et al. ashr: Methods for Adaptive Shrinkage, using Empirical Bayes. 2020. https://github.com/stephens999/ashr.

66. Pagès H, Carlson M, Falcon S, Li N. AnnotationDbi: Manipulation of SQLite-based annotations in Bioconductor. 2020. https://bioconductor.org/packages/AnnotationDbi.

67. Carlson M. org.Mm.eg.db: Genome wide annotation for Mouse. 2020.

68. Xie Y. knitr: A General-Purpose Package for Dynamic Report Generation in R. 2021. https://yihui.org/knitr/.

69. Subramanian A, Subramanian A, Tamayo P, et al. Gene set enrichment analysis: a knowledge-based approach for interpreting genome-wide expression profiles. *Proc Natl Acad Sci U S A*. 2005;102(43):15545-15550. doi:10.1073/pnas.0506580102

70. Mootha VK, Lindgren CM, Eriksson K-F, et al. PGC-1α-responsive genes involved in oxidative phosphorylation are coordinately downregulated in human diabetes. *Nat Genet 2003 343*. 2003;34(3):267-273. doi:10.1038/ng1180

71. Obata Y, Castaño Á, Boeing S, et al. Neuronal programming by microbiota regulates intestinal physiology. *Nature*. 2020;578(7794):284-289. doi:10.1038/s41586-020-1975-8

72. Drokhlyansky E, Smillie CS, Van Wittenberghe N, et al. The Human and Mouse Enteric Nervous System at Single-Cell Resolution. *Cell*. September 2020:1-17. doi:10.1016/j.cell.2020.08.003

73. Anderson MA, Burda JE, Ren Y, et al. Astrocyte scar formation aids central nervous system axon regeneration. *Nature*. 2016;532(7598):195-200. doi:10.1038/nature17623

74. Rao M, Nelms BD, Dong L, et al. Enteric glia express proteolipid protein 1 and are a transcriptionally unique population of glia in the mammalian nervous system. *Glia*. 2015;63(11):2040-2057. doi:10.1002/glia.22876

75. Lee MY, Park C, Berent RM, et al. Smooth Muscle Cell Genome Browser: Enabling the Identification of Novel Serum Response Factor Target Genes. Tang Y, ed. *PLoS One*. 2015;10(8):e0133751. doi:10.1371/journal.pone.0133751

76. Wright CM, Schneider S, Smith-Edwards KM, et al. scRNA-sequencing reveals new enteric nervous system roles for GDNF, NRTN, and TBX3. *Cell Mol Gastroenterol Hepatol*. January 2021:140981. doi:10.1016/j.jcmgh.2020.12.014

77. Schumann T, König J, Henke C, et al. Solute Carrier Transporters as Potential Targets for the Treatment of Metabolic Disease. Michel MC, ed. *Pharmacol Rev*. 2020;72(1):343-379. doi:10.1124/pr.118.015735

78. Eck SR, Ardekani CS, Salvatore M, et al. The effects of early life adversity on growth, maturation, and steroid hormones in male and female rats. *Eur J Neurosci*. 2020;52(1):2664-2680. doi:10.1111/ejn.14609

79. Gayen S, Maclary E, Hinten M, Kalantry S. Sex-specific silencing of X-linked genes by Xist RNA. *Proc Natl Acad Sci*. 2016;113(3):E309-E318. doi:10.1073/pnas.1515971113

80. Li W, Hofer MJ, Songkhunawej P, et al. Type I interferon-regulated gene expression and signaling in murine mixed glial cells lacking signal transducers and activators of transcription 1 or 2 or interferon regulatory factor 9. *J Biol Chem*. 2017;292(14):5845-5859. doi:10.1074/jbc.M116.756510

81. Kreit M, Paul S, Knoops L, De Cock A, Sorgeloos F, Michiels T. Inefficient Type I Interferon-Mediated Antiviral Protection of Primary Mouse Neurons Is Associated with the Lack of Apolipoprotein L9 Expression. *J Virol*. 2014;88(7):3874-3884. doi:10.1128/JVI.03018-13

82. Zhu J, Zhang Y, Ghosh A, et al. Antiviral Activity of Human OASL Protein Is Mediated by Enhancing Signaling of the RIG-I RNA Sensor. *Immunity*. 2014;40(6):936-948. doi:10.1016/j.immuni.2014.05.007

83. Malilas W, Koh SS, Srisuttee R, et al. Cancer upregulated gene 2, a novel oncogene, confers resistance to oncolytic vesicular stomatitis virus through STAT1-OASL2 signaling. *Cancer Gene Ther*. 2013;20(2):125-132. doi:10.1038/cgt.2012.96

84. Liñán-Rico A, Turco F, Ochoa-Cortes F, et al. Molecular Signaling and Dysfunction of the Human Reactive Enteric Glial Cell Phenotype. *Inflamm Bowel Dis*. 2016;22(8):1812-1834. doi:10.1097/MIB.0000000000000854

85. Perschbacher KJ, Deng G, Fisher RA, Gibson-Corley KN, Santillan MK, Grobe JL. Regulators of G protein signaling in cardiovascular function during pregnancy. *Physiol Genomics*. 2018;50(8):590-604. doi:10.1152/physiolgenomics.00037.2018

86. Cifelli C, Rose RA, Zhang H, et al. RGS4 Regulates Parasympathetic Signaling and Heart Rate Control in the Sinoatrial Node. *Circ Res*. 2008;103(5):527-535. doi:10.1161/CIRCRESAHA.108.180984

87. Arnold C, Feldner A, Pfisterer L, et al. <scp>RGS</scp> 5 promotes arterial growth during arteriogenesis. *EMBO Mol Med*. 2014;6(8):1075-1089. doi:10.15252/emmm.201403864

88. Chhatbar C, Detje CN, Grabski E, et al. Type I Interferon Receptor Signaling of Neurons and Astrocytes Regulates Microglia Activation during Viral Encephalitis. *Cell Rep*. 2018;25(1):118-129.e4. doi:10.1016/j.celrep.2018.09.003

89. Chin AC. Neuroinflammation and the cGAS-STING pathway. *J Neurophysiol*. 2019;91:jn.00848.2018. doi:10.1152/jn.00848.2018

90. Madeddu S, Woods TA, Mukherjee P, Sturdevant D, Butchi NB, Peterson KE. Identification of Glial Activation Markers by Comparison of Transcriptome Changes between Astrocytes and Microglia following Innate Immune Stimulation. Basu A, ed. *PLoS One*. 2015;10(7):e0127336. doi:10.1371/journal.pone.0127336

91. John SP, Sun J, Carlson RJ, et al. IFIT1 Exerts Opposing Regulatory Effects on the Inflammatory and Interferon Gene Programs in LPS-Activated Human Macrophages. *Cell Rep*. 2018;25(1):95-106.e6. doi:10.1016/j.celrep.2018.09.002

92. Kotka M, Lieden A, Pettersson S, Trinchieri V, Masci A, D'Amato M. Solute Carriers (SLC) in Inflammatory Bowel Disease. *J Clin Gastroenterol*. 2008;42(Supplement 3):S133-S135. doi:10.1097/MCG.0b013e31815f5ab6

93. Döring A, Gieger C, Mehta D, et al. SLC2A9 influences uric acid concentrations with pronounced sex-specific effects. *Nat Genet*. 2008;40(4):430-436. doi:10.1038/ng.107

94. Brzica H, Abdullahi W, Reilly BG, Ronaldson PT. Sex-specific differences in organic anion transporting polypeptide 1a4 (Oatp1a4) functional expression at the blood–brain barrier in Sprague–Dawley rats. *Fluids Barriers CNS*. 2018;15(1):25. doi:10.1186/s12987-018-0110-9

95. McCarthy NS, Melton PE, Cadby G, et al. Meta-analysis of human methylation data for evidence of sex-specific autosomal patterns. *BMC Genomics*. 2014;15(1):981. doi:10.1186/1471-2164-15-981

96. Stevens B, Allen NJ, Vazquez LE, et al. The Classical Complement Cascade Mediates CNS Synapse Elimination. *Cell*. 2007;131(6):1164-1178. doi:10.1016/j.cell.2007.10.036

97. Luchena C, Zuazo-Ibarra J, Alberdi E, Matute C, Capetillo-Zarate E. Contribution of Neurons and Glial Cells to Complement-Mediated Synapse Removal during Development, Aging and in Alzheimer's Disease. *Mediators Inflamm*. 2018;2018:1-12. doi:10.1155/2018/2530414

98. Barrett ES, Swan SH. Stress and Androgen Activity During Fetal Development. *Endocrinology*. 2015;156(10):3435-3441. doi:10.1210/en.2015-1335

99. Saxena K, Simon LM, Zeng X-L, et al. A paradox of transcriptional and functional innate

interferon responses of human intestinal enteroids to enteric virus infection. *Proc Natl Acad Sci*. 2017;114(4):E570-E579. doi:10.1073/pnas.1615422114

100. O'Mahony SM, Marchesi JR, Scully P, et al. Early Life Stress Alters Behavior, Immunity, and Microbiota in Rats: Implications for Irritable Bowel Syndrome and Psychiatric Illnesses. *Biol Psychiatry*. 2009;65(3):263-267. doi:10.1016/j.biopsych.2008.06.026

101. Silva WI, Maldonado HM, Velázquez G, García JO, González FA. Caveolins in glial cell model systems: from detection to significance. *J Neurochem*. 2007;103(s1):101-112. doi:10.1111/j.1471-4159.2007.04712.x

102. Nagasaka Y, Kaneko H, Terasaki H. Caveolin-1 downregulates glial fibrillary acidic protein and vimentin expression of mouse retina and cultured human Muller cell in pathology of proliferative vitreoretinopathy. | IOVS | ARVO Journals. In: *Investigative Opthalmology & Visual Science*. ; 2018. https://iovs.arvojournals.org/article.aspx?articleid=2692654. Accessed August 7, 2021.

103. Senst L, Baimoukhametova D, Sterley T-L, Bains JS. Sexually dimorphic neuronal responses to social isolation. *Elife*. 2016;5. doi:10.7554/eLife.18726

104. Breznik JA, Schulz C, Ma J, Sloboda DM, Bowdish DME. Biological sex, not reproductive cycle, influences peripheral blood immune cell prevalence in mice. *J Physiol*. 2021;599(8):2169-2195. doi:10.1113/JP280637

CHAPTER FOUR: THE ROLE OF ENTERIC GLIAL STING IN THE ENTERIC NERVOUS SYSTEM

ABSTRACT

Appropriate host-microbe interactions are essential for enteric glial development and subsequent gastrointestinal function but the potential mechanisms for this microbe-glial communication are unclear. Here we tested the hypothesis that enteric glia express the pattern recognition receptor stimulator of interferon genes (STING) and communicate with the microbiome through this pathway to modulate gastrointestinal inflammation. *In situ* transcriptional labeling and immunohistochemistry were used to examine STING and IFNβ expression in enteric neurons and glia. Genetic IFNβ reporter mice (B6.129-*Ifnb1*^{tm1Lky}/J), glial-STING KO mice (*Sox10*$^{CreERT2+/-}$;*STING*$^{fl/fl}$), and IFNβ ELISA were used to characterize the role of enteric glia in canonical STING activation. The role of enteric glial STING in gastrointestinal inflammation was assessed in the DSS colitis model. Enteric glia and neurons express STING and enteric glial STING is reduced in glial-STING KO mice but only enteric neurons express IFNβ. While both the myenteric and submucosal plexuses produce IFNβ with STING activation, enteric glial STING seems to play only a minor role. Furthermore, deleting enteric glial STING does not affect weight loss, colitis severity, or enteric neuronal cell proportions in the 3% DSS colitis model. Taken together, our data support canonical roles for STING and IFNβ signaling in the enteric nervous system through enteric neurons but that enteric glia do not use these same mechanisms. We propose that enteric glial STING may utilize alternative signaling mechanisms and/or is only active in particular disease conditions. Regardless, this study provides the first glimpse of STING signaling in the enteric nervous system and highlights a potential avenue of neuroglial-microbial communication.

INTRODUCTION

Appropriate interactions between gut commensal bacteria and host cells shape microbe-host tolerance that is essential for maintaining gut homeostasis.[1–3] Host cells must also recognize pathogenic agents to defend against infection and disrupting this delicate balance can lead to sustained or repetitive inflammation and ultimately the development of chronic gastrointestinal (GI) diseases such as inflammatory bowel disease (IBD).[1,3,4] The role of host-microbe communication in GI disease is complex and bidirectional communication alters both microbial factors and host response to ultimately contribute to host damage or protection.[5] Known molecular mechanisms of this communication commonly focus on mucosal and immune cells as important regulators of host-dependent factors[1–3] but other cells also communicate and respond to microbial factors to influence gut homeostasis and disease pathogenesis.

The enteric nervous system (ENS) is comprised of neurons and glia that regulate many local GI functions including motility, visceral sensation, secretion, absorption, and mucosal permeability.[6,7] The ENS is also ideally situated to facilitate crosstalk between local microbe-immune interactions and the central nervous system through the brain-gut axis to ultimately modulate systemic health.[8,9] This occurs through both direct interactions between the ENS and gut microbiome and microbial tuning of neuro-immune communication.[9–14] Communication between enteric glial cells and luminal microbes in particular is critical for ENS maintenance and host defense mechanisms. Gut microbiota regulate the formation and replenishment of enteric glia within the mucosa and lamina propria.[15–17] In turn, these glial cells respond to gut dysbiosis and interact with immune cells and the mucosal barrier to produce varying proinflammatory and protective effects.[18–20] Characterized mechanisms of glial-microbe signaling involve S100β and pattern recognition receptors of the toll-like receptor family; however, the mechanisms whereby glia monitor the gut microbiota and initiate functional responses remain mostly uncharacterized.

The stimulator of interferon genes (STING) is a pattern recognition receptor that integrates signals from bacterial, viral, and host molecules to modulate inflammatory response.[21–26] STING

signaling has a complex role in gut homeostasis and disease as demonstrated by experiments in whole body STING knockout mice. Under physiologic conditions, mice lacking STING had abnormal mucosal architecture and mucin gene expression in one study but no noticeable functional or phenotypic differences in another.[27-28] Likewise, ablating STING has been reported as being either protective or detrimental in the dextran sodium-sulfate (DSS) colitis model.[27–29] These apparently conflicting results suggest underlying complexities in STING signaling that dictate its homeostatic and pathologic roles. Most attention related to STING signaling has been focused on its role in immune cells but STING is also present in non-canonical cell types and its roles in these cells could contribute to nuances in STING signaling. STING is expressed by neurons and glia in the CNS and astrocytes activate STING signaling in response to infection and injury.[30,31] Additionally these astrocytes enter a STING-dependent reactive state in injury as measured by glial fibrillary acidic protein (GFAP) upregulation.[30] Enteric glia exhibit similar transcriptional profiles to CNS glia[32,33] and play critical roles in immune communication during colitis.[34,35] Given these similarities, it is plausible that enteric glia express STING and respond to host and microbial mediators to modify GI inflammation through the STING pathway.

The aim of this study was to assess the expression and role of STING signaling with the ENS and study its contributions to GI homeostasis and disease. We hypothesized that like CNS glia, enteric glia also express STING and that glial STING signaling modifies colitis. We tested our hypothesis using immunolabeling and genetic mouse models including cre-lox systems to ablate STING in enteric glia (*Sox10*$^{CreERT2+/-}$;*STING*$^{fl/fl}$). Our results show that STING is expressed by both enteric glia and neurons and plays a complex role in regulating downstream pathways involving IFNβ. Surprisingly, the data show that glial *STING* plays a minor role in canonic IFNβ responses and the pathophysiology of acute DSS colitis. These results show that while STING is a functional mechanism in the ENS, its roles are cell type and context dependent.

MATERIALS AND METHODS

Animal Use

All experimental protocols were approved by the Michigan State University Institutional Animal Care and Use Committee (IACUC) in facilities accredited by the Association for Assessment and Accreditation for Laboratory Care (AAALAC) International. Adult male and female C57BL/6 mice 10-20 weeks of age were used for all experiments unless stated otherwise. Mice were maintained in specific pathogen-free conditions and a temperature-controlled environment (Optimice cage system; Animal Care Systems, Centennial, CO) on a 12:12hr light-dark cycle with *ad libitum* access to water and minimal phytoestrogen diet (Diet Number 2919; Envigo, Indianapolis, IN).

Sox10$^{CreERT2+/-}$;*STING*$^{fl/fl}$ were generated to ablate STING in enteric glia in the GI tract. Briefly, *Sox10*^{CreERT2} mice (gifted by Dr. Vassilis Pachnis, The Francis Crick Institute, London, UK) were crossed with B6;SJL-*Sting1*$^{tm1.1Camb}$ STING flox mice (gifted by Dr. John Cambier, University of Colorado Denver and National Jewish Health, Denver, CO) to generate mice hemizygous for Cre and the floxed allele (*Sox10*$^{CreERT2+/-}$;*STING*$^{fl/wt}$). These mice were then backcrossed with *Sox10*^{CreERT2} mice to generate *Sox10*$^{CreERT2+/-}$/*STING*$^{fl/fl}$ mice. Mice were genotyped by Transnetyx (Cordova, TN) and fed tamoxifen citrate (400mg/kg) for 2 wks to induce Cre activity. IFNβ reporter mice (B6.129-*Ifnb1*^{tm1Lky}/J; Jackson Laboratories, stock number 010818) were purchased and maintained as homozygous.

Acute dextran sodium sulfate (DSS) induced colitis

Acute colitis was induced by adding 3% DSS (colitis grade, M.W. 36-50 kDa; MP Biomedical, Solon, OH) to drinking water (3% w/v) for 7 days. DSS solution was replaced every two days. Bodyweight was recorded daily and animals were monitored for signs of disease activity such as loose stools and fecal blood. Mice were humanely euthanized on day 8 and colon length and the presence/absence of intestinal adhesions were recorded.

Ussing Chamber Experiments

Whole thickness distal colon preparations were mounted in Ussing chambers (aperture 0.3 cm^2; EasyMount Ussing chamber system, Physiologic Instruments, San Diego, CA, USA) as previously described.[36] Tissues were maintained in warmed (37°C) and oxygenated (5% CO_2, 95% O_2) Krebs buffer consisting of (in mM): 121 NaCl, 5.9 KCl, 2.5 $CaCl_2$, 1.2 $MgCl_2$, 1.2 NaH_2PO_4, 25$NaHCO_3$ and 11 glucose. After an initial 30 min equilibration, 500µg/ml of rhodamine B isothiocyante-dextran (RITC-dextan, 10-kDa) and 10µm of bacterial CDN c-di-GMP (Biolog, Bremen, Germany) were added to the luminal chamber and incubated for 1 hour. Krebs buffer in the serosal chamber was sampled before and after incubation and RITC-dextran and c-di-GMP were quantified by fluorescence and absorbance, respectively. RITC fluorescence was measured using excitation/emission wavelengths of 544nm/576nm on an Infinite M1000 PRO microplate reader (Tecan Group Ltd, Mannedorf, Switzerland) using i-control™ microplate reader software version 1.6.19.2 (Tecan). Absorbance for c-di-GMP was measured by the 260/280 ratio on a NanoDrop spectrophotometer (ThermoFisher) as CDNs are nucleic acids and demonstrate similar absorbance patterns.[37] Absorbance for RITC was similarly captured and subtracted from c-di-GMP absorbance measurements. Concentrations of RITC and c-di-GMP were calculated by measuring fluorescence and absorbance standards for each compound, respectively.

Muscularis propria, submucosal and myenteric plexus tissue isolation

Sample of distal colon were obtained from euthanized adult male and female mice and placed in a sylgard-coated petri dish containing ice-cold Dulbecco's Modified Eagle Medium (DMEM/F-12). Luminal contents were flushed using a syringe and tissue was cut open along the mesenteric border and pinned flat with mucosa facing up. For whole mount RNAscope and immunohistochemistry, tissue was subsequently fixed overnight in 4% paraformaldehyde (PFA) at 4°C. Fixed tissue was then washed 3x10mins with 1x phosphate-buffered saline (PBS) and longitudinal muscle-myenteric plexus (LMMP) whole mount preparations were microdissected by

removing overlying mucosa, submucosa, and circular muscle. Live samples for IFNβ ELISA experiments were microdissected to the submucosal plexus (SMP) and muscularis propria by removing the mucosa and SMP separately. Live circular muscle-myenteric plexus (CMMP) preparations were prepared for IFNβ reporter (IFNβ-mob) experiments by removing the mucosa, serosa, and longitudinal muscle as described previously .[38]

RNAscope in whole mount LMMP

RNAscope in whole mount myenteric plexus LMMP tissue was adapted from previous protocols[13] using the RNAscope™ 2.5 HD Assay – RED (ACD Biosciences, Newark, CA) according to manufacturer instructions with the following adjustments for colonic LMMP tissue. Tissues were dehydrated and subsequently rehydrated by a serial ethanol gradient (25%, 50%, 75%, 100% in 1x PBS with 0.1% Triton X-100) prior to H_2O_2 treatment. Tissues were then digested with Protease III for 45 mins and incubated with RNAscope probes overnight at 40°C. Tissues were washed 3x5mins between each step with 1x PBS after protease and FastRED steps and 1x RNAscope™ wash buffer after probe and amplification steps. All RNAscope steps were performed in a 96-well place while wash steps were performed in a 48-well plate. The RNA scope protocol was validated using manufacturer controls and probes for ENS-specific transcripts (see Chapter 2). Immunohistochemistry and tissue mounting was performed following completion of the RNAscope protocol as described below. RNAscope probe details are provided in **Table 4.1**.

Immunohistochemistry in whole mount LMMP

Immunohistochemistry (IHC) was performed as described previously.[34,35] Primary and secondary antibody details are provided in **Table 4.1**. Briefly, LMMP preparations were washed 3x10mins in PBS with 0.1% Triton X-100 followed by 45min incubation in blocking solution (4% normal donkey serum, 0.4% Triton X-100, and 1% bovine serum albumin) at 20°C. Primary antibodies were diluted in blocking solution and incubated with tissue for 24-48hrs at 4°C. Primary

antibodies were removed and tissues were washed 3x10mins in 1x PBS and incubated with secondary antibodies diluted in blocking solution for 2hrs at 20°C. LMMP preparations were then rinsed 2x10mins in 1xPBS followed by 1x10mins in 0.1M phosphate buffer. Tissues were then mounted on slides with Fluoromount-G mounting medium with or without DAPI (Southern Biotech, Birmingham, AL). All antibodies have been validated in prior studies.[34,39–43]

Fixed Frozen Section Immunohistochemistry

Fixed frozen slide IHC was performed as described previously.[34] Distal colons were harvested, pinned at ends in sylgard-coated dishes, and fixed overnight in 4% paraformaldehyde (PFA) at 4°C. Fixed samples were washed 3x10mins in 0.1M phosphate buffer (0.1M PB) and subsequently cryoprotected in a 30% sucrose solution in 0.1M PB for at least 72 hours. Samples were submitted to the Michigan State University HistoPathology Laboratory for cryosectioning and 10-12µm sections were processed for immunolabeling. For IHC, slides equilibrated to 20°C for 2 hours before use. Blocking, labeling, and washes were carried out using the same timing and dilutions as for whole mount IHC and antibodies used are listed in **Table 4.1**.

Histological staining

Cross-sections of distal colon were submerged in 10x volume of Carnoy's fluid (60% ethanol, 30% chroloform, and 10% acetic acid) and fixed for 4 hours at 20°C. Tissues were transferred to 30% ethanol in distilled H_2O prior to staining with hematoxylin & eosin (H&E) or periodic acid-schiff & hematoxylin (PASH) by the Michigan State University HistoPathology Laboratory.

IFNβ reporter experiments

Live CMMP preparations from IFNβ-mob reporter mice (B6.129-*Ifnb1*^{tm1Lky}/J) were incubated with 10µg/ml or 100µg/ml of the STING agonist 5,6-dimethylxanthenone-4-acetic acid

(DMXAA, Invivogen) in DMEM/F-12 plus 100U/ml Penicillin-Streptomycin for 6-18hrs at 37°C (5% CO2, 95% air). Images of YFP reporter expression were captured in the FITC channel at 0, 6, and 18hrs as described below in “Imaging”.

IFNβ ELISA experiments

Muscularis propria and SMP were incubated with STING agonists in DMEM/F-12 plus 100U/ml Penicillin-Streptomycin for 18-24hrs at 37°C (5% CO2, 95% air). Media was collected at the end of the incubation period and transferred to a 1.5ml tube and centrifuged at 2000 x g for 10 mins. Samples were either processed immediately for ELISA or kept at -80°C until further processing. STING agonists used included 100μM c-di-GMP (Biolog), 100μM 2,3-cGAMP (Invivogen), 100μM 3,3-cGAMP (Invivogen), 100μg/ml DMXAA (Invivogen), and ~10^9 viral particles of Ad5-VCA0956[44] (a c-di-GMP producing adenovirus gifted by Dr. Christopher Waters, Michigan State University, MI). C-di-GMP and Ad5-VCA0956 ELISAs were performed after 24h incubations using the Verikine™ Mouse IFN Beta ELISA Kit (PBL Assay Science) while the 2,3-cGAMP, 3,3-cGAMP, and DMXAA ELISAs were performed after 18h incubations using the Mouse IFN beta SimpleStep ELISA® Kit (Abcam). All ELISAs were conducted in duplicate following manufacturer’s protocols and measured on a Synergy H1 Hybrid Multi-Mode Microplate Reader with Gen5 v3.04 software (BioTek, Winooski, VT). Tissue preparations were cut to the same dimensions or normalized to tissue weight.

Imaging

All RNAscope and IHC representative imaging was performed on a Zeiss LSM 880 NLO confocal system (Zeiss, Jena, Germany) using Zen Black software and a 20x objective (0.8 numerical aperture, Plan ApoChromat; Zeiss). 40x images were achieved using digital zoom within the software. IHC images for quantification of $nNOS^+$ or $calbindin^+$ neurons were captured using the 40x objective (0.75 numerical aperture, Plan Fluor; Nikon) of an upright epifluorescence

microscope (Nikon Eclipse Ni) with a Retiga 2000R camera (QImaging, Surrey, BC, Canada) controlled by QCapture Pro 7.0 (QImaging) software. Representative images and those for colitis scoring of histology slides were captured on an Olympus SLIDEVIEW VS200 slide scanner. Images for IFNβ reporter experiments were acquired using a 20x water-immersion objective (LUMPlanFI, 0.8 numerical aperture) of an upright Olympus BX51wI fixed stage microscope (Olympus, Tokyo, Japan) using NIS-Elements software (v.4.5; Nikon, Tokyo, Japan) and an Andor Zyla sCMOS camera (Oxford Instruments, Abingdon, United Kingdom).

Statistical Analysis

All statistical analyses were performed in GraphPad Prism v9.2.0 (GraphPad Software, San Diego, CA) and considered significant at $p < 0.05$. Concentration values for Ussing chamber experiments utilized the least-squares fit model while for ELISAs the sigmoidal 4 parameter curve fit (4PL) was used. A paired *T*-test was used to analyze Ussing chamber experiments while for all other analyses were performed using either a one- or two-way ANOVA with Dunnett's, Tukey's, or Bonferroni's multiple comparison tests where appropriate. Details are specified in respective figure legends.

Histological colitis scoring and neuron counts were performed using FIJI software (National Institutes of Health, Bethesda, MD). Tissue damage was assessed per colonic cross section in histological colitis scoring where the extent of tissue destruction was calculated based on mucosal architecture (0=none, 1=mild damage, 2=moderate damage, and 3=loss of crypt and epithelial structure), cellular infiltration (0=normal, 1=around crypt bases, 2=reaching muscularis mucosa, and 3=reaching submucosa), muscle thickening (0=none, 1=mild, 2=moderate, 3=large), and goblet cell depletion (0=present, 1=decreased in number/modified morphology, or 2=depleted). A score multiplier of 1, 2, 3, or 4 was used based on the % of cross-section affected (25%, 50%, 75%, or 100%, respectively) to reach a maximum score of 44. $nNOS^+$ and $calbindin^+$ neuron counts in the myenteric plexus were assessed as ratios of the number of HuC/D^+ or

peripherin^{+} neurons within each ganglia and ganglionic area for 12 ganglia/mouse in n=3-5 mice/group.

Table 4.1 RNAscope probes and IHC antibodies used in Chapter 4.

RNAscope Probes			
Probe Target	*Vendor*	*Catalog Number*	*Channel*
Tmem173 (Alt. name for *Sting1*)	ACD Bio-Techne	413321	C1
Immunohistochemistry (IHC) Antibodies			
Primary antibodies			
Target	*Vendor*	*Catalog Number*	*Dilution*
Chicken anti-GFAP	Abcam	ab4674	1:1000
Hu C/D (Biotinylated)	Invitrogen	A21272	1:200
Mouse anti-Peripherin	Santa Cruz	sc-377093	1:100
Rat anti-MHCII	Novus	NBP2-21789	1:200
Rabbit anti-Calbindin-D28K	Swant	CD38a	1:500
Rabbit anti-IFNβ	Novus	NBP1-77288	1:200
Rabbit anti-STING	Proteintech	19851-1-AP	1:500
Rabbit anti-S100β	Abcam	ab52647	1:200
Sheep anti-nNOS	Millipore	AB1529	1:200
Secondary antibodies			
Donkey anti-sheep Alexa Fluor 405	Jackson Laboratories	713-475-147	1:400
Goat anti-chicken Dylight 405	Jackson Laboratories	103-475-155	1:400
Donkey anti-chicken Alexa Fluor 488	Jackson Laboratories	703-545-155	1:400
Donkey anti-mouse Alexa Fluor 488	Jackson Laboratories	715-545-150	1:400
Donkey anti-rabbit Alexa Fluor 488	Jackson Laboratories	711-545-152	1:400
Donkey anti-sheep Alexa Fluor 488	Jackson Laboratories	713-475-147	1:400
Donkey anti-rabbit Alexa Fluor 594	Jackson Laboratories	711-585-152	1:400

Table 4.1 (cont'd)

Goat anti-rat Alexa Fluor 594	Jackson Laboratories	112-585-003	1:400
Streptavidin Alexa Fluor 594	Jackson Laboratories	016-580-084	1:400
Donkey anti-rabbit Alexa Fluor 647	Jackson Laboratories	711-605-152	1:400
Donkey anti-rat Alexa Fluor 647	Jackson Laboratories	712-605-150	1:400

RESULTS

STING is expressed in enteric neurons and glia

STING is expressed by neurons and glia in the CNS[30,31] but whether it is expressed in the ENS is unknown. We began assessing potential STING expression in the ENS using publicly available RNA-sequencing datasets for enteric glia that were generated by our laboratory and other groups.[45,46] Our RNA-sequencing data is represented in **Fig 4.1a** (data 1 unpublished, see Chapter 3; data 2 available from Delvalle et al. 2018[46]) while publicly available data is represented in **Fig 4.1b** (available from Drokhlyansky et al. 2020[45] and accessed through the Single Cell Portal, Broad Institute). The canonical STING signaling cascade involves STING forming a complex with TANK-binding kinase (*Tbk1*) to activate transcription factors interferon regulatory factor (*Irf3*) and NF-κB (*Nfkb1* and *Rela*) that stimulate the production of type I IFNs such as IFNβ.[21] Type I IFNs bind to the IFNα/β receptor (*Ifnar1* + *Ifnar2*) and activate interferon-stimulated gene factor 3 (comprised of *Stat1*, *Stat2*, and *Irf9*) that induce transcription of IFN-stimulated genes.[21,47] The transcriptional data show that enteric glia express STING (gene *Sting1,* alternate gene name *Tmem173*), its directly downstream signaling molecules, and genes for the proteins induced by type I IFN binding in both mice (**Fig 4.1a-b**) and humans (**Fig 4.1b'**). We confirmed these results by visualizing *Sting1* expression within the myenteric plexus using RNAscope *in situ* hybridization. RNAscope labeling shows that *Sting1* is expressed in both enteric glia and neurons of the myenteric plexus in WT mice (**Fig 4.1c**, white and yellow arrows, respectively) and that labeling for *Sting1* is reduced in enteric glia from glial-STING KO (*Sox10*$^{CreERT2+/-}$;*STING*$^{fl/fl}$) mice. *Sting1* expression within cell types was defined as visible RNAscope puncta colocalizing with nuclei and either immunolabeled S100β for glia or peripherin for neurons. Taken together, these data suggest that enteric glia express the necessary genes to utilize STING signaling through its prototypical signaling cascade and additionally respond to downstream type I IFN signaling.

We next determined whether STING protein is expressed by enteric neurons and/or glia using immunohistochemistry. STING immunoreactivity was observed in both neurons and glia

throughout the myenteric plexus in WT mice (**Fig 4.2a**). Immunoreactivity for STING was also observed in neighboring MHCII$^+$ immune cells, which are likely resident muscularis macrophages (yellow arrows). Interestingly, STING is also expressed in endothelial cells[21] and positive immunolabeling of blood vessels adjacent to ganglia was observed (tan arrow). Immunoreactivity for STING in macrophages and endothelial cells serves as an internal positive control for the antibody since these are known cellular locations of STING. The highly overlapping nature of enteric neurons and glia that express STING and the diffuse pattern of STING staining made appreciating overt differences in enteric glial STING labeling difficult between samples from WT and glial-STING KO mice. However, loss of STING expression in enteric glia was evident in regions surrounding enteric neurons (white arrows denote glial cell bodies surrounded by GFAP$^+$ processes in WT and KO panels) which led to an apparent increased definition of neuronal cell bodies (**Fig 4.2a**). Immunolabeling in cross-section of colon showed clear labeling in the myenteric plexus including neurons and enteric glia (white arrow denotes a glial cell body surrounded by GFAP$^+$ processes) (**Fig 4.2b**) and stronger STING labeling of MHCII$^+$ immune cells in the muscularis propria and mucosa/lamina propria (yellow arrows). These data suggest that enteric neurons and glia express STING, albeit at lower levels than immune cells.

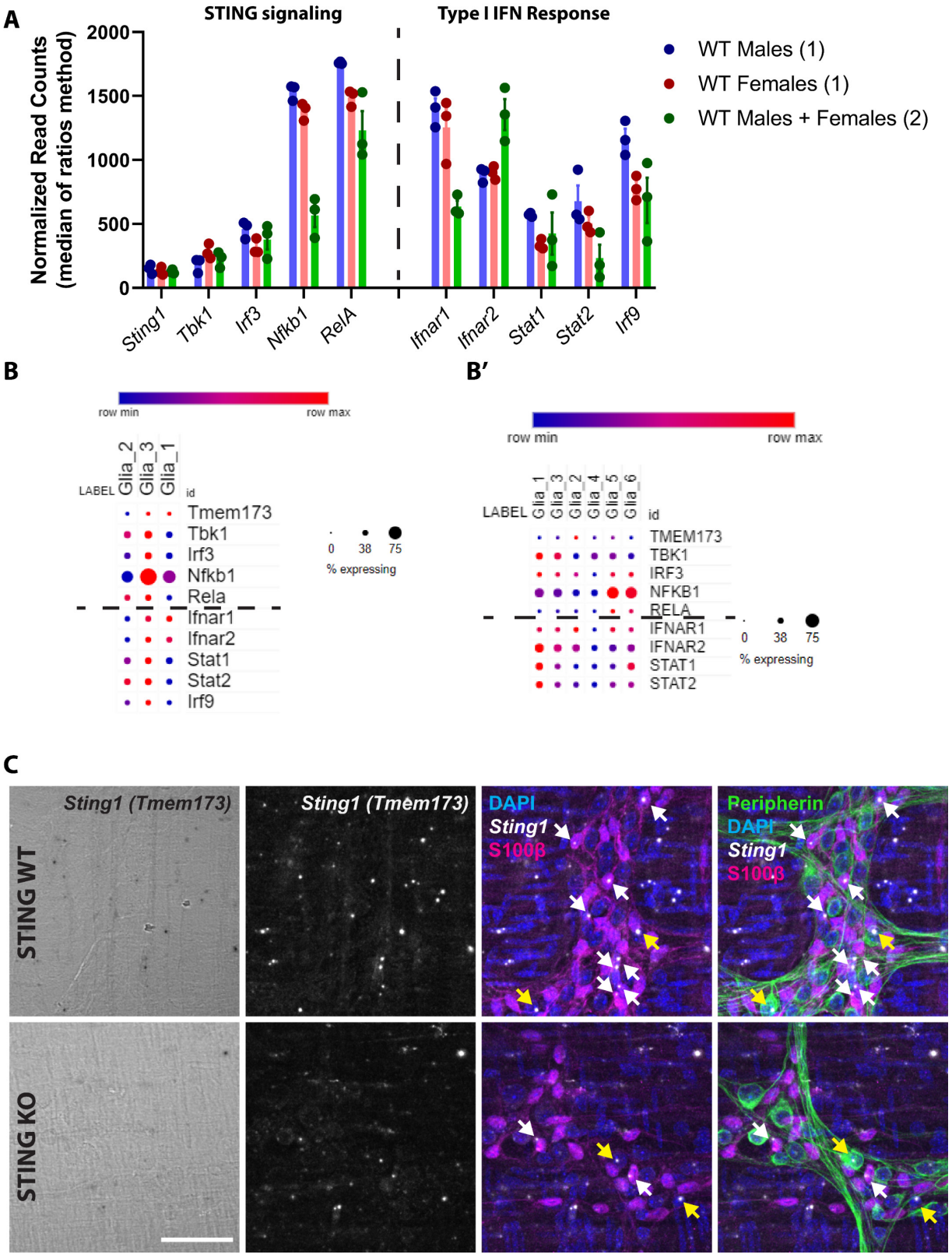

Figure 4.1 Transcripts of STING and its downstream signaling molecules are expressed in colonic enteric glia across RNA-seq datasets and in situ.

(A) Gene expression of STING and related genes in normalized read counts generated through DESeq2[48] analysis from colonic enteric glia in control mice. Data are from two separate RNA-seq datasets from our lab; (1) unpublished, see chapter 3 of n=3mice/group and (2)previously published,[46] n=3 mice. Glia from both experiments display consistent expression of STING (*Sting1*), its downstream targets, and type I IFN downstream targets. **(B-B')** These genes are also expressed in colonic enteric glia from mice **(B)** and humans **(B)** in a publicly available single cell RNA-seq dataset[45] (accessed through the Single Cell Portal, Broad Institute). In these data the STING gene is referred to by another alternate name, *Tmem173.* Relative expression level is denoted by color while percentage of expressing cells is estimated by circle size. Dotted lines in **A-B** separate genes for proteins involved in STING activation and genes for proteins in type I IFN response. **(C)** *In situ* hybridization RNAscope labeling for *Sting1* (grayscale) in myenteric plexus samples from WT (*top*) and glial-STING KO (*Sox10*$^{CreERT2+/-}$;*STING*$^{fl/fl}$, *bottom*) mice co-labeled with antibodies against S100β (magenta) for glia and peripherin (green) for neurons. Enteric glial *Sting1* expression is highlighted by white arrows while enteric neuronal expression is marked by yellow arrows. Images representative of labeling in n=3 mice. Scale bar represents 50μm.

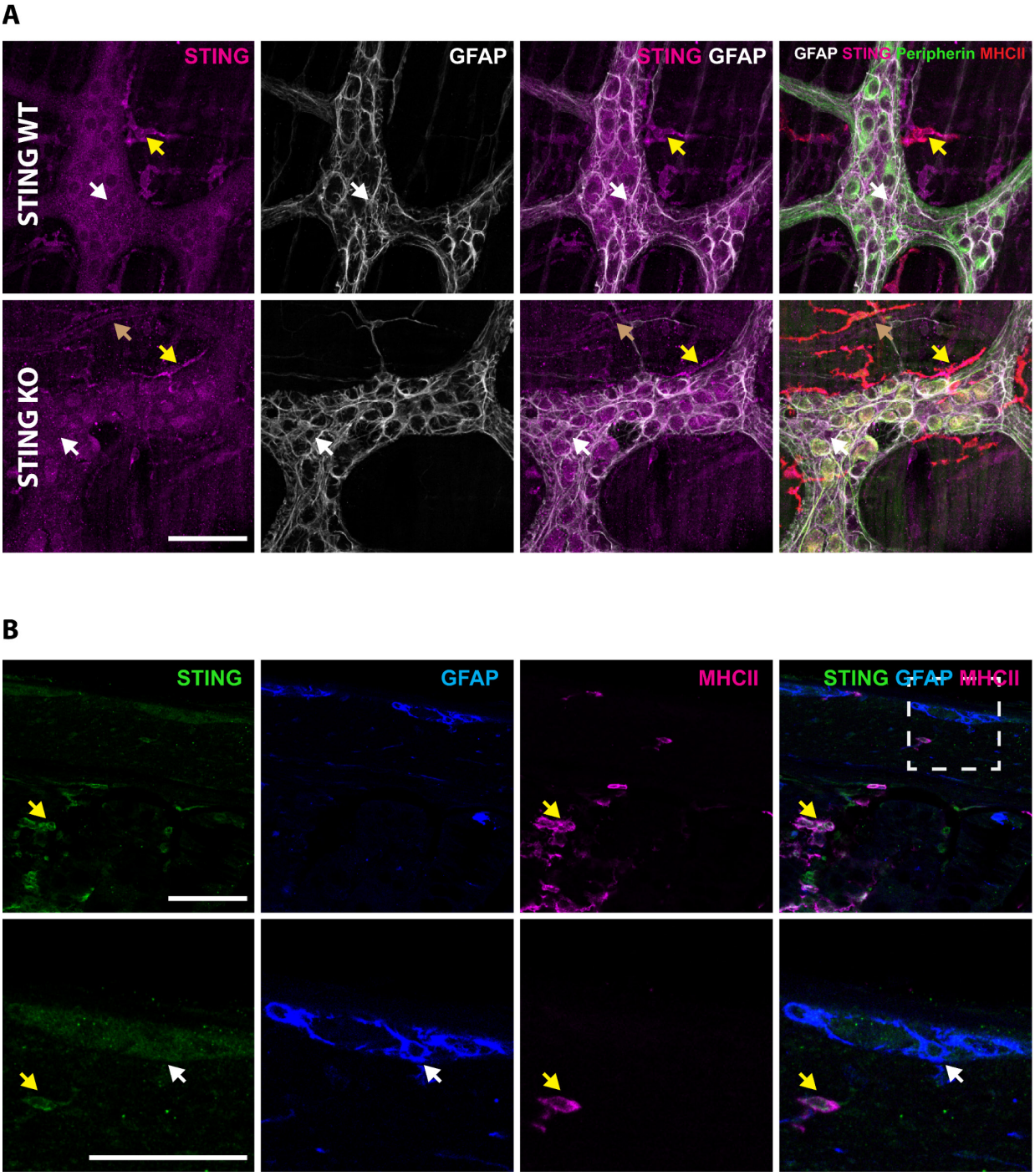

Figure 4.2 STING protein is expressed in enteric glia and neurons in the myenteric plexus, and by resident macrophages.

(A) Immunolabeling for STING (magenta), GFAP (grayscale; glia), peripherin (green; neurons), and MHCII (red; macrophages) in myenteric ganglia from WT (*top*) and glial-STING KO (*Sox10*$^{CreERT2+/-}$;*STING*$^{fl/fl}$, *bottom*) mice. STING labeling is observed throughout myenteric ganglia

and loss of expression in glial STING-KO mice (*Sox10::*$^{CreERT2+/-}$/*STING*$^{fl/fl}$) is mainly appreciable by accentuation of STING within neuronal cell bodies and adjacent reduced STING expression indicative of glial cell bodies (white arrows). STING is also expressed by resident endothelial cells (brown arrow) and resident muscularis macrophages (yellow arrows). **(B)** Immunolabeling for STING (green), GFAP (blue; glia), and MHCII (magenta; macrophages) in cross-sections of the mouse colon. The serosa is at the top of each image while mucosa is at the bottom. Immunolabeling for STING is present in the ENS and resident immune cells in the muscularis and lamina propria. White arrows indicate enteric glial STING expression while yellow arrows point to MHCII^{+} immune cell expression. The boxed area in the top row of panels is magnified in the images shown in the second row. Images representative of labeling in n=2-4 mice. Scale bars represent 50μm.

Myenteric plexus IFNβ is primarily localized in enteric neuron cell bodies and neuronal and/or glial processes and fiber tracts

Given that enteric neurons and glia express STING RNA and protein, we assessed whether type I IFNs, the primary mediator of STING activitity[21], are also expressed by these cells. We began by examining expression of the gene encoding IFNβ (*Ifnb1*) in enteric glial transcriptional datasets. Interestingly, *Ifnb1* was not expressed at detectable levels in bulk enteric glial RNA-sequencing datasets[46] and was negligible in single cell transcriptional sequencing datasets for enteric glia (data not shown)[45] suggesting that enteric glia do not express IFNβ. We confirmed this data by conducting experiments in IFNβ-mob reporter mice (B6.129-*Ifnb1*^{tm1Lky}/J) that express YFP with IFNβ transcription [49] and with immunohistochemistry for IFNβ. YFP expression in IFNβ-mob reporter mice was primarily observed in neuronal cell bodies within the myenteric plexus with no apparent fluorescence in glia (**Fig 4.3a**). Reporter expression in this line is supported by ganglionic IFNβ immunolabeling that was observed to primarily localizes to neuronal fiber tracts (**Fig 4.3b**). These data suggest that enteric neurons are responsibly for IFNβ in the ENS and that enteric neurons traffic IFNβ along their processes. We conducted labeling in cross-section of mouse colon to visualize the extent of IFNβ expression in the gut wall and relative expression in other cell types compared to the ENS. Similar to STING, IFNβ is primarily expressed in the myenteric plexus and mucosa/lamina propria (**Fig 4.3c**). However, unlike STING the relative expression of IFNβ in the ENS (denoted by white arrows) is comparable or potentially even higher as compared to MHCII^{+} immune cells (denoted by yellow arrows). This supports IFNβ as a functional immune mediator in the ENS and enteric neurons whether through STING-dependent or –independent pathways.

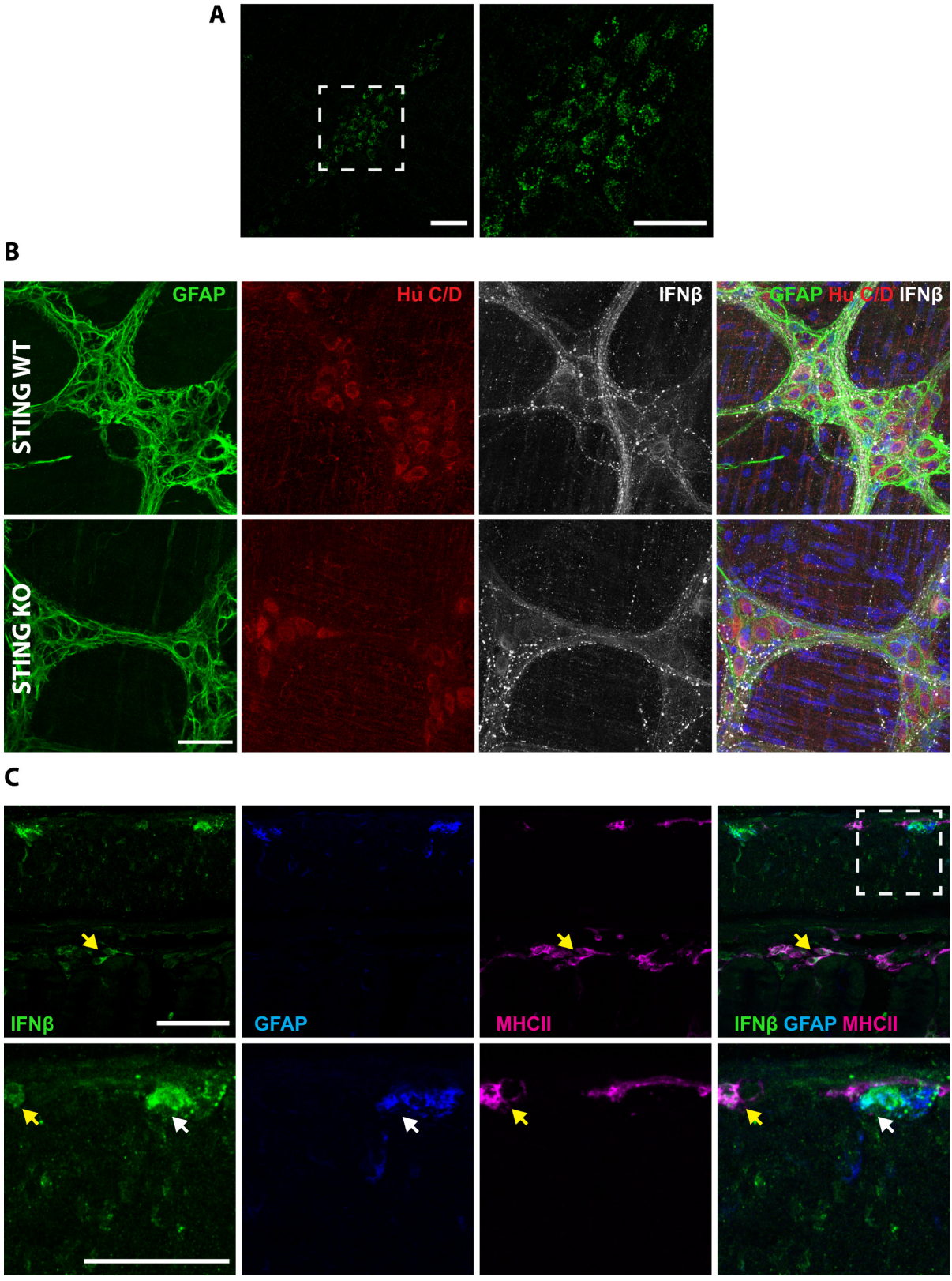

Figure 4.3 IFNβ in the ENS is primarily located to enteric neurons and resident immune cells.

(A) Image showing native YFP fluorescence in the myenteric plexus of a IFNβ-mob reporter mouse (B6.129-*Ifnb1*^{tm1Lky}/J) and demonstrates expression primarily in enteric neuronal cell bodies. Image within white dotted box in the left panel is magnified in the right panel. **(B)** Immunolabeling for IFNβ (grayscale), GFAP (green; glia), and Hu C/D (red; neurons) in myenteric ganglion from the colons of WT (*top*) and glial-STING KO (*Sox10*$^{CreERT2+/-}$;*STING*$^{fl/fl}$, *bottom*) mice. **(C)** Immunolabeling in cross-sections of WT mouse colon showing IFNβ (green), GFAP (blue), and MHCII (red). The serosal side is at the top of each image while mucosa is at the bottom. Images representative of labeling in n=2-3 mice. Scale bars represent 50μm.

Enteric glial STING does not affect ENS IFNβ production

Since STING and IFNβ are both expressed in the ENS we next sought to determine if ENS STING could be activated to produce IFNβ and whether enteric glial STING contributed to this response. Canonical STING signaling responds to cyclic dinucleotide (CDN) molecules produced by microbes and in response to self-leaked DNA during host damage to upregulate type I IFNs.[21] While host-dependent CDNs may originate in the deeper gut layers, bacterial CDNs must reach the ENS from the lumen to activate STING. While this may occur readily in disease states that compromise the mucosal barrier, whether bacterial CDNs utilize physiological mechanisms of trans- and paracellular permeability to reach the ENS is not understood. We tested this by mounting the full-thickness colon samples in Ussing chambers and incubating the luminal chamber with the bacterial CDN c-di-GMP. The physiologic barrier of the samples was fully intact and without leakage as confirmed by lack of passage of the 10-kDa molecule RITC-dextran to the serosal chamber (**Fig 4.4a**, *left*). Furthermore, c-di-GMP was identified in the serosal chamber after 1h incubation ($P < 0.001$; **Fig 4.4a**, *right*), suggesting that c-di-GMP is capable of reaching the ENS from the gut lumen even when the mucosal barrier is intact.

ENS IFNβ production with STING activation was measured by ELISA from supernatants of ENS preparations incubated *in vitro* with STING ligands for 18-24h (**Fig 4.4b-c**). First, muscularis propria tissue housing the myenteric plexus was incubated with either the bacterial CDN c-di-GMP or an adenovirus construct designed to promote host c-di-GMP production (AdVCA or Ad-VCA0956).[44] An adenovirus containing no transgenetic material (AdNull) was used as an additional negative control. The myenteric plexus produced IFNβ in response to both c-di-GMP and AdVCA ($P < 0.01$; **Fig 4.4b**) indicating that ENS STING can be canonically activated by bacterial c-di-GMP. However, there are a variety of other STING ligands including CDNs derived from different bacterial species such as 3,3-cGAMP, the host-produced CDN 2,3-cGAMP, and the murine pharmacologic agonist DMXAA.[21,23,24,50,51] Differential responses to these ligands by the ENS may suggest specified function of ENS STING and therefore, we tested IFNβ in

response to these ligands as well. Both the myenteric ($P < 0.01$; **Fig4.4c**, *left*) and submucosal ($P < 0.001$; **Fig4.4c**, *middle*) plexuses produce IFNβ in response to STING ligands. However, IFNβ production between ligands was not significantly different in either the myenteric or submucosal plexus suggesting that ENS STING responds fairly equally to these STING ligands. Interestingly IFNβ production in response to all ligands was higher in the submucosal than myenteric plexus ($P < 0.0001$; **Fig4.4c**, *right*). This is likely due to the additional $STING^+$ cell types that reside within and adjacent to this layer (**Fig4.2b**) and thus it is unclear to what degree enteric neurons and/or glia contribute to total IFNβ production in the submucosal plexus. However, IFNβ production in the myenteric plexus can be visualized with IFNβ-mob mice and increased transcription is appreciated in enteric neuronal cell bodies after a 6h incubation with 100μg/ml DMXAA (**Fig 4.2e**). This supports that at least in the myenteric plexus STING activation leads to IFNβ in enteric neurons.

Even though ENS IFNβ is primarily produced in enteric neurons, glial STING may still indirectly contribute to IFNβ production. STING transcription is induced by type I IFNs and STING in turn potentiates CDN-triggered type I IFN production.[52] Neuronal IFNβ could potentiate STING in enteric glia and in turn, enteric glial STING could potentiate neighboring neurons. CNS neuroglia complete STING signaling between different cell types[53] and enteric neurons and glia also divide and share other signaling cascades like that of the antioxidant glutathione.[41] Thus, we performed ELISA on supernatants from glial-STING WT and KO mice after 18h incubations with 100μg/ml DMXAA. Genotype did not significantly affect IFNβ production in either the myenteric (**Fig 4.4d**, *left*) or submucosal (**Fig 4.4d**, *right*) plexus. We then hypothesized the contribution of enteric glial STING to IFNβ production may be more subtle and only appreciated locally so we immunostained the myenteric plexus after incubation. However, there are no appreciable differences in IFNβ staining within the myenteric ganglia of glial-STING WT and KO mice (**Fig 4.4f**) suggesting that enteric glial STING does not play a significant role in ENS IFNβ production.

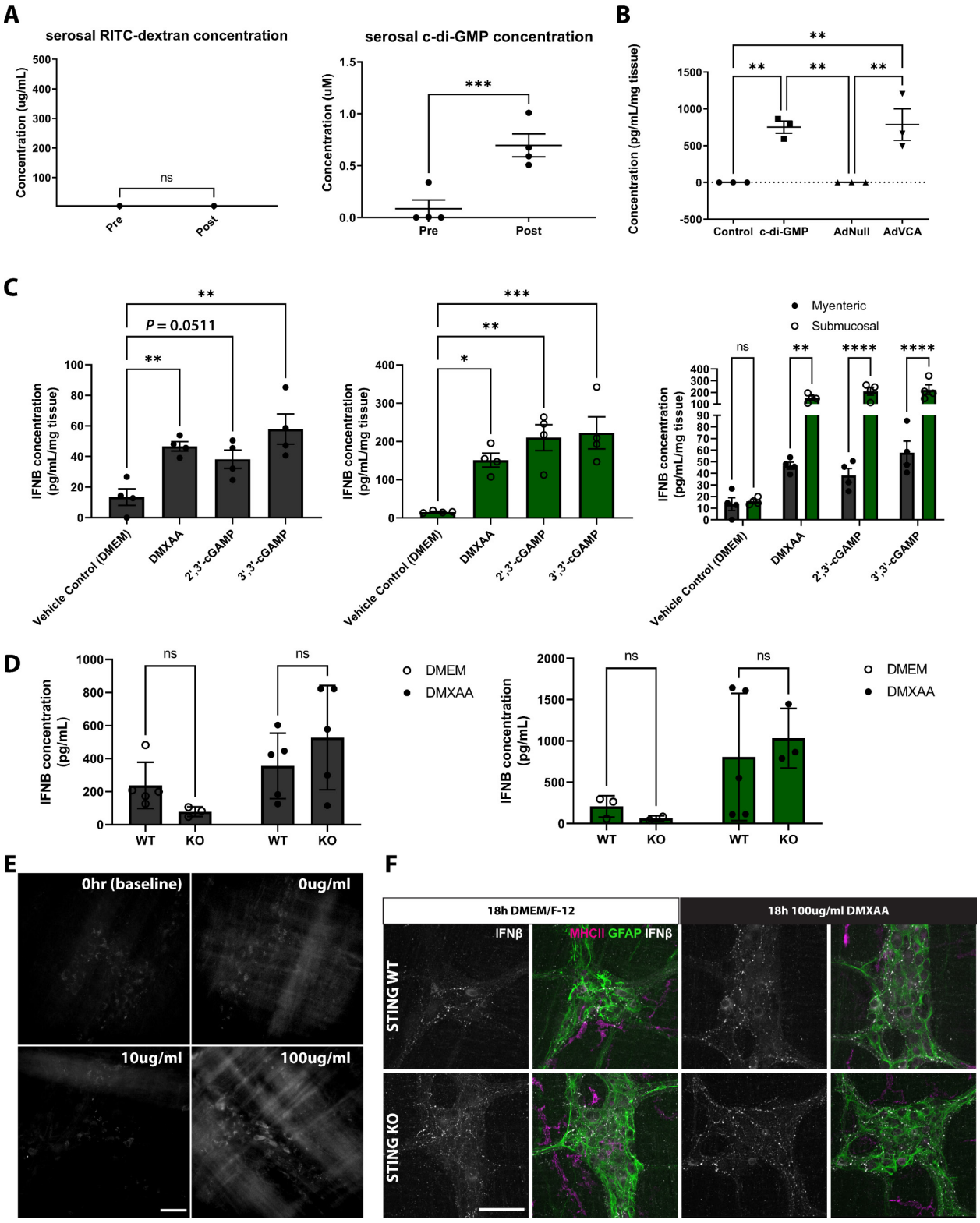

Figure 4.4 The gastrointestinal wall is permeable to bacterial STING agonist c-di-GMP and enteric glial STING does not significantly contribute to ENS IFNβ response.

(A) Ussing chamber data demonstrating no RITC-dextran flux to the serosal side of chamber at the end of the experiment (*left)* to demonstrate mucosal barrier integrity and that the gut wall is permeable to the bacterial STING agonist c-di-GMP (*right),* suggesting that luminal CDNs are capable of reaching the ENS. C-di-GMP concentrations in the serosal chamber were assessed after 1h incubation by 260/280 absorbance. Ussing chamber experiments were analyzed by paired Student's *T* test with n=4 mice. **(B-C)** IFNβ production by ENS whole mounts in response to STING agonists as assessed by ELISA. **(B)** Muscularis propria tissue housing the myenteric plexus was incubated for 24h with 100μM c-di-GMP or ~10^9 viral particles of Ad-VCA0956,[44] an adenovirus that promotes c-di-GMP production within infected cells. Negative controls also included a mutant adenovirus carrying no transgenic material (Ad5-null). Data were analyzed by one-way ANOVA with Tukey's multiple comparison test from n=3 mice/group. **(C)** Both submucosal (*left*) and muscularis propria (*middle*) tissue were incubated with STING agonists 100μg/mL DMXAA, 100μM 2',3-cGAMP, or 100μM 3',3'-cGAMP for 18h. While both layers produce IFNβ in response to all STING agonists the SMP produces more IFNβ than the LMMP (*right*). Data represents analysis from n=4 mice/group. **(D)** Glial STING KO does not significantly alter ENS IFNβ production. Muscularis propria (*left*) and submucosal plexus (*right*) preparations from glial-STING WT and KO mice were incubated with 100μg/mL DMXAA for 18h. Both layers were significant for DMXAA treatment but not genotype ($P = 0.0156$ for myenteric and $P = 0.0357$ for submucosal). Data analyzed from n=5 mice/group. **(E)** Enteric neurons produce IFNβ after 6h of incubation with 100μg/ml DMXAA as visualized by YFP fluorescence in IFNβ-mob mice. **(F)** IFNβ localized to the myenteric plexus is not appreciably different after 18h incubation with 100μg/ml DMXAA in either glial-STING WT (*top*) or KO (*bottom*) mice. Data were analyzed with one- and two-way ANOVA and Dunnett's or Bonferroni's multiple comparison tests respectively. Data shown as mean ± SEM. *$P < 0.05$, **$P < 0.01$, ***$P < 0.001$, ****$P < 0.0001$, ns = not significant. Images representative of labeling in n= 2-3 mice/group. Scale bars represent 50μm.

Enteric glial STING does not play a major role in GI health or ENS neuronal populations in acute DSS colitis

The pathogenesis of DSS colitis involves compromised mucosal barrier integrity and increased exposure of deeper gut layers to luminal contents including bacterial metabolites.[54,55] This makes DSS colitis an appropriate method to study the role of pattern recognition receptors such as STING in GI disease. Prior work assessing the susceptibility of whole-body STING KO mice to acute 3% DSS colitis reported opposing results where STING may either exacerbate or ameliorate colitis.[28,29] This suggests more complex and specific factors may influence STING's role in acute DSS colitis and understanding the roles of cell-specific responses would help determine this. Therefore, we tested whether enteric glial STING contributes to disease in the acute 3% DSS colitis model. Glial-STING WT and KO males and females were given 3% DSS in their drinking water for 7 days during and euthanized on day 8 (**Fig 4.5a**). Significant weight loss ($P < 0.0001$; **Fig 4.5b**) and colonic shortening ($P < 0.0001$; **Fig 4.5b'**) occurred in 3% DSS treated mice compared to controls with no significant difference between genotypes, suggesting that enteric glial STING does not significantly contribute to these DSS-induced responses. DSS colitis is reportedly more severe in males than females[29,56] so we then hypothesized that enteric glial STING may produce a male-specific response and analyzed body weight loss and colonic shortening in males only. Genotype did not have a significant effect in male-specific weight loss (**Fig 4.5c**) or colonic shortening (**Fig 4.5c'**). However, glial-STING KO DSS males exhibited a delay in weight loss compared to WT controls. This may be indicative of subtle differences in DSS response due to glial STING but further research is required.

DSS colitis causes colonic mucosal damage, immune cell infiltration, and edematous muscle thickening that can be appreciated in histological staining. Since studies of whole-body STING KO suggest STING may ameliorate or exacerbate damage on this scale as well[28,29] we investigated this in our glial-STING KO mice to see if glial STING contributed to one of these responses. We utilized a standardized method for assessing colonic histological pathology that

incorporates assesses cellular destruction and infiltrate throughout the gut wall and assigns a damage score based on the severity of these parameters known as the disease activity index. Destruction of mucosal architecture, degree of cellular infiltration, and muscle thickening were observed using H&E staining (**Fig 4.6a**) while goblet cell loss was observed using PASH staining (**Fig 4.6b**). 3% DSS treatment significantly increased disease score in both sexes ($P < 0.0001$; **Fig 4.6c**) and males only ($P < 0.0001$; **Fig 4.6c'**) but was not significantly different between glial-STING WT and KO mice, suggesting glial STING does not play a role in these whole-colon disease processes.

Acute DSS colitis causes notable effects within the ENS and can alter proportions of cholinergic and nitrergic neurons in the colonic myenteric plexus.[57–60] We assessed neurochemical coding in glial-STING WT and KO mice using immunolabeling for the cholinergic marker calbindin and the nitrergic marker nNOS (**Fig 4.7a**). Positive cells were counted per ganglion and normalized to ganglionic area. DSS-treated mice exhibited increased proportions of calbindin$^+$ neurons ($P < 0.0001$; **Fig 4.7b**, *left*) which is consistent with prior reports.[57,58] However, DSS-treated mice also exhibited an increase in the proportion of nNOS$^+$ nitrergic neurons ($P < 0.0001$; **Fig 4.7b**, *right*) where previous studies reported no difference or loss of nitrergic neurons[58–60]. Genotype did not have a significant effect on the proportions of cholinergic or nitrergic neurons. Taken together, these data support the conclusion that enteric glial STING does not play a major role in acute DSS colitis.

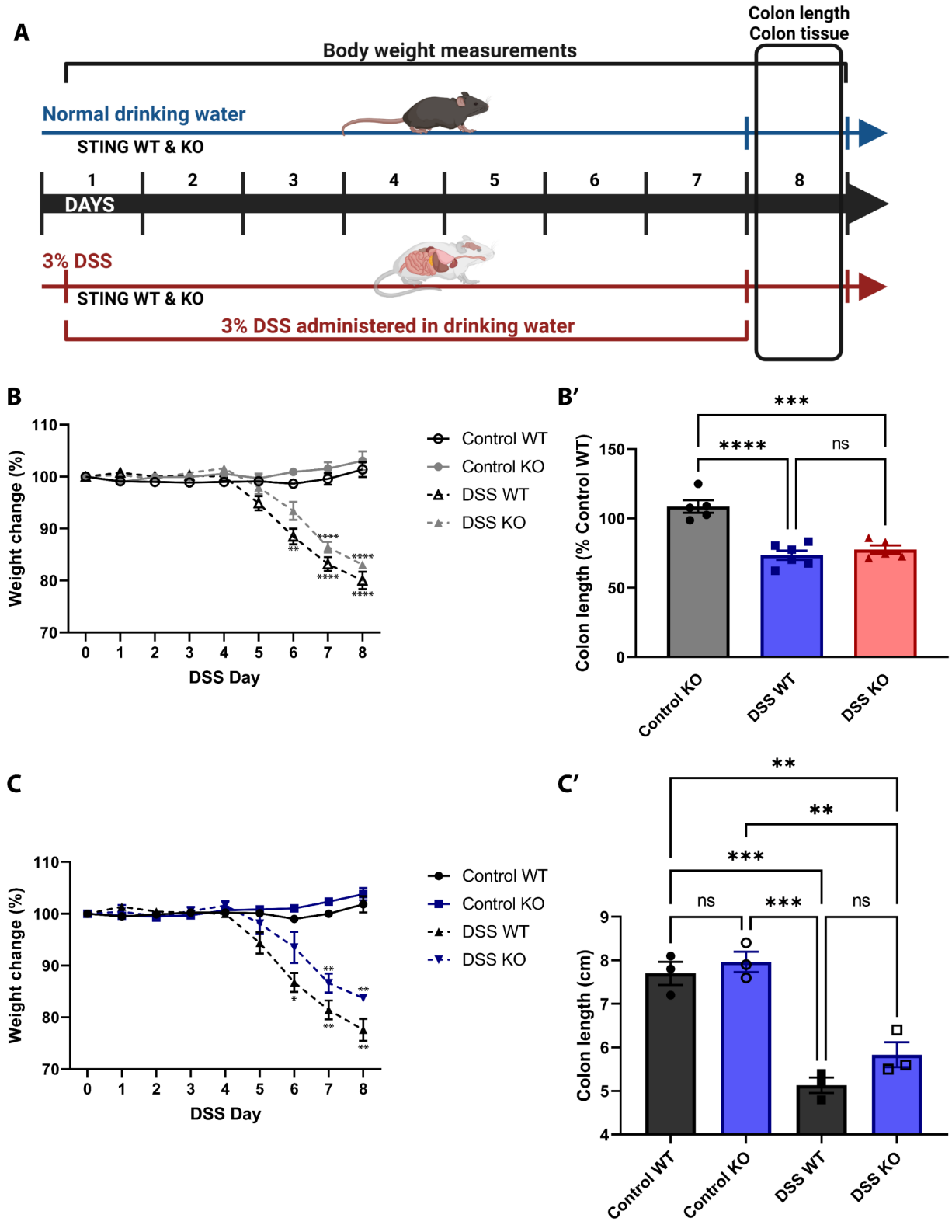

Figure 4.5 Enteric glial STING does not play a major role in DSS colitis-induced weight loss or colonic shortening.

(A) Schema of timeline for acute 3% DSS colitis and data collection (created with Biorender.com). **(B-B)** Loss of enteric glial STING does not significantly affect DSS colitis-induced weight loss **(B)** or colonic shortening (represented by %control WT to allow combined sex comparisons) **(B')** in male and female mice. **(C-C')** Since DSS colitis affects males more severely than females[29] we analyzed our male data separately as well to see if any sex-specific effects occurred. However, enteric glial STING still did not significantly affect DSS colitis-induced weight loss **(C)** or colonic shortening **(C')**. For weight changes, STING KO DSS mice were significantly different from both control groups for days 7 and 8 while STING WT DSS mice were significantly different from both control groups for days 6-8. Weight change data were analyzed with a mixed-model two-way ANOVA and Dunnett's multiple comparison test while colon length data were analyzed with a one-way ANOVA and Tukey's multiple comparison test. All data are expressed as mean ± SEM. **P* < 0.05, ***P* < 0.01, ****P* < 0.001, *****P* < 0.0001, ns = not significant. Data analyzed from n=3-5 mice/group.

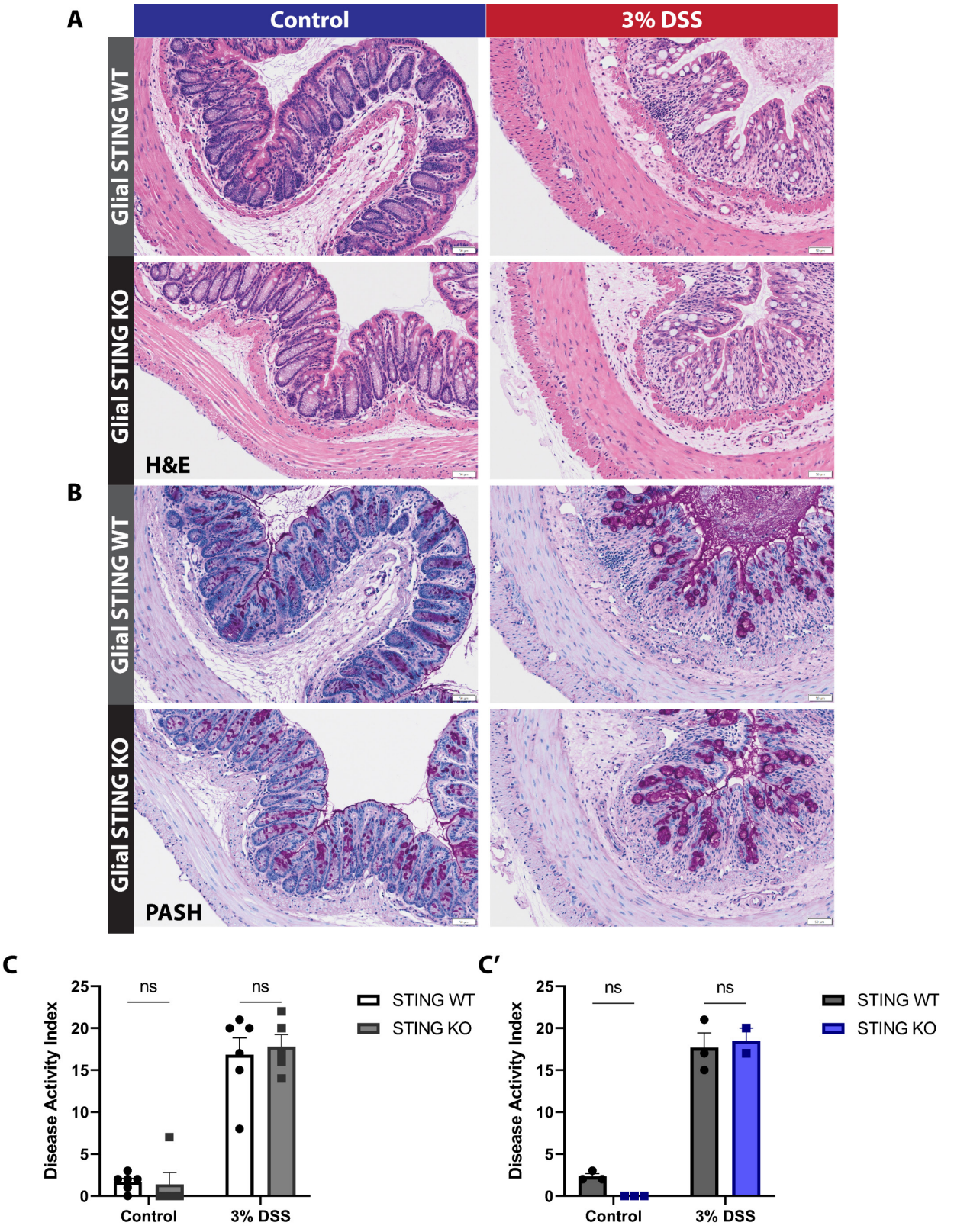

Figure 4.6 Enteric glial STING does not significantly alter histological disease scoring of colonic tissue in acute DSS colitis.

(A-B) Representative H&E **(A)** and PASH **(B)** images used to determine histological disease activity index in STING WT (rows with gray headers) and glial STING KO (rows with black headers) mouse colon. H&E and PASH collectively highlight damage in DSS-treated tissue based on assessment of mucosal morphology, goblet cell numbers, cellular infiltrate, and muscle layer thickening but no differences in response to glial STING-KO are appreciated. Scale bars represent 50μm. **(C)** Quantitative scoring and statistical analysis of histological damage demonstrates no significant difference between WT and glial STING-KO mice in mixed sex **(C)** or male only **(C')** response to acute 3% DSS treatment. Data were analyzed using two-way ANOVA and Tukey's or Bonferroni's multiple comparison test from n=5 mice/ group. Data are expressed as mean ± SEM. Ns = not significant. Images representative of labeling in n=5 mice/group. Scale bars represent 50μm.

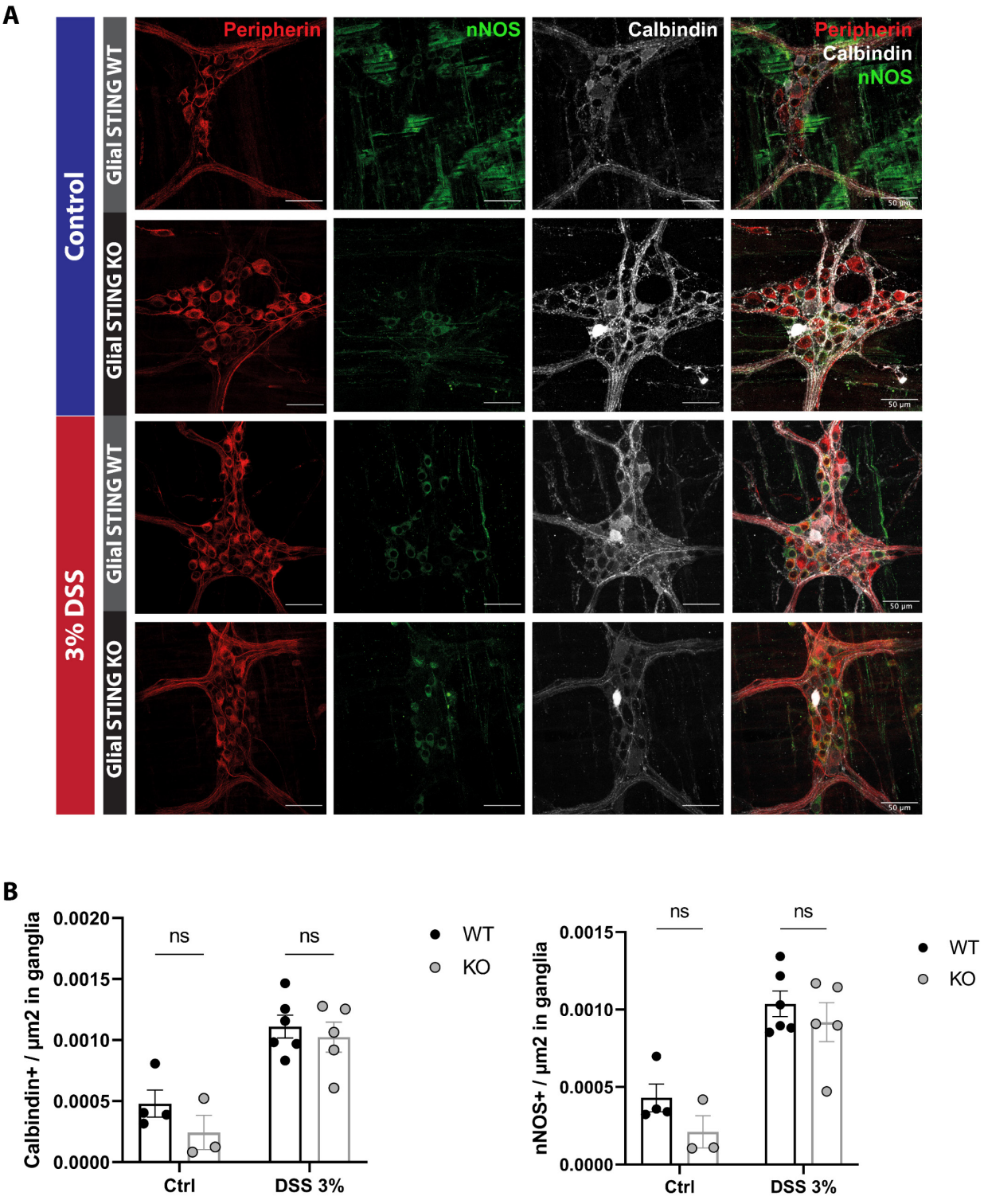

Figure 4.7 Enteric glial STING does not alter cholinergic and nitrergic myenteric neuron populations in acute DSS colitis.

(A) Representative images of cholinergic (Calbindin$^+$, gray) and nitrergic (nNOS$^+$, green) enteric neuron populations in the myenteric plexus from control and DSS-treated glial STING WT (rows with gray headers) and KO (rows with black headers) mice. Total neurons are represented by peripherin in red. While relative increases in both cholinergic and nitrergic populations are appreciable with acute 3% DSS treatment there is no difference between genotypes. **(B)** Quantification of nitrergic nNOS$^+$ (*left*) and cholinergic Calbindin$^+$ (*right*) enteric neurons normalized to ganglionic area. Data are representative of 12 ganglia/mouse. Both neuronal subpopulations are increased with acute 3% DSS treatment ($P < 0.0001$) but unaffected by genotype. Data were analyzed using two-way ANOVA and Bonferroni's multiple comparison test from n=5 mice/group. Data are expressed as mean ± SEM. Ns = not significant. Images representative of labeling in n=5 mice/group. Scale bars represent 50μm.

DISCUSSION

Appropriate host-microbial communication is essential for both tolerance of commensal microbes and anti-pathogen defense where perturbations in the signaling result in inflammatory damage and disease.[1–5] The stimulator of interferon genes (STING) responds to microbial cues to modulate inflammation[21,22,24,25] to play a complex role in acute colitis and can either exacerbate or ameliorate colonic damage.[27–29] We hypothesized that cell-specific STING activation contributes to STING's detrimental or protective role and enteric glial STING plays a part in this balance. We provide the first known examination of STING and IFNβ expression in the ENS and determined that STING is expressed in both neurons and glia of the myenteric plexus while IFNβ is primarily expressed in enteric neurons. We also showed that ENS STING can be activated to produce IFNβ and this process occurs in enteric neurons and is likely glial-independent. Finally we demonstrated that enteric glial STING does not play a major role during acute DSS colitis in whole-colon and ENS-specific damage responses. Our data provide the first investigation of STING and IFNβ expression and activation in the ENS and potential roles of ENS STING signaling in disease.

Neurons and glia in the central nervous system express STING in culture and *in situ* albeit at lower levels that professional immune cells such as microglia.[30,31,61] Our *in situ* transcriptional labeling and immunohistochemistry support similar STING expression patterns within enteric neurons and glial compared to resident MHCII$^+$ immune cells (**Figs 4.1c** and **4.2**). Furthermore transcriptional datasets support enteric glial expression of other components of the STING signaling cascade (**Fig 4.1a-b**). Thus enteric glia express the necessary genes to signal through the STING pathway. Enteric glia express genes for NF-κB (*Nfkb1* and *RelA*) at relatively higher levels than other STING components. While relative gene expression does not necessarily correlate to protein expression or activity this likely reflects the less specific role of NF-κB than other STING signaling components as it is involved in many other immune signaling pathways including other pattern recognition receptors.[62] This could suggest a role for other STING-like

cytosolic DNA sensors in enteric glia as they are expressed in central nervous system glia and induced in neurodegenerative disease.[61] Future research could examine the role of these other cytosolic DNA sensors in the ENS and enteric glia.

It is interesting that while STING is expressed in both ENS neurons and glia IFNβ is only expressed in enteric neurons. This is supported by both gene expression (**Figs 4.1a-b** and **4.3a**) and protein localization *in situ* (**Fig 4.3b-c**). IFNβ has not been previously investigated in the ENS and our results support enteric neuron IFNβ production and trafficking suggesting that this may play a functional role in GI health and/or disease. In the brain IFNβ plays a neuroprotective role during HIV infection but it is unclear whether this IFNβ is produced within neurons themselves or other cell types.[63] Additionally IFNβ is detectable but relatively lowly expressed in the brain during basal conditions[64,65] and increased during viral infection[63] suggesting that it more likely plays are role during pathology and not homeostatic conditions. This is contrasted in the ENS as our data demonstrated relatively high expression of IFNβ in enteric neurons even compared to resident $MHCII^+$ immune cells (**Fig 4.3c**). Furthermore IFNβ increases in enteric neurons with STING activation (**Fig 4.4e**). Taken together these data suggest enteric neuronal IFNβ may play a role in physiologic and infectious conditions but further investigation is required to elucidate this. Our ELISA data support ENS STING activation and IFNβ production in both the myenteric and submucosal plexus (**Fig 4.4b-c**). Since we used *in vitro* tissue preparations to assess this some IFNβ produced is likely from to $STING^+$ immune cells that reside within these layers. However it is also likely that enteric neurons contribute to this response as their intracellular IFNβ increases with DMXAA incubation (**Fig 4.4e**). This is also supported by IFNβ induction in the muscularis propria by Ad5-VCA0956 (**Fig 4.4b**) as serotype 5 can infect neurons.[66,67] Therefore it may be enteric neurons and not enteric glia that utilize STING-dependent IFNβ signaling in the ENS. This would be interesting to investigate in future studies and additionally compare to central nervous system STING expression and activation in neurons and glia. To date central neuroglia work supports higher STING expression in glia than neurons and glial STING activation in disease

states[30,31,53] and perhaps this contrasts with the ENS where neuronal STING plays are more active role. However this could simply mean central neuronal STING function is less frequently investigated.

Even though enteric glia do not affect canonic STING signaling to produce type I IFNs in response to CDNs (**Figs 4.4d** and **4.4f**) there are reports of specialized STING signaling mechanisms and perhaps enteric glial STING is activated in these situations. For instance STING can respond to etoposide-induced DNA damage to produce IFNβ response in keratinocytes and fibroblasts.[68] This represents a unique signaling mechanism for STING as although the downstream signaling cascade involves the same proteins this activation is independent of CDNs. STING can also activate autophagy in an IFN-independent mechanism in fibroblasts.[69] Interestingly the role of STING in autophagy is thought to evolutionarily predate its ability to stimulate type I IFNs as research on STING from sea anemone *Nematostella vectensis* can induce autophagy but not type I IFNs with STING activation.[69] In parallel to this the ENS is a highly immune organ in primordial creatures as well and integral to regulating host-microbe interactions in *Hydra*.[70] Recent work in mice support a continued immune role for enteric glia in mammals[34,35] and even specifically highlight mechanisms by which glia utilize autophagy during inflammation to communicate with lymphocytes.[34] Taken together these findings support the potential for enteric glial STING to retain this primordial autophagy-related function independently of its capacity to induce type I IFNs.

It is also possible that the role of enteric glial STING in ENS and GI function is more specialized and this is why we do not see any significant effects in acute DSS colitis between glial-STING WT and KO mice (**Figs 4.5-4.7**). Traumatic brain injury induces STING-dependent reactivity in central nervous system glia[30] and perhaps enteric glia are important in GI disease states more similar this. The pathophysiology of traumatic brain injury is highly dependent on autophagy dysfunction[30,71–74] and thus further supports both these specialized signaling mechanisms and functional responses in enteric glia. Another possibility is that enteric glia do

play a role in inflammatory disease but only in chronic conditions and not during the acute state. Type I IFNs play opposing roles in acute and chronic DSS colitis through myeloid cells where IFN signaling was protective during the acute phase of injury but prevented resolution of inflammation in chronic settings.[75] While our data suggest enteric glia do not express IFNβ or use type I signaling in homeostasis or acute colitis. It is possible these genes could be upregulated only during chronic inflammatory states. It is also possible that even in these states enteric glia themselves do not produce the IFNβ initially but instead response to production from other cell types. This in turn may potentiate STING expression as is seen in other reports[52] and ultimately activate glial STING to produce type I IFN-dependent or –independent responses. This is possible as enteric glia express the IFNβ receptor and its downstream signaling molecules (**Fig 4.1a-b**).

A chronic colitis-specific role is the case for connexin-43 hemichannel signaling in enteric glia as KO of this channel did not produce any appreciable differences in DSS colitis during the acute phase but exacerbated colonic hypersensitivity and myenteric plexus macrophage recruitment during the chronic phase.[35] Perhaps STING plays a similarly specific role. It is even possible that the role of enteric glial connexin-43 and STING intersect in chronic colitis as central nervous glia participate in STING signaling in combination other cell types where STING ligands are passed from other cells to glia through connexin-43 hemichannels in order to produce type I IFNs and other proinflammatory cytokines.[53] This is specifically observed between central neuroglia and metastatic cancer cells highlighting a role for glia in cancer. STING signaling is also involved in the development of colon cancer in chronic inflammation[21,27] and perhaps enteric glial STING in these disease states involves connexin-43-mediated transfer of signaling components. Taken together these data support the mechanistic potential for enteric glial STING to be important in specialized signaling functions and/or disease states that future research could determine.

One potential limitation of our findings is the efficacy of our genetic STING KO as it is difficulty to appreciate certain loss of labeling in enteric glia *in situ* by either RNAscope or

immunolabeling due to the highly overlapping nature of enteric glia with enteric neurons and the diffuse expression of STING across the myenteric ganglia (**Figs 4.1c** and **4.2a**). This could mean our lack of glial STING contribution to IFNβ production and acute DSS colitis are due to ineffective glial STING reduction. However both our *Sox10*^{CreERT2} cre line and the floxed STING line (B6;SJL-*Sting1*$^{tm1.1Camb}$) are independently validated[76,7778,79] and it is therefore likely that these are working as expected. We additionally were limited by sample size in some experiments. Additional mice in WT and KO ELISAs would have allowed for stratification by sex to see if this contributed to variability. Similarly in the DSS experiments this would have allowed female-only comparisons. Furthermore the male-only body weight data appears to trend towards differences between glial-STING WT and KO and additional mice could help solidify or remove this perceived difference. However given the current nature of the data (even the male body weights were still $P > 0.2$) we think it is unlikely this would change major results. Another limitation is in our quantification of myenteric cholinergic and/or nitrergic neurons in acute DSS colitis. Due to the shortened colon length in acute DSS especially in female mice it is possible that some of our preparations for immunohistochemistry are more proximal than others and this influenced our calculations. We corrected for this by normalizing to ganglionic size instead of total neuronal number as the proximal colon has different proportions of neuronal types and total neuronal numbers.[6,80,81] However this still may account for our finding of increased nNOS^{+} neurons in acute DSS compared to previous studies that reported no changes or decreased proportions[58–60] as the number of nitrergic neurons in relatively higher in proximal than distal colon.[81] However, another difference that could account for this phenomena is that those studies utilized 5% DSS instead and therefore nNOS neuronal alterations in DSS colitis may be bimodal and dependent on disease severity.

Overall this research represents the first known investigation of STING signaling and IFNβ production in the ENS. Our data support novel important findings including the potential of enteric neurons to utilize STING and IFNβ signaling while enteric glial STING is potentially important in

more specialized roles as it does not impact homeostatic IFNβ response or colonic inflammation in acute DSS colitis. Furthermore we discuss other potential mechanisms that enteric glial STING could be useful for and future research into these pathways could uncover critical roles for enteric glial STING elsewhere. Understanding what circumstances enteric glial STING is active in and the mechanisms of this activation can help us further characterize the role of enteric glia in micro-immune communication and additional potential mechanisms for STING in GI health and disease.

REFERENCES

REFERENCES

1. Round JL, Mazmanian SK. The gut microbiota shapes intestinal immune responses during health and disease. *Nat Rev Immunol*. 2009;9(5):313-323. doi:10.1038/nri2515

2. Zheng D, Liwinski T, Elinav E. Interaction between microbiota and immunity in health and disease. *Cell Res*. 2020;30(6):492-506. doi:10.1038/s41422-020-0332-7

3. Hill DA, Artis D. Intestinal Bacteria and the Regulation of Immune Cell Homeostasis. *Annu Rev Immunol*. 2010;28(1):623-667. doi:10.1146/annurev-immunol-030409-101330

4. Honda K, Littman DR. The Microbiome in Infectious Disease and Inflammation. *Annu Rev Immunol*. 2012;30(1):759-795. doi:10.1146/annurev-immunol-020711-074937

5. Casadevall A, Pirofski L. The damage-response framework of microbial pathogenesis. *Nat Rev Microbiol*. 2003;1(1):17-24. doi:10.1038/nrmicro732

6. Furness JB. *The Enteric Nervous System*. (Furness JB, ed.). Malden, Massachusetts, USA: Blackwell Publishing; 2006. doi:10.1002/9780470988756

7. Furness JB. The enteric nervous system and neurogastroenterology. *Nat Rev Gastroenterol Hepatol*. 2012;9(5):286-294. doi:10.1038/nrgastro.2012.32

8. Endres K, Schäfer K-H. Influence of Commensal Microbiota on the Enteric Nervous System and Its Role in Neurodegenerative Diseases. *J Innate Immun*. 2018;10(3):172-180. doi:10.1159/000488629

9. Jacobson A, Yang D, Vella M, Chiu IM. The intestinal neuro-immune axis: crosstalk between neurons, immune cells, and microbes. *Mucosal Immunol*. 2021;14(3):555-565. doi:10.1038/s41385-020-00368-1

10. De Vadder F, Grasset E, Mannerås Holm L, et al. Gut microbiota regulates maturation of the adult enteric nervous system via enteric serotonin networks. *Proc Natl Acad Sci*. 2018;115(25):6458-6463. doi:10.1073/pnas.1720017115

11. Matheis F, Muller PA, Graves CL, et al. Adrenergic Signaling in Muscularis Macrophages Limits Infection-Induced Neuronal Loss. *Cell*. 2020;180(1):64-78.e16. doi:10.1016/j.cell.2019.12.002

12. Muller PA, Matheis F, Schneeberger M, Kerner Z, Jové V, Mucida D. Microbiota-modulated CART + enteric neurons autonomously regulate blood glucose. *Science (80-)*. 2020;6176(August):eabd6176. doi:10.1126/science.abd6176

13. Obata Y, Castaño Á, Boeing S, et al. Neuronal programming by microbiota regulates intestinal physiology. *Nature*. 2020;578(7794):284-289. doi:10.1038/s41586-020-1975-8

14. Obata Y, Pachnis V. The Effect of Microbiota and the Immune System on the Development and Organization of the Enteric Nervous System. *Gastroenterology*. 2016;151(5):836-844. doi:10.1053/j.gastro.2016.07.044

15. Kabouridis PS, Lasrado R, McCallum S, et al. Microbiota Controls the Homeostasis of Glial Cells in the Gut Lamina Propria. *Neuron*. 2015;85(2):289-295. doi:10.1016/j.neuron.2014.12.037

16. Kabouridis PS, Lasrado R, McCallum S, et al. The gut microbiota keeps enteric glial cells on the move; prospective roles of the gut epithelium and immune system. *Gut Microbes*. 2015;6(6):398-403. doi:10.1080/19490976.2015.1109767

17. Seguella L, Gulbransen BD. Enteric glial biology, intercellular signalling and roles in gastrointestinal disease. *Nat Rev Gastroenterol Hepatol*. March 2021. doi:10.1038/s41575-021-00423-7

18. Turco F, Sarnelli G, Cirillo C, et al. Enteroglial-derived S100B protein integrates bacteria-induced Toll-like receptor signalling in human enteric glial cells. *Gut*. 2014;63(1):105-115. doi:10.1136/gutjnl-2012-302090

19. Benvenuti L, D'Antongiovanni V, Pellegrini C, et al. Enteric Glia at the Crossroads between Intestinal Immune System and Epithelial Barrier: Implications for Parkinson Disease. *Int J Mol Sci*. 2020;21(23):9199. doi:10.3390/ijms21239199

20. Kimono D, Sarkar S, Albadrani M, et al. Dysbiosis-Associated Enteric Glial Cell Immune-Activation and Redox Imbalance Modulate Tight Junction Protein Expression in Gulf War Illness Pathology. *Front Physiol*. 2019;10(OCT):1229. doi:10.3389/fphys.2019.01229

21. Barber GN. STING: Infection, inflammation and cancer. *Nat Rev Immunol*. 2015;15(12):760-770. doi:10.1038/nri3921

22. Burdette DL, Monroe KM, Sotelo-Troha K, et al. STING is a direct innate immune sensor of cyclic di-GMP. *Nature*. 2011;478(7370):515-518. doi:10.1038/nature10429

23. Gao P, Ascano M, Wu Y, et al. Cyclic [G(2′,5′)pA(3′,5′)p] Is the Metazoan Second Messenger Produced by DNA-Activated Cyclic GMP-AMP Synthase. *Cell*. 2013;153(5):1094-1107. doi:10.1016/j.cell.2013.04.046

24. Sun L, Wu J, Du F, Chen X, Chen ZJ. Cyclic GMP-AMP Synthase Is a Cytosolic DNA Sensor That Activates the Type I Interferon Pathway. *Science (80-)*. 2013;339(6121):786-791. doi:10.1126/science.1232458

25. Woodward JJ, Iavarone AT, Portnoy DA. c-di-AMP Secreted by Intracellular Listeria monocytogenes Activates a Host Type I Interferon Response. *Science (80-)*. 2010;328(5986):1703-1705. doi:10.1126/science.1189801

26. Wu J, Sun L, Chen X, et al. Cyclic GMP-AMP Is an Endogenous Second Messenger in Innate Immune Signaling by Cytosolic DNA. *Science (80-)*. 2013;339(6121):826-830. doi:10.1126/science.1229963

27. Ahn J, Son S, Oliveira SC, Barber GN. STING-Dependent Signaling Underlies IL-10 Controlled Inflammatory Colitis. *Cell Rep*. 2017;21(13):3873-3884. doi:10.1016/j.celrep.2017.11.101

28. Canesso MCC, Lemos L, Neves TC, et al. The cytosolic sensor STING is required for intestinal homeostasis and control of inflammation. *Mucosal Immunol*. 2018;11(3):820-

834. doi:10.1038/mi.2017.88

29. Martin GR, Blomquist CM, Henare KL, Jirik FR. Stimulator of interferon genes (STING) activation exacerbates experimental colitis in mice. *Sci Rep*. 2019;9(1):14281. doi:10.1038/s41598-019-50656-5

30. Abdullah A, Zhang M, Frugier T, Bedoui S, Taylor JM, Crack PJ. STING-mediated type-I interferons contribute to the neuroinflammatory process and detrimental effects following traumatic brain injury. *J Neuroinflammation*. 2018;15(1):1-17. doi:10.1186/s12974-018-1354-7

31. Reinert LS, Lopušná K, Winther H, et al. Sensing of HSV-1 by the cGAS-STING pathway in microglia orchestrates antiviral defence in the CNS. *Nat Commun*. 2016;7. doi:10.1038/ncomms13348

32. Rao M, Nelms BD, Dong L, et al. Enteric glia express proteolipid protein 1 and are a transcriptionally unique population of glia in the mammalian nervous system. *Glia*. 2015;63(11):2040-2057. doi:10.1002/glia.22876

33. Grubišić V, Gulbransen BD. Enteric glia: the most alimentary of all glia. *J Physiol*. 2017;595(2):557-570. doi:10.1113/JP271021

34. Chow AK, Grubišić V, Gulbransen BD. Enteric Glia Regulate Lymphocyte Activation via Autophagy-Mediated MHC-II Expression. *Cell Mol Gastroenterol Hepatol*. June 2021. doi:10.1016/j.jcmgh.2021.06.008

35. Grubišić V, McClain JL, Fried DE, et al. Enteric Glia Modulate Macrophage Phenotype and Visceral Sensitivity following Inflammation. *Cell Rep*. 2020;32(10):108100. doi:10.1016/j.celrep.2020.108100

36. Grubišić V, Gulbransen BD. Enteric glial activity regulates secretomotor function in the mouse colon but does not acutely affect gut permeability. *J Physiol*. 2017;595(11):3409-3424. doi:10.1113/JP273492

37. Zhou J, Zheng Y, Roembke BT, et al. Florescent analogs of cyclic and linear dinucleotides as phosphodiesterase and oligoribonuclease activity probes. *RSC Adv*. 2016.

38. Fried DE, Gulbransen BD. In Situ Ca^{2+} Imaging of the Enteric Nervous System. *J Vis Exp*. 2015;(95):1-7. doi:10.3791/52506

39. Luo X, Li H, Ma L, et al. Expression of STING Is Increased in Liver Tissues From Patients With NAFLD and Promotes Macrophage-Mediated Hepatic Inflammation and Fibrosis in Mice. *Gastroenterology*. 2018;155(6):1971-1984.e4. doi:10.1053/j.gastro.2018.09.010

40. McClain JL, Mazzotta EA, Maradiaga N, et al. Histamine-dependent interactions between mast cells, glia, and neurons are altered following early-life adversity in mice and humans. *Am J Physiol Liver Physiol*. 2020;319(6):G655-G668. doi:10.1152/ajpgi.00041.2020

41. Brown IAM, Gulbransen BD. The antioxidant glutathione protects against enteric neuron death in situ, but its depletion is protective during colitis. *Am J Physiol Liver Physiol*.

2017;314(1):G39-G52. doi:10.1152/ajpgi.00165.2017

42. Peng Y, Zhuang J, Ying G, et al. Stimulator of IFN genes mediates neuroinflammatory injury by suppressing AMPK signal in experimental subarachnoid hemorrhage. *J Neuroinflammation*. 2020;17(1):165. doi:10.1186/s12974-020-01830-4

43. Hernandez S, Fried DE, Grubišić V, McClain JL, Gulbransen BD. Gastrointestinal neuroimmune disruption in a mouse model of Gulf War illness. *FASEB J*. 2019;(1):fj.201802572R. doi:10.1096/fj.201802572R

44. Koestler BJ, Seregin SS, Rastall DPW, et al. Stimulation of innate immunity by in vivo cyclic di-GMP synthesis using adenovirus. *Clin Vaccine Immunol*. 2014;21(11):1550-1559. doi:10.1128/CVI.00471-14

45. Drokhlyansky E, Smillie CS, Van Wittenberghe N, et al. The Human and Mouse Enteric Nervous System at Single-Cell Resolution. *Cell*. September 2020:1-17. doi:10.1016/j.cell.2020.08.003

46. Delvalle NM, Dharshika C, Morales-Soto W, Fried DE, Gaudette L, Gulbransen BD. Communication Between Enteric Neurons, Glia, and Nociceptors Underlies the Effects of Tachykinins on Neuroinflammation. *Cell Mol Gastroenterol Hepatol*. 2018;6(3):321-344. doi:10.1016/j.jcmgh.2018.05.009

47. Kaur S, Platanias LC. IFN-β-specific signaling via a unique IFNAR1 interaction. *Nat Immunol*. 2013;14(9):884-885. doi:10.1038/ni.2686

48. Love M, Anders S, Huber W. DESeq2: Differential gene expression analysis based on the negative binomial distribution. 2021. https://github.com/mikelove/DESeq2.

49. Scheu S, Dresing P, Locksley RM. Visualization of IFNβ production by plasmacytoid versus conventional dendritic cells under specific stimulation conditions in vivo. *Proc Natl Acad Sci U S A*. 2008;105(51):20416-20421. doi:10.1073/pnas.0808537105

50. Li Y, Wilson HL, Kiss-Toth E. Regulating STING in health and disease. *J Inflamm (United Kingdom)*. 2017;14(1):1-21. doi:10.1186/s12950-017-0159-2

51. Prantner D, Perkins DJ, Lai W, et al. 5,6-Dimethylxanthenone-4-acetic Acid (DMXAA) Activates Stimulator of Interferon Gene (STING)-dependent Innate Immune Pathways and Is Regulated by Mitochondrial Membrane Potential. *J Biol Chem*. 2012;287(47). doi:10.1074/jbc.M112.382986

52. Ma F, Li B, Yu Y, Iyer SS, Sun M, Cheng G. Positive feedback regulation of type I interferon by the interferon-stimulated gene <scp>STING</scp>. *EMBO Rep*. 2015;16(2):202-212. doi:10.15252/embr.201439366

53. Chen Q, Boire A, Jin X, et al. Carcinoma–astrocyte gap junctions promote brain metastasis by cGAMP transfer. *Nature*. 2016;533(7604):493-498. doi:10.1038/nature18268

54. Eichele DD, Kharbanda KK. Dextran sodium sulfate colitis murine model: An indispensable tool for advancing our understanding of inflammatory bowel diseases pathogenesis. *World J Gastroenterol*. 2017;23(33):6016-6029.

doi:10.3748/wjg.v23.i33.6016

55. Chassaing B, Aitken JD, Malleshappa M, Vijay-Kumar M. Dextran Sulfate Sodium (DSS)-Induced Colitis in Mice. *Curr Protoc Immunol*. 2014;104(1):Unit. doi:10.1002/0471142735.im1525s104

56. Mähler M, Bristol IJ, Leiter EH, et al. Differential susceptibility of inbred mouse strains to dextran sulfate sodium-induced colitis. *Am J Physiol Liver Physiol*. 1998;274(3):G544-G551. doi:10.1152/ajpgi.1998.274.3.G544

57. Belkind-Gerson J, Graham HK, Reynolds J, et al. Colitis promotes neuronal differentiation of Sox2+ and PLP1+ enteric cells. *Sci Rep*. 2017;7(1):1-15. doi:10.1038/s41598-017-02890-y

58. Winston JH, Li Q, Sarna SK. Paradoxical regulation of ChAT and nNOS expression in animal models of Crohn's colitis and ulcerative colitis. *Am J Physiol Liver Physiol*. 2013;305(4):G295-G302. doi:10.1152/ajpgi.00052.2013

59. Mizuta Y, Isomoto H, Takahashi T. Impaired nitrergic innervation in rat colitis induced by dextran sulfate sodium. *Gastroenterology*. 2000;118(4):714-723. doi:10.1016/S0016-5085(00)70141-7

60. Kono T, Chisato N, Ebisawa Y, et al. Impaired nitric oxide production of the myenteric plexus in colitis detected by a new bioimaging system. *J Surg Res*. 2004;117(2):329-338. doi:10.1016/j.jss.2003.11.004

61. Cox DJ, Field RH, Williams DG, et al. DNA sensors are expressed in astrocytes and microglia in vitro and are upregulated during gliosis in neurodegenerative disease. *Glia*. 2015;63(5):812-825. doi:10.1002/glia.22786

62. Liu T, Zhang L, Joo D, Sun S-CC. NF-κB signaling in inflammation. *Signal Transduct Target Ther*. 2017;2(April):17023. doi:10.1038/sigtrans.2017.23

63. Thaney VE, O'Neill AM, Hoefer MM, Maung R, Sanchez AB, Kaul M. IFNβ Protects Neurons from Damage in a Murine Model of HIV-1 Associated Brain Injury. *Sci Rep*. 2017;7(1):46514. doi:10.1038/srep46514

64. Abt MC, Osborne LC, Monticelli LA, et al. Commensal Bacteria Calibrate the Activation Threshold of Innate Antiviral Immunity. *Immunity*. 2012;37(1):158-170. doi:10.1016/j.immuni.2012.04.011

65. Kawashima T, Kosaka A, Yan H, et al. Double-Stranded RNA of Intestinal Commensal but Not Pathogenic Bacteria Triggers Production of Protective Interferon-β. *Immunity*. 2013;38(6):1187-1197. doi:10.1016/j.immuni.2013.02.024

66. O'Carroll SJ, Cook WH, Young D. AAV Targeting of Glial Cell Types in the Central and Peripheral Nervous System and Relevance to Human Gene Therapy. *Front Mol Neurosci*. 2021;13:256. doi:10.3389/fnmol.2020.618020

67. Benskey MJ, Kuhn NC, Galligan JJ, et al. Targeted gene delivery to the enteric nervous system using AAV: A comparison across serotypes and capsid mutants. *Mol Ther*. 2015;23(3):488-500. doi:10.1038/mt.2015.7

68. Dunphy G, Flannery SM, Almine JF, et al. Non-canonical Activation of the DNA Sensing Adaptor STING by ATM and IFI16 Mediates NF-κB Signaling after Nuclear DNA Damage. *Mol Cell*. 2018;71(5):745-760.e5. doi:10.1016/j.molcel.2018.07.034

69. Gui X, Yang H, Li T, et al. Autophagy induction via STING trafficking is a primordial function of the cGAS pathway. *Nature*. 2019;567(7747):262-266. doi:10.1038/s41586-019-1006-9

70. Klimovich A V., Bosch TCG. Rethinking the Role of the Nervous System: Lessons From the Hydra Holobiont. *BioEssays*. 2018;40(9):1800060. doi:10.1002/bies.201800060

71. Choi AMK, Ryter SW, Levine B. Autophagy in Human Health and Disease. *N Engl J Med*. 2013;368(7):651-662. doi:10.1056/NEJMra1205406

72. Clark RSB, Bayir H, Chu CT, Alber SM, Kochanek PM, Watkins SC. Autophagy is increased in mice after traumatic brain injury and is detectable in human brain after trauma and critical illness. *Autophagy*. 2008;4(1):88-90. doi:10.4161/auto.5173

73. Smith CM, Chen Y, Sullivan ML, Kochanek PM, Clark RSB. Autophagy in acute brain injury: Feast, famine, or folly? *Neurobiol Dis*. 2011;43(1):52-59. doi:10.1016/j.nbd.2010.09.014

74. Sarkar C, Zhao Z, Aungst S, Sabirzhanov B, Faden AI, Lipinski MM. Impaired autophagy flux is associated with neuronal cell death after traumatic brain injury. *Autophagy*. 2014;10(12):2208-2222. doi:10.4161/15548627.2014.981787

75. Rauch I, Hainzl E, Rosebrock F, et al. Type I interferons have opposing effects during the emergence and recovery phases of colitis. *Eur J Immunol*. 2014;44(9):2749-2760. doi:10.1002/eji.201344401

76. Jin L, Waterman PM, Jonscher KR, Short CM, Reisdorph NA, Cambier JC. MPYS, a Novel Membrane Tetraspanner, Is Associated with Major Histocompatibility Complex Class II and Mediates Transduction of Apoptotic Signals. *Mol Cell Biol*. 2008;28(16):5014-5026. doi:10.1128/mcb.00640-08

77. Jin L, Hill KK, Filak H, et al. MPYS Is Required for IFN Response Factor 3 Activation and Type I IFN Production in the Response of Cultured Phagocytes to Bacterial Second Messengers Cyclic-di-AMP and Cyclic-di-GMP. *J Immunol*. 2011;187(5):2595-2601. doi:10.4049/jimmunol.1100088

78. McClain JL, Gulbransen BD. The acute inhibition of enteric glial metabolism with fluoroacetate alters calcium signaling, hemichannel function, and the expression of key proteins. *J Neurophysiol*. 2017;117(1):365-375. doi:10.1152/jn.00507.2016

79. Memic F, Knoflach V, Morarach K, et al. Transcription and Signaling Regulators in Developing Neuronal Subtypes of Mouse and Human Enteric Nervous System. *Gastroenterology*. 2018;154(3):624-636. doi:10.1053/j.gastro.2017.10.005

80. Li Z, Hao MM, Van den Haute C, Baekelandt V, Boesmans W, Vanden Berghe P. Regional complexity in enteric neuron wiring reflects diversity of motility patterns in the mouse large intestine. *Elife*. 2019;8. doi:10.7554/eLife.42914

81. Takahashi T, Owyang C. Regional differences in the nitrergic innervation between the proximal and the distal colon in rats. *Gastroenterology*. 1998;115(6):1504-1512. doi:10.1016/S0016-5085(98)70029-0

CHAPTER FIVE: KEY FINDINGS AND FUTURE DIRECTIONS FOR CHARACTERIZING EXPRESSIONAL NETWORKS OF ENTERIC GLIAL-ENVIRONMENTAL COMMUNICATION

KEY FINDINGS

The enteric nervous system (ENS) consists of neurons and glia that contribute to essential gastrointestinal (GI) functions including motility, visceral sensation, secretion, absorption, neuroimmune communication, and permeability.[1,2] Specialized “omics” tools have already begun to revolutionize our understanding of enteric neuronal genetic architecture in homeostatic and pathologic roles in addition to providing gene expression databases invaluable for future research directions and mechanistic insights.[3–7] However these types of studies rarely focus on enteric glia and as such there are relatively few enteric glial omics databases to date.[3,6,8,9] Thus a major focus of this dissertation was to develop and utilize genetic technologies to characterize enteric glia. In particular these genetic tools are ideal for investigating key regulatory networks that govern how enteric glia respond to dynamic environmental factors including stress and the gut microbiota. Furthermore these networks are likely intricate and characterizing them in complex models is essential for placing them in the context of GI disease. We utilized large-scale and *in situ* gene expression techniques to investigate two modalities of glial-environmental communication. First we assessed the impact of psychosocial stressors during critical development periods, defined as early life stress, and characterized gene expression networks and altered expression patterns in this complex model between sexes to help understand sexual dimorphism in enteric glial communication and stress response. Next we investigated potential mechanisms enteric glia use to communicate with gut bacteria by characterizing the expression and activation of stimulator of interferon genes (STING) in enteric glia and neurons. We supplemented our gene expression results with *in situ* RNAscope and immunolabeling to visualize these molecular findings in their structural environment.

Enteric glial have sexually dimorphic expression patterns in homeostasis and response to early life stress

We discovered fundamental differences between sexes in how enteric glia communicate and respond to early life stress that may contribute to the sexual dimorphism of GI disease and

symptom presentation.[10–16] For instance gene expression of G protein-coupled receptor (GPCR) signaling cascades are differently expressed between males and females. GPCR signaling is a major established means of enteric glial communication[17–20] and these expressional differences may underlie fundamental sex-specific ways enteric glia communicate that are typically overlooked by male-only and mixed-sex experiments. This is also supported by recent work characterizing sexually dimorphic responses of enteric glia to unidirectional ganglionic stimulation that suggest structural and/or molecular differences in enteric glial connectivity (Ahmadzai et al. accepted at *PNAS*). However very little research has investigated the role of sex on enteric glial function and thus our findings are incredibly novel and likely shift the framework of how we should approach mechanistic research involving the ENS and subsequently disease pathogenesis and presentation.

These sex differences are made all the more interesting by the gene expression response in male mice following early life stress where they shift partially toward female-like expression patterns. In particular enteric glia from male mice alter expression of genes involved in known GI and neurological disease and related molecular pathways such as glial-immune communication through interferon signaling. Considering early life stress is a disease modifier we typically associate with females,[13,14,16,21] seeing more dramatic results in males is unexpected and characterizing these differences is likely integral to our understanding of sex-specific effects of early life stress on GI disease. Since pathway analysis focuses on gene sets associated with inflammation and disease states it is logical to consider that these expressional shifts after early life stress confer disease risk in males. However interferon signaling-related genes are actually decreased in males after early life stress and what this means for disease development and presentation could be complex. This downregulation could be indicative of an anti-inflammatory response. Furthermore since these same pathways are decreased in non-stressed females compared to non-stressed males further mechanistic research is integral to understanding whether these expressional similarities reflect functional similarities or alternatively sexually

dimorphic responses to similar gene expression patterns. What is protective in one instance may actually confer disease risk in another and this could be especially difficult to ascertain in immune-related pathways where complex factors ultimately regulate if a response is exacerbating or protective. Type I interferon signaling in the gut emulates this paradigm as it protects against acute inflammation but promotes the development of chronic inflammation in colitis models[22] and therefore decreased expression of these same genes in stressed males and non-stressed females could have entirely different consequences on gut health.

STING is a functional mechanism within the ENS but its role is cell type- and context-dependent

This complexity in glial-immune communication is further exemplified by our examination of STING signaling in the ENS. Since type I interferons are a potentially important signaling mediator in the enteric glia we sought to characterize the role of STING and type I interferon response as a mechanism of glial-microbial communication. While we hypothesized STING would be active in enteric glia based on prior literature[23,24] our data suggests this canonical activation of STING signaling to promote type I interferon response occurs in primarily in enteric neurons and not enteric glia. Furthermore while general STING signaling does impact GI inflammation and damage during the dextran sodium sulfate (DSS) model of acute colitis,[25,26] enteric glial STING does not have a major impact. This may once again highlight complexity in enteric glial immune signaling where STING plays a more specialized role. An interesting alternative signaling role for STING is in autophagy and is considered a primordial role for STING conserved in other nonimmune cell types.[27] Autophagy was recently established as a non-canonical role of major histocompatibility complex II (MHCII) in enteric glia and enteric glial MHCII does not participate in prototypical antigen processing and presentation.[28] Perhaps both MHCII and STING highlight evolutionarily conserved genes that maintain their primordial functions within enteric glia from previous organisms where the ENS also served as a rudimentary immune organ.[29] Perhaps as professional immune cells evolved and began utilizing these signaling molecules for specialized

functions enteric glia instead retained them only with their original use. Regardless of its evolutionary trajectory, the potential role of enteric glial STING in autophagy would support considering alternative signaling mechanisms and subsequent functions of other prototypical immune biomolecules expressed in nonprofessional immune cells like enteric glia.

STUDY LIMITATIONS

Limited sample size has varying implications across some of our experiments. In RNA-sequencing increased samples would have helped to understand the nature of expressional variability seen in enteric glia from female mice. This may be a true phenomenon and gene expression patterns between females vary more than males or this could be due to other confounding factors such as estrus cycling. Assessing changes to variability patterns with more samples in addition to estrus staging would allow better interpretation of the significance of this phenomenon in females. Additionally many differentially expressed genes in enteric glia from females are likely false negatives due to this variability and with the increased power afforded from more samples we could better characterize gene expression shifts in females following early life stress. However, while these would strengthen our findings they do not discount the current results. Estrus staging is not a strong indicator of female variability in immune cells[30] and therefore may not play a major role in enteric glia as well. Additionally we are still able to highlight some changes in enteric glia from females after early life stress that have important and functionally relevant implications.

Additional samples for our RNAscope data would allow us to assess RNAscope signaling quantitatively and identify the most consistently and highly differentially expressed genes that may be key regulators in networks functionally relevant to sex-specific responses to early life stress. Of course the magnitude of up- or downregulation is not the same as functional impact and thus any validated expressional differences could be worth investigating. Finally since enteric glia have sex-specific regulation of type I interferon signaling additional samples in our STING experiments

would have allowed for sex-stratification of results to see if STING contributed to sex-dependent interferon signaling in enteric glia. However given that our current data suggests STING may not use canonical type I interferon signaling in enteric glia under homoeostatic or acute inflammatory conditions it is unlikely that sex stratification would have produced any additional results.

FUTURE DIRECTIONS

Investigating the functional implications of differential gene expression on enteric glial GPCR and interferon signaling

In addition to adding samples to both our Sox10-RiboTag RNA-sequencing and RNAscope experiments to further strengthen our data we would like to assess the functional significance of key differentially expressed genes. Understanding this in enteric glia based on sex and/or early life stress exposure helps connect these large-scale patterns of expression and molecular networks with tangible effects and means of modifying GI function. For instance the gene for regulator of G-protein signaling (*Rgs5*) is increased in non-stressed females compared to non-stressed males and also decreases in female mice following early life stress (**Fig 3.6**). Rgs5 alters Gα- and Gq-mediated signaling in arteriolar smooth muscle cells[31] and therefore could have similar functions in enteric glia to modify signaling patterns throughout the glial network. Gq-signaling in enteric glia in particular can be relatively easily measured and quantified *in situ*[32] to assess changes in signaling patterns with Rgs5 inhibition or over expression. Even characterizing the baseline differences in these signaling patterns between non-stressed and early life stressed mice has not been done before and would provide valuable additional functional information to connect to differential gene expression. IFN signaling in enteric glia is also sexually dimorphic and contributes to feminization of male enteric glia following early life stress (**Fig 3.7**). The effects of interferon signaling on enteric glial functionally connectivity can be initially characterized in a similar manner by incubating *ex vivo* myenteric plexus preparations with interferon-α/β or interferon-γ and following then assessing functional activation of enteric glia in response to stimulation. Comparing glial responses with changes in these signaling pathways with the

responses of enteric glia in mice following early life stress would help characterize the impact of GPCRs and interferon signaling on enteric glial intercellular communication and the functional connectivity of the ENS.

Performing RNA-sequencing on male and female mice with and without early life stress to assess enteric neuronal expression

Since enteric neurons are also an important factor in altering the functional connectivity of enteric glia understanding tandem molecular changes in these cells that are sex-dependent and follow early life stress could provide valuable information about key pathways that affect the entire ENS and identify mechanisms of communication between enteric neurons and glia use to alter gut function after early life stress. Therefore we are creating a parallel dataset for enteric neurons using BAF53b-Cre mice (Tg(Actl6b-Cre)4092Jiwu/J; Jackson Laboratories, stock number 027826) combined with the RiboTag model. The BAF53b-Cre line has been used to perform single-cell RNAs-sequencing from enteric neurons[5] and is expressed specifically in enteric neurons of the myenteric plexus (**Fig 5.1**). We crossed this line with *GCaMP5g-Tdt* mice (PC::G5-tdT mice (B6;129S6-Polr2a$^{tm1(CAG-GCaMP5g,-tdTomato)Tvrd}$/J; Jackson Laboratory, stock number 024477) so that both Tdt and Ca^{2+} indicator GCaMP5g would be expressed under the BAF53b promoter (*Baf53b$^{Cre+/-}$;GCaMP5g-tdT$^{+/-}$*). We then assessed Tdt and GCaMP5g expression in the myenteric plexus in live (**Fig 5.1a**) and fixed (**Fig 5.1b**) tissue. Both Tdt and GCaMP5g (labeled for by antibodies for Tdt and GFP respectively) are neuron-specific and display no overlap with glial cell bodies as determined by S100β antibody labeling (**Fig 5.1b**, *third panels*). Additionally we immunolabeled fixed frozen slides from these mice to investigate *Baf53b* expression throughout the entire gut wall. *Baf53b* expression is primarily localized to ganglia within the myenteric and submucosal plexus with some expression through intramuscular and mucosal ENS processes (**Fig 5.1b**, *bottom panels*).

We then crossed homozygous BAF53b-Cre mice with homozygous RiboTag mice (B6N.129-*Rpl22*$^{tm1.1Psam}$/J; Jackson Laboratories, stock number 011029) to generate *Baf53b*$^{Cre+/-}$*;Rpl22*$^{+/-}$ mice (Baf53b-RiboTag). Since RiboTag mice express the HA tag on ribosomes we immunolabeled myenteric tissue with an antibody against HA and characterized its co-localization with neuronal cell bodies (labeled by peripherin) and glial cell bodies (outlined by GFAP). HA is expressed specifically in neurons and not enteric glia (**Fig 5.1c**) further supporting BAF53b-Cre as an appropriate driver line to study neuronal signaling. Once RNA-sequencing from Baf53b-RiboTag male and female mice with and without early life stress is completed, we will run these data through the same analysis pipeline used for enteric glial Sox10-RiboTag mice. We will then utilize different pathway analysis pipelines to understand expressional differences between enteric neurons and glia and even suggest specific ligand-receptor interactions that may be altered by sex or early life stress. Others have used similar methods to study enteric glial and neuronal interactions with other cell types.[3,33] Performing this analysis will provide putative mechanistic targets for downstream investigation that could have major implications for driving sex-specific functional connectivity with the ENS.

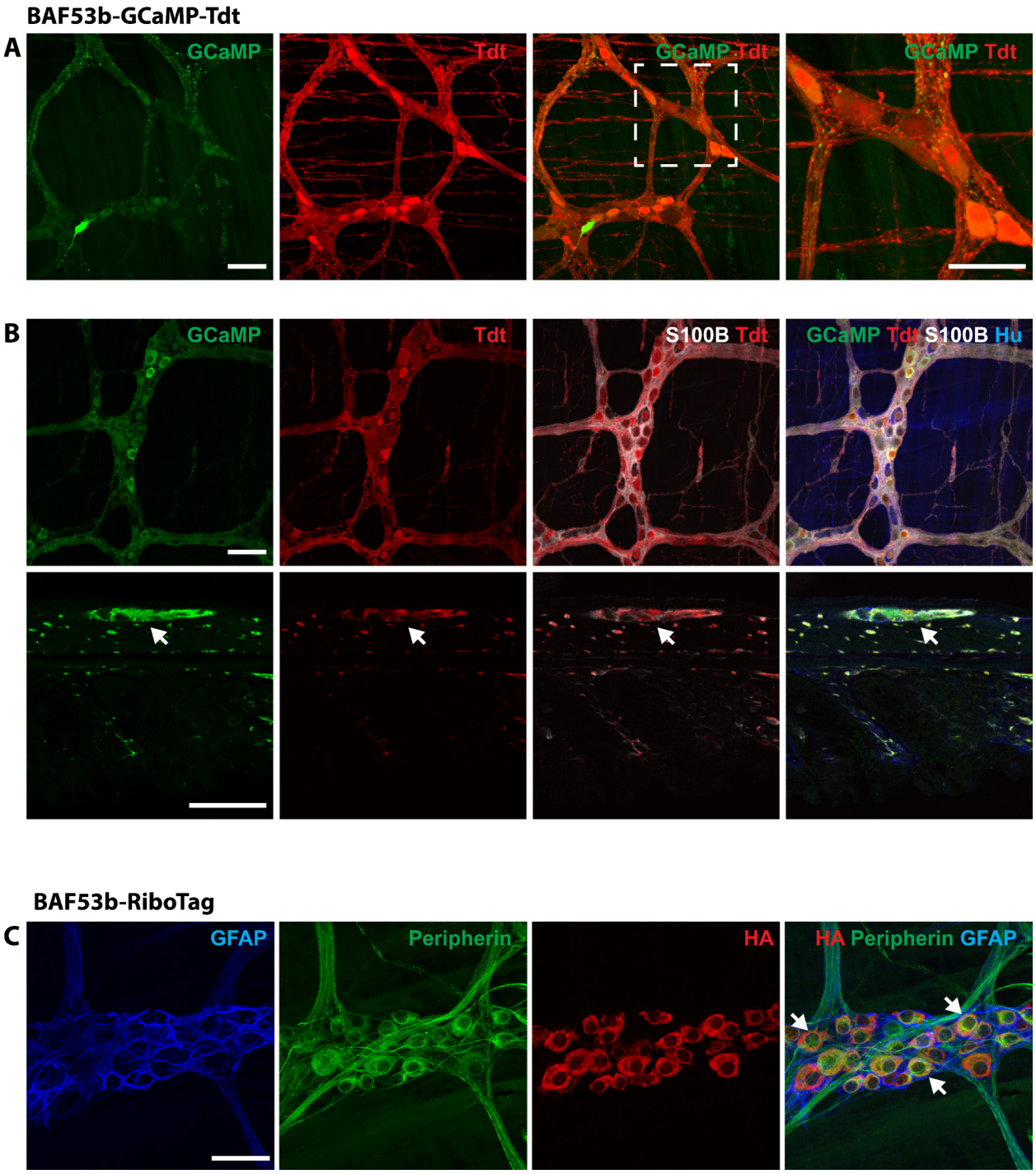

Figure 5.1 The BAF53b-Cre driver line is specific for enteric neurons with the intestine.

(A) GCaMP5g (green) and Tdt (red) reporter expression in live myenteric tissue from *Baf53b*$^{Cre+/-}$*;GCaMP5g-tdT*$^{+/-}$ mice demonstrates labeling specifically in enteric neuron cell bodies and fiber tracts. Area within the dotted rectangle is magnified in the final panel. **(B)** This is confirmed by co-

labeling for enteric glial (S100β, white) and neuronal (Hu C/D, blue) markers in myenteric plexus whole mounts (*top panels*) where S100β$^+$ glial cell bodies and Tdt expression are non-overlapping. Furthermore, *Baf53b* is mainly expressed in ENS ganglia (white arrow) and intermuscular and mucosal fiber tracts throughout the gut wall (*bottom panels*). In these images the serosal side is at the top while the mucosal side is at the bottom. **(C)** Immunolabeling demonstrates co-localization of the HA tag with peripherin$^+$ neuronal cell bodies (green) and not enteric glial cell bodies (indicated by small cells enveloped by GFAP$^+$ processes, blue). Representative HA$^+$ neurons are indicated by white arrows. Images representative of n= 2-3 mice/group and captured using a Zeiss LSM 880 NLO confocal system (Zeiss, Jena, Germany) using Zen Black software and a 20x objective (0.8 numerical aperture, Plan ApoChromat; Zeiss). Scale bars represent 50μm.

Investigating the role of enteric glial STING in autophagy

Our lab recently determined that enteric glial MHCII is used in autophagy during interferon-γ and lipopolysaccharide (LPS) stimulation.[28] This was characterized by quantifying expression of MHCII in enteric glia in combination with the autophagy agonist rapamycin and inhibitor 3-MA over a 16-hour time course. We could perform similar experiments with STING expression to see if enteric glial STING is altered in autophagy as measured by localization and intensity of STING within enteric glial cells. However we have yet to assess changes in enteric glial STING expression in the interferon-γ + LPS inflammatory model so it is unclear if this will be an appropriate method to use. However this model does alter STING expression in cardiomyocytes and alveolar macrophages[34,35] and thus may also do so in enteric glia. This could also be used in other models of inflammation or that are known to promote autophagy including the DSS colitis model[36] we used to investigate STING in the ENS instead if interferon-γ + LPS do not stimulate response. Since these experiments are already performed in our lab it would be relatively simple to use them to characterize STING expression in autophagy as well.

In conclusion this dissertation provides novel genetic tools and data to further uncover molecular functions in enteric glia and their role in GI and systemic health. Using these methods we discovered entirely novel molecular interaction effects between sex and early life stress that shift the framework of these risk factors in GI disease. Furthermore we highlight a novel potential mediator of ENS-microbe communication with STING. Together these data further characterize the molecular patterns used by glia in response to complex environmental factors and highlight unique heterogeneity in glial intercellular communication. We hope that our future work in these studies will build on this framework to further characterize key networks regulating glial-neuronal functional circuitry and glial-immune communication.

REFERENCES

REFERENCES

1. Furness JB. *The Enteric Nervous System*. (Furness JB, ed.). Malden, Massachusetts, USA: Blackwell Publishing; 2006. doi:10.1002/9780470988756

2. Furness JB. The enteric nervous system and neurogastroenterology. *Nat Rev Gastroenterol Hepatol*. 2012;9(5):286-294. doi:10.1038/nrgastro.2012.32

3. Drokhlyansky E, Smillie CS, Van Wittenberghe N, et al. The Human and Mouse Enteric Nervous System at Single-Cell Resolution. *Cell*. September 2020:1-17. doi:10.1016/j.cell.2020.08.003

4. May-Zhang AA, Tycksen E, Southard-Smith AN, et al. Combinatorial transcriptional profiling of mouse and human enteric neurons identifies shared and disparate subtypes in situ. *Gastroenterology*. 2020;160(3):1-16. doi:10.1053/j.gastro.2020.09.032

5. Morarach K, Mikhailova A, Knoflach V, et al. Diversification of molecularly defined myenteric neuron classes revealed by single-cell RNA sequencing. *Nat Neurosci*. December 2020. doi:10.1038/s41593-020-00736-x

6. Wright CM, Schneider S, Smith-Edwards KM, et al. scRNA-sequencing reveals new enteric nervous system roles for GDNF, NRTN, and TBX3. *Cell Mol Gastroenterol Hepatol*. January 2021:140981. doi:10.1016/j.jcmgh.2020.12.014

7. Zeisel A, Hochgerner H, Lönnerberg P, et al. Molecular Architecture of the Mouse Nervous System. *Cell*. 2018;174(4):999-1014.e22. doi:10.1016/j.cell.2018.06.021

8. Delvalle NM, Dharshika C, Morales-Soto W, Fried DE, Gaudette L, Gulbransen BD. Communication Between Enteric Neurons, Glia, and Nociceptors Underlies the Effects of Tachykinins on Neuroinflammation. *Cell Mol Gastroenterol Hepatol*. 2018;6(3):321-344. doi:10.1016/j.jcmgh.2018.05.009

9. Rao M, Nelms BD, Dong L, et al. Enteric glia express proteolipid protein 1 and are a transcriptionally unique population of glia in the mammalian nervous system. *Glia*. 2015;63(11):2040-2057. doi:10.1002/glia.22876

10. Bradford K, Shih W, Videlock EJ, et al. Association Between Early Adverse Life Events and Irritable Bowel Syndrome. *Clin Gastroenterol Hepatol*. 2012;10(4):385-390.e3. doi:10.1016/j.cgh.2011.12.018

11. Chitkara DK, van Tilburg MAL, Blois-Martin N, Whitehead WE. Early Life Risk Factors That Contribute to Irritable Bowel Syndrome in Adults: A Systematic Review. *Am J Gastroenterol*. 2008;103(3):765-774. doi:10.1111/j.1572-0241.2007.01722.x

12. Chang L, Di Lorenzo C, Farrugia G, et al. Functional Bowel Disorders: A Roadmap to Guide the Next Generation of Research. *Gastroenterology*. 2018;154(3):723-735. doi:10.1053/j.gastro.2017.12.010

13. Medland JE, Pohl CS, Edwards LL, et al. Early life adversity in piglets induces long-term upregulation of the enteric cholinergic nervous system and heightened, sex-specific

secretomotor neuron responses. *Neurogastroenterol Motil*. 2016;28(9):1317-1329. doi:10.1111/nmo.12828

14. Pohl CS, Medland JE, Mackey E, et al. Early weaning stress induces chronic functional diarrhea, intestinal barrier defects, and increased mast cell activity in a porcine model of early life adversity. *Neurogastroenterol Motil*. 2017;29(11):e13118. doi:10.1111/nmo.13118

15. Prusator DK, Greenwood-Van Meerveld B. Sex-related differences in pain behaviors following three early life stress paradigms. *Biol Sex Differ*. 2016;7(1):29. doi:10.1186/s13293-016-0082-x

16. Chaloner A, Greenwood-Van Meerveld B. Sexually Dimorphic Effects of Unpredictable Early Life Adversity on Visceral Pain Behavior in a Rodent Model. *J Pain*. 2013;14(3):270-280. doi:10.1016/j.jpain.2012.11.008

17. Gulbransen BD. Enteric Glia. *Colloq Ser Neuroglia Biol Med From Physiol to Dis*. 2014;1(2):1-70. doi:10.4199/C00113ED1V01Y201407NGL002

18. Grubišić V, Gulbransen BD. Enteric glia: the most alimentary of all glia. *J Physiol*. 2017;595(2):557-570. doi:10.1113/JP271021

19. McClain JL, Fried DE, Gulbransen BD. Agonist-Evoked Ca2+ Signaling in Enteric Glia Drives Neural Programs That Regulate Intestinal Motility in Mice. *Cell Mol Gastroenterol Hepatol*. 2015;1(6):631-645. doi:10.1016/j.jcmgh.2015.08.004

20. Brown IAMM, McClain JL, Watson RE, Patel BA, Gulbransen BD. Enteric Glia Mediate Neuron Death in Colitis Through Purinergic Pathways That Require Connexin-43 and Nitric Oxide. *Cell Mol Gastroenterol Hepatol*. 2016;2(1):77-91. doi:10.1016/j.jcmgh.2015.08.007

21. Rosztóczy A, Fioramonti J, Jármay K, Barreau F, Wittmann T, Buéno L. Influence of sex and experimental protocol on the effect of maternal deprivation on rectal sensitivity to distension in the adult rat. *Neurogastroenterol Motil*. 2003;15(6):679-686. doi:10.1046/J.1350-1925.2003.00451.X

22. Rauch I, Hainzl E, Rosebrock F, et al. Type I interferons have opposing effects during the emergence and recovery phases of colitis. *Eur J Immunol*. 2014;44(9):2749-2760. doi:10.1002/eji.201344401

23. Abdullah A, Zhang M, Frugier T, Bedoui S, Taylor JM, Crack PJ. STING-mediated type-I interferons contribute to the neuroinflammatory process and detrimental effects following traumatic brain injury. *J Neuroinflammation*. 2018;15(1):1-17. doi:10.1186/s12974-018-1354-7

24. Reinert LS, Lopušná K, Winther H, et al. Sensing of HSV-1 by the cGAS-STING pathway in microglia orchestrates antiviral defence in the CNS. *Nat Commun*. 2016;7. doi:10.1038/ncomms13348

25. Canesso MCC, Lemos L, Neves TC, et al. The cytosolic sensor STING is required for intestinal homeostasis and control of inflammation. *Mucosal Immunol*. 2018;11(3):820-834. doi:10.1038/mi.2017.88

26. Martin GR, Blomquist CM, Henare KL, Jirik FR. Stimulator of interferon genes (STING) activation exacerbates experimental colitis in mice. *Sci Rep*. 2019;9(1):14281. doi:10.1038/s41598-019-50656-5

27. Gui X, Yang H, Li T, et al. Autophagy induction via STING trafficking is a primordial function of the cGAS pathway. *Nature*. 2019;567(7747):262-266. doi:10.1038/s41586-019-1006-9

28. Chow AK, Grubišić V, Gulbransen BD. Enteric Glia Regulate Lymphocyte Activation via Autophagy-Mediated MHC-II Expression. *Cell Mol Gastroenterol Hepatol*. June 2021. doi:10.1016/j.jcmgh.2021.06.008

29. Klimovich A V., Bosch TCG. Rethinking the Role of the Nervous System: Lessons From the Hydra Holobiont. *BioEssays*. 2018;40(9):1800060. doi:10.1002/bies.201800060

30. Breznik JA, Schulz C, Ma J, Sloboda DM, Bowdish DME. Biological sex, not reproductive cycle, influences peripheral blood immune cell prevalence in mice. *J Physiol*. 2021;599(8):2169-2195. doi:10.1113/JP280637

31. Arnold C, Feldner A, Pfisterer L, et al. <scp>RGS</scp> 5 promotes arterial growth during arteriogenesis. *EMBO Mol Med*. 2014;6(8):1075-1089. doi:10.15252/emmm.201403864

32. Fried DE, Gulbransen BD. In Situ Ca^{2+} Imaging of the Enteric Nervous System. *J Vis Exp*. 2015;(95):1-7. doi:10.3791/52506

33. Wangzhou A, Paige C, Neerukonda S V, Dussor G, Ray PR, Price TJ. A pharmacological interactome platform for discovery of pain mechanisms and targets. 2020.

34. Li N, Zhou H, Wu H, et al. STING-IRF3 contributes to lipopolysaccharide-induced cardiac dysfunction, inflammation, apoptosis and pyroptosis by activating NLRP3. *Redox Biol*. 2019;24:101215. doi:10.1016/j.redox.2019.101215

35. Ning L, Wei W, Wenyang J, Rui X, Qing G. Cytosolic DNA-STING-NLRP3 axis is involved in murine acute lung injury induced by lipopolysaccharide. *Clin Transl Med*. 2020;10(7):e228. doi:10.1002/ctm2.228

36. Shao B-Z, Yao Y, Zhai J-S, Zhu J-H, Li J-P, Wu K. The Role of Autophagy in Inflammatory Bowel Disease. *Front Physiol*. 2021;12:63. doi:10.3389/fphys.2021.621132